1-23-2013

Chemically Modified Proteins as Functional Biomaterials

Vindya K. Thilakarathne
vindyakalani@gmail.com

Chemically Modified Proteins as Functional Biomaterials

Vindya Kalani Thilakarathne, PhD

University of Connecticut, 2013

The goal of this thesis was to explore how to improve the functionality of proteins as biomaterials by chemical modification of the surface of the protein. In order to achieve this goal protein surfaces were decorated with small amine molecules and large synthetic polymers. The introduced functionality by the facile modification, allowed the protein to behave as a successful biocatalysts, biosensor and a useful scaffolding platform.

Thorough characterization was performed using various biochemical, bioanalytical biophysical methods to evaluate the structural integrity, enzymatic activity , thermodynamic and kinetic stability of chemically modified proteins/enzymes. Improved stability and reversible thermal denaturation were key stand out properties observed with chemical modification.

The study was further expanded to understand the effect of modification for the interaction between chemically modified protein and macromolecules. As a model system triethylenetetramine modified hemoglobin and polyacrylic acid were used to investigate the charge dependency on thermodynamics of protein/polymer interaction. A collaborative research project between Kasi and Kumar groups exploit the protein/polymer interaction towards a development of biosensor to detect small molecules.

Furthermore we studied the chemically modified bovine serum albumin (BSA) as a scaffolding platform for construction of protein and DNA based artificial antenna complex to capture solar energy. Chemical modification allows BSA to reverse its negative charge and facilitate the binding to DNA. Donors and acceptor chromophores were loaded in DNA/BSA scaffold and functioned as an efficient and stable antenna complex. Thus, functionalities introduced to the protein by chemical modification have shown a major influence towards the application of proteins as successful functional biomaterials.

Chemically Modified Proteins as Functional Biomaterials

Vindya Kalani Thilakarathne

B.Sc University of Peradeniya, Sri Lanka , 2006

A dissertation

Submitted in Partial Fulfillment of the

Requirement for the Degree of

Doctor of Philosophy

at the

University of Connecticut

2013

APPROVAL PAGE

Doctor of Philosophy Dissertation

Chemically Modified Proteins as Functional Biomaterials

Presented by Vindya Kalani Thilakarathne

Major Advisor ……..
Dr. Challa V. Kumar

Associate Advisor …….
Dr. Rajeswari M. Kasi

Associate Advisor …….
Dr. Xudong Yao

Associate Advisor …….
Dr. Fatma Selampinar

Associate Advisor …….
Dr. Yao Lin

University of Connecticut

2013

Acknowledgements

Successful completion of a doctoral dissertation is impossible without all the help given to us during our PhD career. It is my greatest pleasure to thank all those who were encouraged me and helped me to achieve a successful doctoral dissertation. I would like to express my sincere gratitude to my advisor Prof.C.V.Kumar for his enormous support, guidance and encouragement he had offered me to achieve my career goals. His great mentorship allowed me to grow as a confident independent thinker throughout my PhD career.

I would also like to thank Dr.R.M. Kasi for all her guidance and support. Having been working with her nearly four years she has became my second advisor, and always willing to offer her help and guidance during challenging situations. I also thank my teaching supervisor Dr.Fatma Selampinar, for she exposed me to explore width and breath of teaching experience. Her support and the training have prepared me well for challengers in teaching. I also thankful for Dr. Lin and Dr.Yao, for their comments and suggestions.

I'm fortunate to have wonderful colleagues to work with during my five years of research work. I would like to express my gratitude to my past group members, especially Dr. Duff for teaching me experimental techniques and instrumentations. To all current group members, thank you very much for bringing fun and humor to some stressful days in the lab. Thank you Inoka for being there with me during all those ups and downs in this journey to achieve PhD. I'm also grateful to Victoria for being a wonderful collaborator. I learned a lot from her. I will miss all of you in the lab and I wish you best of luck with achieving your goals in life !!!

Finally and most importantly I would like to thank all my family members whose love, concern and support strengthen me during all these years. My sincere gratitude goes to my dear loving mother to whom this dissertation is dedicated to. Her encouragement and support meant immense to my life. Words are not enough to express my gratitude to my husband Neranjan for his patience, support and encouragement during this endeavor.

Table of Contents

List of Schemes

List of Tables

List of Figures

Figure 1.4. Agarose gels of GO (lane 1) , GO-Lysine (lane 2) , GO-NH_4Cl (lane 3) and GO-TETA (lane 4) in 40 mM Tris acetate, gels were run at specific pHs, as indicated.When pI of the protein equals to the pH of the running buffer, protein does not move out of the well, which are located in the middle of the gel. Mid point of each protein band as indicated was taken as the distance migrated in the agarose gel. Distance and charge relationship of the modified GO derivatives, relative to the distance and charge of unmodified GO, were estimated using imageJ 1.46r software from NIH and average charge at pH 7 was tabulated in **Table 1.2.**

Figure 1.5. Plot of pH vs charge of (A) GO, (B) GO-Lysine, (C) GO-NH_4Cl and (D) GO-TETA. The Y-intercept of each is the corresponding isoelectric point (pI).

Figure 1.6. SDS PAGE of **A.** the modified glucose oxidase. Lane, 1 is the molecular weight marker and lane 2 is unmodified glucose oxidase. Lanes 3 to 6 are glucose oxidase samples modified with TETA, PEI, NH_4Cl and L-lysine, respectively. The extent of crosslinking in each of these lanes is indicated under the gel; **B**. modified hemoglobin, Lane 1 is the molecular weight marker and lane 2 is unmodified hemoglobin. Lanes 3 to 5 are modified carbonic anhydrase, synthesized using L-lysine, TETA and NH_4Cl, respectively; **C**. modified carbonic anhydrase, Lane 1 is the molecular weight marker and lane 2 is unmodified carbonic anhydrase. Lanes 3 to 5 are modified carbonic anhydrase, synthesized using L-lysine, TETA and NH_4Cl, respectively.

Figure 1.7. The far UV CD spectra of (**A)** glucose oxidase (black line) before and after modification with 20 mM TETA (red line), 100 mM NH_4Cl (blue line) and 1 mM PEI (Green line); and note that the CD spectra of modified GO are similar to that of the

corresponding GO, which indicates retention of native-like structure to a significant extent.

Figure 1.8. Far UV CD spectra of **A**. carbonic anhydrase and hemoglobin before and after modification with 20 mM TETA (red line), 200 mM NH_4Cl (blue line) and 200 mM L-lysine (Green line) recorded in 10 mM K_2HPO_4 50 mM NaCl pH 7.2 buffer. Note that in all cases, the CD spectra of modified enzymes have significant overlaps with those of the corresponding unmodified ones.

Figure 1.9. Comparison of activities of: **A**. GO **B. CA** and **C.** Hb before and after chemical modification. Activities were monitored using 1 μM protein solution in 10 mM K_2HPO_4 50 mM NaCl pH 7.2 buffer in room temperature according to the procedure explained in experimental section. The particular amines used for the modification are as marked in the graph.

Figure 1.10: The plot of relative specific activities (Relative to the initial activity) of unmodified and modified glucose oxidase vs time in hours . Time taken for the relative specific activity to be half was take as the half life of each sample. Note that the half life of unmodified GO is around 50 hrs and all the modified GOs have half life above 160 hours.

Figure 1.11: The plot of half life in hours vs isoelectric point of GO and modified GO. Note that the half life of unmodified GO is around 50 h and highest half life was >300 h, >500% improvement.

Figure 1.12: The plot of half life vs isoelectric point of hemoglobin and carbonic anhydrase. Note that the highest half life among hemoglobin samples were observed with lysine modified Hb which has pI around 7.5. Amine modified carbonic

anhydrase samples do not show any correlation between the half life and isoelectric point.

Figure 1.13. Thermograms of modified GO, recorded in 10 mM K_2HPO_4 pH 7.2, at a scan rate of 2 ˚C/min. GO (black), GO-TETA (red), GO-NH_3 (blue) and GO-PEI (green).

Figure 1.14. Molar heat capacity profile of CA (**A**) and hemoglobin **(B)**, unmodified (black), modified with TETA (red), NH_4Cl (blue) and L-lysine (green) in corresponding buffers at a scan rate of 2 ˚C/min.

Figure 1.15. (A) .Plot of denaturation temperatures (T_m/˚C) of GO, CA and Hb derivatives vs their corresponding half lives (● Unmodified enzyme, ■ NH_4Cl derivative, ◆ TETA derivative, ▼ Lysine derivative). Unmodified and modified derivatives of GO show a clear correlation between the denaturation temperature and half life while CA and Hb derivatives don't show any such correlation. **(B) .** The plot of half life of enzyme vs corresponding amine conjugation of each enzyme. The plot indicates higher half life with modified glucose oxidase which has 120 acidic amino acids. Hemoglobin and carbonic anhydrase, which contains 60 and 30 acidic amino acids respectively, does not show a significant increase in half life.

Figure 2.1 Absorption spectra of Hb, Hb-PAA and Hb/PAA (1 μM protein) recorded in phosphate buffer (10 mM K_2HPO_4 pH 7.2, 1 cm pathlength). The Soret bands of Hb (blue line) and Hb-PAA (red line) are nearly superimposable while that of Hb/PAA mixture (green line) indicated minor decrease in Soret band intensity.

Figure 2.2 Gel electrophoresis image of agarose gel run at pH 6.5 tris acetate buffer, Hb-PAA conjugate (1), Hb/PAA mixture (2) and Hb (3).

Figure 2.3 TEM images of (a) Hb-PAA (0.2 wt% PAA) (b) Hb/PAA (0.2 wt% PAA) (c) Hb and (d) PAA (0.2 wt% PAA), stained by RuO_4.

Figure 2.4. Far UV CD spectra (**Figure 2.4a**) of unmodified Hb (black line) and Hb-PAA conjugate (red line), as well as those of a physical mixture of Hb and PAA (green line). All three samples contained same amount of Hb (4 μM protein in 10 mM K_2HPO_4 pH 7.2 buffer). Soret CD (**Figure 2.4b**) of Hb and Hb-PAA (4 μM protein in 10 mM K_2HPO_4 pH 7.2 buffer). Soret CD peak position of the conjugate is the same as that of Hb.

Figure 2.5. Redox activities of Hb (**Figure 2.5a**) and Hb-PAA conjugate (**Figure 2.5b**) (1 μM protein in 10 mM K_2HPO_4 pH 7.2 buffer) as indicated by the Soret absorption bands, upon the addition of sodium dithionite and sodium ferricyanide (20 μM). Redox activity of the heme moiety is retained in Hb-PAA conjugate.

Figure 2.6 The peroxidase-like activity of Hb, Hb-PAA and Hb/PAA (1 μM protein) by the addition of 2-methoxyphenol (2.5 mM) and H_2O_2 (1 mM) as monitored by following the absorbance of the product at 470 nm (10 mM K_2HPO_4 pH 7.2 buffer at room temperature). Activity of Hb-PAA (red line) is almost the same as that of Hb (blue line) or Hb/PAA mixture (green line). Activities were normalized to the concentration of Hb in each sample. Conjugation of the polymer with the protein did not alter Hb activity.

Figure 2.7 The DSC thermograms of Hb, PAA, Hb-PAA and Hb/PAA. The molar heat capacity profiles of Hb (8 μM protein, blue line), PAA (4.4 μM, black line), Hb/PAA (8 μM protein, 4.4 μM PAA, green line), and Hb-PAA (8 μM protein, 4.4 μM PAA, red line) recorded in 10 mM K_2HPO_4 pH 7.2 buffer at a scan rate of 2 ˚C /min. The quantitative values of the corresponding thermodynamic parameters are listed in Table 1.

Figure 2.8 Peroxidase activities after steam sterilization and cooling to room temperature. Activities were measured with with1 mM H_2O_2 and 2.5 mM 2-methoxyphenol in 10 mM K_2HPO_4 pH 7.2 buffer, at room temperature. The data has been normalized to the concentration of Hb in each sample. Activity of Hb-PAA (broken red line) after steam sterilization is similar to the activities of Hb (broken blue line) and Hb/PAA (broken green line). There are no measureable differences among the three samples.

Figure 2.9. The effect of pH on heme Soret peak from pH 7 to 11, (Hb (blue line) Hb-PAA (red line), 4.4μM PAA, 8μM Hb in PBS pH 7.4 buffer at 25°C). The peak shifted from 406 nm to higher values upon addition of NaOH and the transition was reversible with little or no hysteresis.

Figure 2.10 Change in specific activity of the Hb-PAA as a function of time. Specific activities of Hb (*blue line*), Hb/PAA mix (*green line*) and Hb-PAA conjugate (*red line*) are compared, as a function of time. 1 mM H_2O_2 and 2.5 mM 2-methoxyphenol in 10 mM K_2HPO_4 pH 7.2 were used to measure the peroxidase-like activities of the samples. Specific activity at time t was divided by specific activity at time 0 to compare the three sets of data.

Figure 3.1. Titration of Hb (486 μM) with PAA (0.7 μM) in PBS, pH 7.4 at 25 ˚C. (A) Change in power vs time plot when PAA solution was titrated with Hb solution. (B) Enthalpy change vs [Hb]/[PAA] for titration. Red line is the best fit to the data, according to the single, identical, non-interacting binding site model. Best fit indicated a binding stoichiometry of 14 Hb per mole of PAA, binding constant of $3.2x10^5$ M^{-1}, ΔH and ΔS values of -7.4 kcal/mol of Hb bound and 0.1715 cal/mol, respectively.

Figure 3.2. Hb association dissociation curve for 10μM Hb binding to PAA in PBS pH 7.4 (500μRIU PAA immobilized). (black – Hb binding curve, red- data fit by Scrubber software)

Figure 3.3. Agarose gel electrophoresis of Hb-TETA and Hb-Ammonia derivatives at pH 7 (samples spotted at the center of the gel). Lane 1 is Hb and lanes 2-4 are Hb-TETA40-7, Hb-TETA40-5 and Hb-TETA80-5, respectively, while lanes 5-8 are the Hb-Ammonia derivatives, Hb-Ammonia400-5, Hb-Ammonia800-5, Hb-Ammonia1k-5, Hb-Ammonia1.5k-5, respectively, produced under specific reaction conditions.

Figure 3.4. Agarose gels of chemically modified hemoglobin derivatives at pH 6, 8, and 9 (A through C respectively). Lane 1 in each gel is Hb and lanes 2, 3, & 4 are Hb-TETA40-7, Hb-TETA40-5 and Hb-TETA80-5 respectively. Lanes 5-8 are Hb-NH_4Cl400-5, Hb-NH_4Cl800-5, Hb-NH_4Cl1k-5, Hb-NH_4Cl1.5k-5, respectively. Mid point of each protein band as indicated was taken as the distance migrated in the agarose gel. Distance and charge relationship of the modified Hb derivatives, relative to the distance and charge of Hb, were calculated using imageJ 1.46r software from NIH and tabulated in **Table 3.2.**

Figure 3.5. Agarose gels of chemically modified hemoglobin derivatives at pH 6, 6.8, 7.5 and 8.7. Lane 1 in each gel is Hb and lanes 2, 3, 4, 5and 6 are Hb-TETA40-7, Hb-TETA40-5 , Hb-TETA80-5, Hb-TETA60-7 and Hb-TETA60-7 respectively. Mid point of the protein band in lane 5 and 6 was taken as the distance migrated in the agarose gel. Distance and charge relationship of the modified Hb derivatives, relative to the distance and charge of Hb, were calculated using imageJ 1.46r software from NIH and tabulated in **Table 3.3**.

Figure 3.6. Plot of pH vs charge of Hb and Hb-TETA and Hb-NH_4Cl derivatives. Y Intercept of each curve was taken as the isoelectric point (pI). Charge of each derivative at pH 6.4 where ITC measurements were take were also extracted from the plot.

Figure 3.7. Far UV CD spectra of unmodified Hb (black line), Hb-TETA40-7 (Blue line), Hb-TETA40-5 (Red line) and Hb-TETA80-5 (Green line). All samples contained same amount of protein in PBS pH 6.4 buffer. Note that the peak positions and intensities of Hb did not change upon chemical modification.

Figure 3.8. Far UV CD spectra of unmodified Hb and Hb-TETA derivatives in the absence (black line) and in the presence (Blue dash line) of PAA. All samples contained same amount of protein and PAA that was used for ITC measurements and were in PBS pH 6.4 buffer. CD spectra imply that there are no major distortions in protein secondary structure when bound to PAA.

Figure 3.9. Soret CD spectra of unmodified Hb and Hb-TETA derivatives in the absence (black line) and in the presence (Blue dash line) of PAA. All samples contained same amount of protein and PAA that was used for ITC measurements and were in PBS pH 6.4 buffer.

Figure 3.10. **A**. Change in power due to the addition of Hb-TETA80-5 (60 μM) to PAA (9 μM, polymer) (black curve), the dilution of Hb-TETA80-5 (60 μM) (blue curve), and dilution of PAA (9 μM) (red curve). **B**. Change in power due to the binding of Hb-TETA80-5 to PAA, after correcting for the dilutions of Hb-TETA80-5 and PAA (PBS, pH 6.4, 25 ˚C). These peaks were integrated to extract the corresponding ΔH values.

Figure 3.11. Binding enthalpies of Hb-TETA (blue dots) and Hb-Ammonia derivatives (black dots) (60 μM) to PAA (9 μM) as a function of their charge. Slopes of the linear

fits to the TETA and ammonia derivatives are – 3.8 and -1.0 kcal/mol per unit charge, respectively (PBS, pH 6.4, 25 ˚C).

Figure 3.12. Comparison of activities of modified and unmodified Hb (1 μM) in the presence and absence of PAA (0.15 μM) in PBS buffer pH 6.4 at room temperature.

Figure 3.13. Relative activities of Hb-derivatives (1 μM) in the presence or absence of PAA (0.15 μM), with respect to that of Hb, in PBS, pH 6.4, at 25 ˚C.

Figure 4.1: Agarose gel of unmodified BSA (lane 1) and BSA modified with TETA (cBSA) (lanes 2, 40 mM Tris acetate, gel run at pH 6) and samples were loaded into wells at the middle of the gel (dotted line).

Figure 4.2 : Overlap of absorbance and emission spectra of the four chromophores used to make the artificial antenna complex. Abbreviations of dyes are ; **H** for Hoechst (Blue), **C** for C540A (Green), **F** for Fluorescein (yellow) and **R** for Rhodamine (red).

Figure 4.3 : Emission spectra of the self-assembled system showing the contribution of each chromophore to the energy transfer cascade. (Abbreviations of dyes are ; **H** for Hoechst, **C** for C540A, **F** for Fluorescein and **R** for Rhodamine). **A**) Note that the Hoechst emission was quenched and Rhodamine emission was increased in the presence of primary and secondary acceptors, C540 and Fluorescein respectively. **B**) Clear evidence of step-wise energy transfer cascade has shown since elimination of each intermediate results in decrease in Rhodamine emission and increase in corresponding donor emission.

Figure 4.4. A) Increase in quenching of Fluorescein emission by increasing Rhodamine concentration. B) Plot of ln Φ_0/Φ vs quencher (Rhodamine) concentration. Note that the plot is non linear. C) Plot of ln Φ_0/Φ vs quencher (Rhodamine) concentration. Linear plot implies the quenching follows Perrin model.

Figure 4.5 A) C540 emission was decreased concomitantly by increasing quencher (Fluorescein) concentration. B) Plot of ln Φ_0/Φ vs quencher (Fluorescein) concentration. Quenching radius between C540 and Fluorescein was extracted from this Perrin plot. C). Decrease of emission spectra of Hoechst due to the increase in C540 which as the immediate acceptor for Hoechst emission according spectra overlaps. D) Plot of ln Φ_0/Φ vs quencher (C540) concentration. Quenching radius between Hoechst and C540 was extracted from this Perrin plot.

Figure 4.6 Energy transfer efficiency as a function of donor concentrations monitored using excitation spectra. Emission was monitored at 650 nm. A) Increase in concentration of Hoechst. B) Increase in concentration of C540A. C) Increase in concentration of Rhodamine.

Figure 4.7 SEM image of protein-DNA-Dye film.

Figure 4.8 Emission intensity at 586 nm (emission of Rhodamine) vs time of incubation of DNA/cBSA/dye film and DNA/cBSA/Rhodamine film at 80 ^{0}C. Films were cooled down to room temperature for 2-3 hours before taking the collecting spectra.

Chapter 1: Chemical Modification of Proteins Using Polyamines: As a Tool to Improve Enzyme Stability

1.1 Abstract

Enzyme-water interface could influence enzyme stability, and controlling the nature of this interface is a challenge. Here, we tested the hypothesis that net charge at the enzyme-water interface contributes to protein stability by systematically controlling this interface. Controlled amidation of the surface carboxyl groups of glucose oxidase (GO), carbonic anhydrase (CA) and hemoglobin (Hb) by reaction with NH_4Cl, triethylenetetramine (TETA), L-lysine or polyethyleneimine (PEI) resulted in chemically modified derivatives of these enzymes. Amidation, as expected, raised the isoelectric points (pI) of all 12 derivatives, but it did not alter enzyme structure or their catalytic activities to a significant extent, as monitored by gel electrophoresis, circular dichroism and activity studies. Storage half lives of all 12 enzyme derivatives increased, consistent with modified enzyme charge, and we show that protein stability can be exquisitely controlled by chemical modification. Thus, enzyme-water interface plays a very important role in controlling enzyme stability and this physical insight provides benign chemical methods to increase enzyme stability in a systematic manner. Control of enzyme stability is important for applications in biocatalysis and biosensing and current results point to new opportunities to control enzyme stability.

1.2 Introduction

Chemically modified enzymes provide unique opportunities to control enzyme behavior at the molecular level. For example, the surface residues of enzymes were chemically modified to facilitate the formation of novel enzyme-enzyme and enzyme-DNA complexes, which are not formed otherwise.[1,2] Chemically modified enzymes also provided opportunities to enhance their solubility in organic media.[3,4,5] Conjugation of polycations, polyols, small molecules or peptides to enzymes has been used to increase the affinities these enzymes for selected targets.[6,7,8] Ethylenediamine modified bovine serum albumin (BSA), for example, showed stronger affinity for afflotoxin and increased antibody production.[9] Enzymes conjugated with amines showed high efficiency for the cellular uptake of DNA, proteins and small molecules, due to favorable interactions of the newly introduced amine groups with the negatively charged cell membranes.[10.11,12,13] Amine conjugates of catalase and GO bind to the epithelial cells and prevent oxidative cellular damage.[14,15,16] Carboxyl-modified pepsin indicated enhanced thermal stability, but the underlying reasons for increased stability are not investigated.[17] Here, we systematically control enzyme-water interface by chemical modification and show that this molecular control provides new opportunities to improve enzyme stability in a systematic manner.

Our hypothesis is that decrease of charge at the enzyme-water interface, via limited chemical conversion of the surface carboxylate functions (**Scheme 1.1**), would stabilize the native state of the enzyme. This is fundamentally due to a decrease in the charge-charge repulsion (coulombic explosion) in the native state and this repulsion contributes to the propensity for denaturation.[18]

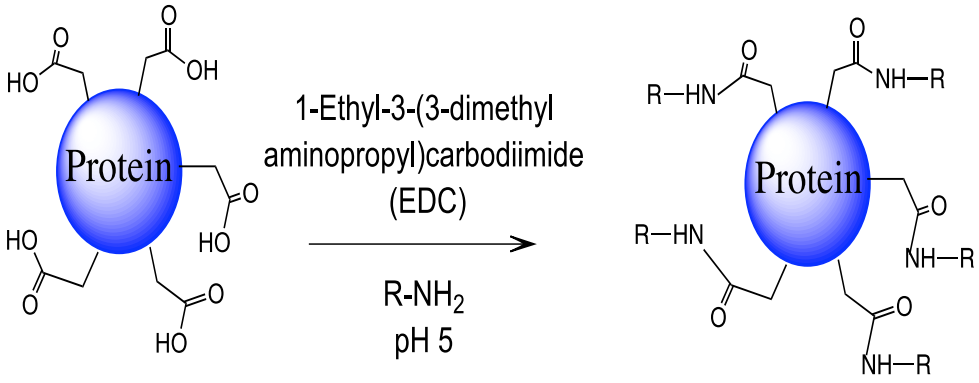

Scheme 1.1: Amidation of the carboxyl groups of enzymes using EDC chemistry, under mild reaction conditions.

Conversely, a reduction in charge-charge repulsion would stabilize the enzyme. For the current study, we have chosen glucose oxidase (GO), hemoglobin (Hb) and carbonic anhydrase (CA), which carry 126, 60 and 30 carboxyl functions, respectively. Limited conversion of these carboxyl groups to the corresponding amides, under controlled conditions, is expected to reduce charge repulsion by replacing negatively charged carboxyl groups by charge-neutral amide functions. Note that all three enzymes are negatively charged at pH 7, and alleviation of this unfavorable charge repulsion is expected to stabilize the native state and thereby increase its stability.

The amidation was carried out by the reaction of COOH groups with NH_3, triethylenetetrammine (TETA), L-lysine or polyethyleneimine (PEI), to produce the corresponding -CO-NH_2, -CO-TETA, -CO-Lysine and -CO-PEI, respectively. Both TETA and PEI provide additional basic sites for side chain protonation and they have the potential for additional reduction of negative charges. Controlled carboxyl-modification, therefore, can lower the net negative charge on the enzyme, while decorating the surface with strongly polar, amide groups. All 12 carboxyl-modified enzyme derivatives reported here, showed increased stability, and stabilities correlated with the extent of charge reduction at the enzyme-water interface. Details of our investigations are presented.

1.3 Experimental

1.3.1 Materials: Glucose oxidase (GO, *Aspergillus niger*), peroxidase type 1 from horseradish (HRP), bovine met-hemoglobin (Hb), triethylenetetraamine (TETA), L-lysine, NH_4Cl, glucose, sodium phosphate, NaCl, acetonitrile, PEI (mol. wt. 2000) and p-nitrophenyl acetate were purchased from Sigma-Aldrich Co (St. Louis, MO). Bovine carbonic anhydrase (CA) from US biological (Swampscott, MA) and N-(3-dimethlaminopropyl)-N-ethylcarbodiimide (EDC) from TCI America (Portland, OR).

1.3.2 Chemical Modification of Enzymes: Surface groups of enzymes were modified by reacting the carboxyl functions of enzymes with appropriate amines by adopting reported procedures.[19] (*25*). GO (3 mg/ml) in deionized water (DI) was stirred with TETA (20 mM, pH adjusted to 5) for half an hour followed by the addition of EDC (10 mM). The mixture was stirred for four hours at room temperature and unreacted EDC, TETA and other byproducts were removed by dialysis against phosphate buffer (K_2HOP_4 (10 mM), NaCl (50 mM) pH 7.2). This approach was also used for enzyme modification with other amines. The degree of modification was carefully controlled by adjusting amine concentration, pH of the reaction mixture, enzyme concentration and the reaction time until all the natural enzyme has been consumed to form the modified enzyme. These details are collected in **Table 1.1**. Modified enzymes were examined by native agarose gel elctrophoresis[21] and SDS PAGE[22] for purity, charge modification and for the presence of any crosslinked products.

Table 1.1. Reaction conditions used for the bioconjugate preparation. Optimized concentrations of amines (mM) and enzymes (2 mg/ml) (pH 4.5 or 5.0) in K_2HPO_4 (10 mM), NaCl (10 mM) at 25 ^{0}C. Reaction time was 4 hours.

Enzyme /Amine Used (2 mg/ml)	NH_4Cl pH 4.5	TETA pH 5.0	PEI pH 5.0	L-Lysine pH 5.0
Glucose oxidase	100 mM	20 mM	1 mM	100 mM
Carbonic anhydrase	200 mM	20 mM	NA	200 mM
Hemoglobin	200 mM	20 mM	NA	200 mM

1.3.4 Agarose Gel Electrophoresis: Native agarose gel electophoresis was performed using horizontal gel electrophoresis apparatus (Gibco model 200, Life Technologies Inc, MD) and agarose (0.5% w/w) in Tris acetate (40 mM) pH 7.2 buffer was used. Modified enzymes were loaded with 50% loading buffer (50% v/v glycerol and 0.01% w/w bromophenol blue). Running buffer used for all the samples was Tris acetate (40 mM) pH 7.2, and samples have been spotted into wells placed at the middle of the gel so that the enzyme could migrate toward the negative or the positive electrode depending on its net charge at pH 7.2. A voltage of 100 V was applied for appropriate duration, which depended on the enzyme and the extent of reaction. Gels were stained overnight with 10% v/v acetic acid, 0.02% w/w Coomassie blue and destained in 10% v/v acetic acid over night.

1.3.5 SDS PAGE: The purity and the presence of crosslinked products of the bioconjugates were also assessed using SDS PAGE by following a reported method.[22] After synthesis, following dialysis, enzyme samples were completely dried in a SpeedVac (Savant Speedvac concentrator, Savant Inc, NY) for 2 h, and 24 μl of loading buffer (SDS (7% v/v), glycerol (13% v/v), Tris-HCl (50 mM), mercaptoethanol (2 % v/v) and bromophenol blue (0.15% v/v) pH 6.8) were added to dissolve enzymes. The mixture was heated for 60 seconds in boiling water and sample (8 μl) was loaded into 9% acrylamide gel containing separating and stacking gels. The separating gel contained acrylamide, gel buffer, 80% glycerol, 10% ammonium per sulfate (APS) and TEMED (N, N, N, N-tetramethylethylenediamine), and deionized water. Stacking gel contained

acrylamide, gel buffer, deionized water, 10% APS and TEMED. Potential of 60 V was applied until the dye passed through the stacking gel and after that the voltage increased to 110 V for an additional 2 h. Gel was first stained for 1 h with stain 1 which contained 20% v/v 2-propanol, 20% v/v acetic acid, 0.02% w/w Coomassie Blue and staining was continued with stain ll which contained 20% v/v acetic acid. 0.02% m/m Coomassie Blue for additional 24 h. Then, gels were destained in 10% acetic acid for 24 h and scanned using CanonScan Lide200 scanner. To estimate the molecular weights, a standard curve was plotted by using the mobilities of known MW standards. NIH image v1.1.6 software (NIH, U. S. A) was used to quantify the per cent yield of dimerization, if any.

1.3.6 Determination of the pI of Bioconjugates*:* Agarose gel electrophoresis was performed at specific pH values of the running buffer, in order to determine the isoelectric points of the bioconjugates.[21] Based on the assumption that the size of the modified enzyme is nearly the same as unmodified enzyme, which is a reasonable assumption given the small size of the polyamines that are being used for modification, the pI values were evaluated. Charge on the enzyme is proportional to its electrophoretic mobility, and when the buffer pH corresponds to the pI of the sample, enzyme will have a net charge of zero with no electrophoretic mobility in the gel.

1.3.7 Determination of amount of TETA reacted using Cu^{+2} titration*:* The number of TETA molecules reacted per GO molecule was estimated using TETA-Cu complexation reaction. After the reaction between TETA and GO in the presence of EDC, unreacted TETA was dialysed into DI water. Unreacted TETA was complexed with excess Cu^{+2} for 0.5 h and the TETA-Cu absorption was measured at 260 nm[23]. Amount of unreacted TETA was determined by using a previously constructed calibration plot. From the initial mole numbers of TETA and unreacted TETA, the number of moles of TETA reacted per mole of GO was estimated.

1.3.8 Circular Dichroism (CD) Studies: The CD spectra were recorded on a JASCO J-710 spectropolarimeter using 4 μM enzyme dissolved in K_2HPO_4 (10 mM), NaCl (50 mM), pH 7.2 buffer and the baseline obtained with buffer alone.[24] While collecting data, step resolution was kept at 0.2 nm per data point and scan speed was 50 nm/min. Sensitivity was kept at 20 millidegrees with a bandwidth of 1.0 nm. Each sample was scanned from 190 to 260 nm and an average of four accumulations was recorded using 0.05 cm path length cuvette.

1.3.9 Enzyme Activity Studies: Activities of natural and modified lipase were determined using p-nitrophenyl acetate as the substrate by following reported methods.[25] To the enzyme solution (2 μM) in phosphate buffer (K_2HPO_4, 10 mM), NaCl (50 mM), pH 7.2, p-nitrophenyl acetate (1.6 mM in 5% acetonitrile) was added, and product formation has been monitored (absorbance at 410 nm) as a function of time. The kinetic data have been analyzed to calculate specific activities from the initial rates of these reactions.

GO activity was determined by following a reported method.[26] To GO (1 μM), in phosphate buffer, was added a solution of glucose (0.2 mM), guaiacol (10 mM) and horseradish peroxidase (2 μM). Oxidation of the substrate was monitored by recording the product absorbance at 470 nm as a function of time.

Peroxidase-like activity of Hb was determined by adopting a reported method[28] . To Hb (0.5 μM, in phosphate buffer) was added o-methoxyphenol (2.5 mM) and H_2O_2 (1 mM). and product formation monitored at 470 nm as a function of time.

Activities of natural and modified CA were evaluated by a reported method, with minor modifications.[28] To CA (2 μM) in Tris buffer, p-nitrophenyl acetate (1.6 mM in 5% acetonitrile) was added and the rate of product formation has been recorded by monitoring absorbance at 410 nm as a function of time.

In all activity studies, the kinetic traces were plotted using Kaleidagraph (V. 4.0) to determine initial rates and specific activities. Each experiment was repeated three times and data have been averaged.

1.3.10 Half-Lives of Enzymes: Enzyme stabilities were measured by monitoring their activities as a function of time. Modified and unmodified enzyme conjugates were stored at 30 ^{0}C and activities have been measured at room temperature at intervals of 24 hrs until the activity is closer to zero. All activity studies performed in phosphate buffer (K_2HPO_4 10 mM, NaCl 50 mM, pH 7.2), according to procedures described above. Specific activities vs time were plotted (average of three measurements) and time taken to reduce the activity of the bioconjugate to half of its original activity (half-life) has been estimated from these data.

1.3.11 Differential Scanning Calorimetry (DSC): Thermograms of natural and modified enzymes were recorded using a 6100 Nano II differential scanning calorimeter (Calorimetry Sciences Corporation, CSC Utah) by following a previously reported procedure.[29] All solutions were degassed 10 minutes prior to loading and constant pressure of 3 atm was applied to prevent solvent evaporation during the scan. Baseline was recorded with buffer versus buffer scans, where both cells were loaded with 10 mM Na_2HPO_4 50 mM NaCl pH 7.2 buffer. The cells were first equilibrated for 10 minutes at 20˚C and scanned from 20 – 100 ˚C at a scan rate of 2 ˚C $minute^{-1}$. After the buffer scan, sample cell was emptied, washed, and filled with the enzyme solution (4 μM) in phosphate buffer (10 mM Na_2HPO_4 50 mM NaCl pH 7.2). Heating and cooling scans were recorded using the same parameters, as the buffer versus buffer scan. During data processing, buffer scan data were subtracted from sample scan and normalized to enzyme concentration. The extent of reversibility of the transition was checked by repeating the heating scan after the first cycle, and none of the samples indicated reversible denaturation. Hence, only the model independent parameters such as denaturation temperature (T_m) and $\Delta H_{denaturation}$ (area under the curve) were calculated from the DSC data.

1.4 Results

We tested the hypothesis that charge-charge repulsion contributes significantly to enzyme instability (coulomb explosion), and therefore, controlled carboxyl-modification with amines could reduce charge and thereby stabilize the native state of the enzyme. Our data show that, when modifications are few, mild, sparse, and controlled, this approach could produce modified enzymes with increased isoelectric points (pI) and enhanced stabilities. The half lives of the modified enzymes correlated with the net charge on the enzyme, and this provided a physical insight into controlling enzyme stability by chemical modification.

1.4.1 Synthesis of Chemically Modified Enzymes*:* Covalent coupling of amines to the carboxyl functions of enzymes was carried out under mild conditions by carbodiimide chemistry (**Scheme 1.1**). Coupling with ammonia, L-lysine, triethylenetetramine (TETA) and polyethyleneimine (PEI, mol. wt., 2000), under specific conditions, produced enzymes with reduced negative charge. Care was taken not to crosslink the enzymes by using excess of amine and by limiting the reaction time.

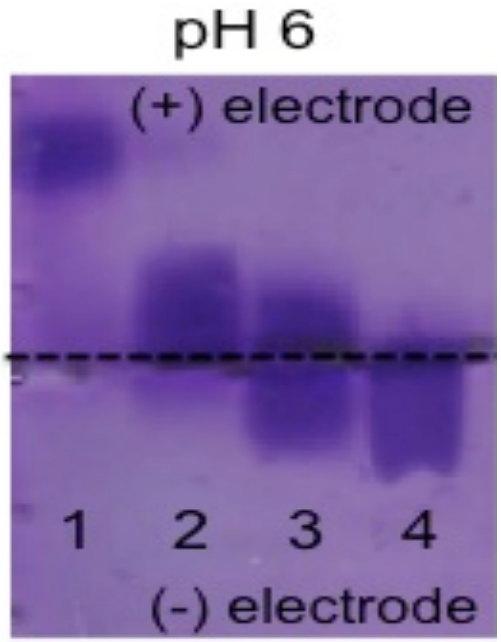

Figure 1.1: Agarose gel of GO (lane 1) and GO modified by reaction with L-lysine, NH_4Cl and TETA (lanes 2, 3 and 4, respectively, 40 mM Tris acetate, gel has been run at pH 6,) and samples were loaded into wells at the middle of the gel (dotted line).

Reaction progress was monitored by agarose gel electrophoresis, where the protein is subjected an electric filed. Net charge on the enzyme is proportional to the distance of its migration in the agarose gel and the direction of migration is indicative of the sign of charge. For example, GO is negatively charged at pH 6, and it migrated toward the positive electrode (**Figure 1.1**, lane 1). Chemical conversion of a portion of its carboxyl groups to amides with L-lysine, ammonia or TETA resulted in GO-derivatives that migrated less toward the positive electrode (lanes 2 and 3) or started to migrate toward the negative electrode (lane 4). Thus, reaction progress has been monitored using agarose gel electrophoresis and the reaction was stopped when the charge is adjusted as desired (**Figure 1.1**).

Since the samples were spotted at the center of the gel, the enzyme could migrate toward the anode or the cathode depending on the sign of its charge, at the pH of the buffer used for electrophoresis. The gel obtained at pH 6 (**Figure 1.1**) shows complete conversion of GO to the modified enzyme, and none of the lanes indicated unreacted GO. Thus, net charge on GO diminished in the case of lane 2 and charge on modified GO in lane 4 indicated a net positive charge. The attachment of amines can potentially introduce a number of positive charges per conjugation event, and this provided a simple method to systematically adjust enzyme charge at a given pH, as desired.

In a similar fashion, controlled chemical modification with the above four amines was carried out with CA and Hb, and in all cases the reaction conditions were optimized (**Table 1.1**) for the complete conversion of the unmodified enzyme to the corresponding cationized enzymes. The products were examined in agarose gel electrophoresis (**Figure 1.2**), and amidation was stopped when all the starting

material has been consumed. Next, we examined the net charge of the modified enzyme as a function of pH to estimate the isoelectric points of these bioconjugates.

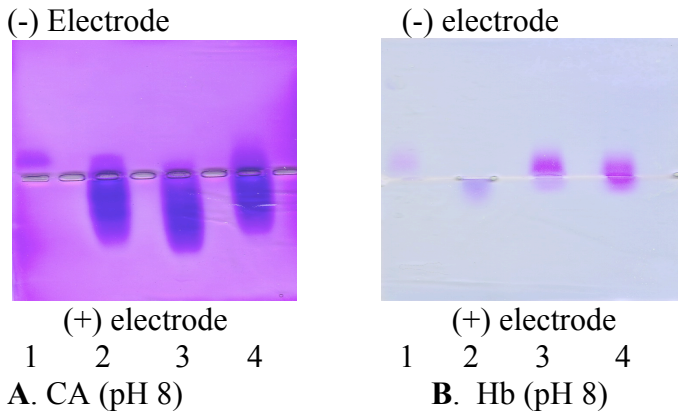

Figure 1.2. A. Agarose gel of unmodified carbonic anhydrase (lane 1), and modified CA, (lanes 2, 3, 4) synthesized with L-lysine, TETA and NH_4Cl, respectively according to the conditions listed in Table 1. (running buffer, 40 mM Tris acetate, pH 8). **B**. Agarose gel of unmodified hemoglobin (lane 1), and modified hemoglobin, (lanes 2, 3, 4) synthesized with TETA, L-lysine and NH_4Cl respectively according to the conditions listed in Table 1. (running buffer, 40 mM Tris acetate, pH 8).

1.4.2 Characterization of Modified Enzymes: The newly produced enzyme derivatives are characterized by a battery of biophysical and biochemical techniques, prior to measuring their thermodynamic stabilities. These included the determination of isoelectric points, circular dichroism spectra, and activity studies.

1.4.2.1 Isoelectric Points and Charge determination*:* We further characterized modified enzymes by determining their isoelectric points (pI), the pH where the enzyme net charge is zero. When pH of the running buffer is the same as the pI of the enzyme, net charge on the enzyme must be zero, and therefore, the sample should not move out of the wells, when the electric field is applied. On the other hand, when the net charge on the enzyme is not zero at a given pH, it will migrate out of the wells either toward the positive electrode or the negative electrode depending on the sign and magnitude of its charge. Thus, gel electrophoresis is a simple and quick method to determine the pI values by running a set of agarose gels at specific pHs.

Accordingly, we ran multiple agarose gels at specific pHs and a representative set of gels are shown in **Figure 1.3**, where the sample is loaded into the wells at the center of each gel (the thin dotted line).

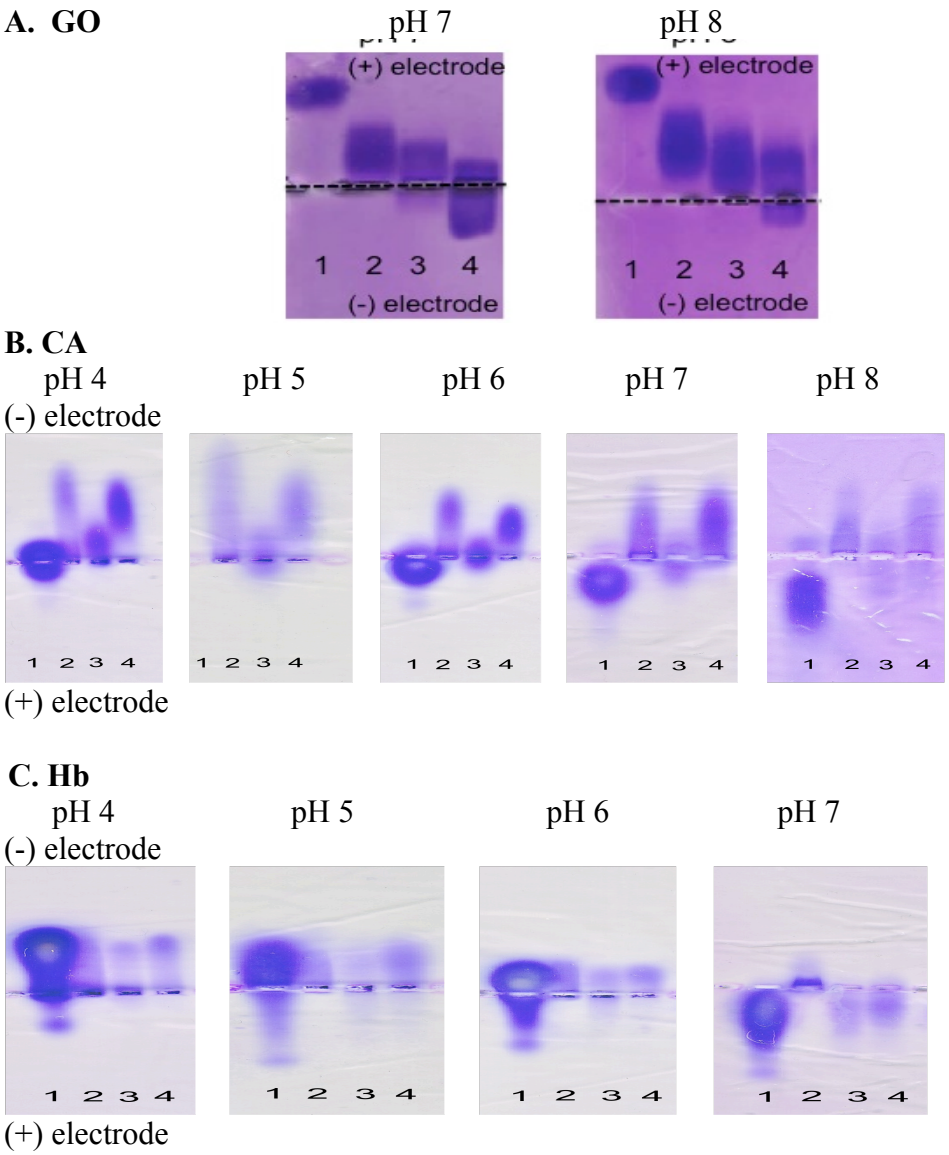

Figure 1.3A. Agarose gels of modified GO (lane 1) and GO modified by reaction with with L-lysine, NH_4Cl and TETA (lanes 2, 3 and 4, respectively, 40 mM Tris acetate, gels were run at specific pHs, as indicated). **B.** Agarose gels of modified CA in 40 mM Tris acetate at room temperature. In each gel, lane 1 contained to unmodified CA, lane 2 is CA modified with 20 mM TETA and lanes 3 and 4 were CA modified with 200 mM L-lysine and 200 mM NH_4Cl, respectively. **C**. Agarose gels of modified Hb in 40 mM Tris acetate at room temperature. In each gel, lane 1 contained unmodified Hb, lane 2 is hemoglobin has been modified with 20 mM TETA at pH 5 and lanes 3 and 4 were Hb modified with 200 mM lysine (pH 5) and 200 mM NH_4Cl (pH 5), respectively.

Lane 1 in all gels contained unmodified enzyme while lanes 2-4 contained enzymes modified with L-lysine, NH_4Cl and TETA, respectively. The pI values were deduced from these gels by monitoring the distance of migration in each lane as a function of the pH of the buffer used for electrophoresis. For example, GO, CA and Hb indicated pI values of 4, 6, and 7 which are in good agreement with literature values of 4.2, 5.6 and 7, respectively.[30] Lanes 2-4 in each gel correspond to enzymes modified with L-lysine, NH_4Cl and TETA, respectively. The pI values estimated from these gels are collected in **Table 1.2** and the pI values are to be compared with the corresponding pKa values of amines used, L-lysine (2.2, 10.53), ammonia (7) and TETA (3.37, 6.62, 9.09, 9.69), respectively[31]. This small set of modified enzymes (12) along with the 3 unmodified ones, with pI values over a wide range (4-10), are suitable to test the above hypothesis.

Table 1.2. Isoelectric points of modified and unmodified enzymes as estimated by agarose gel electrophoresis.

Enzyme/Amine Used	Unmodified	L-Lysine	NH_4Cl	TETA
Glucose oxidase	~4[32] ± 0.25	5 ± 0.5	6 ± 0.5	7 ± 0.7
Carbonic anhydrase	5.6[33]	6-8	> 10	> 10
Hemoglobin	6.5[34]	7-8	7-8	> 8

The net charge on chemically modified GO samples were estimated from the distance of migration of that sample, when compared to that of unmodified GO and from the known charge of unmodified GO at the corresponding pH[35] (**Figure 1.4**).

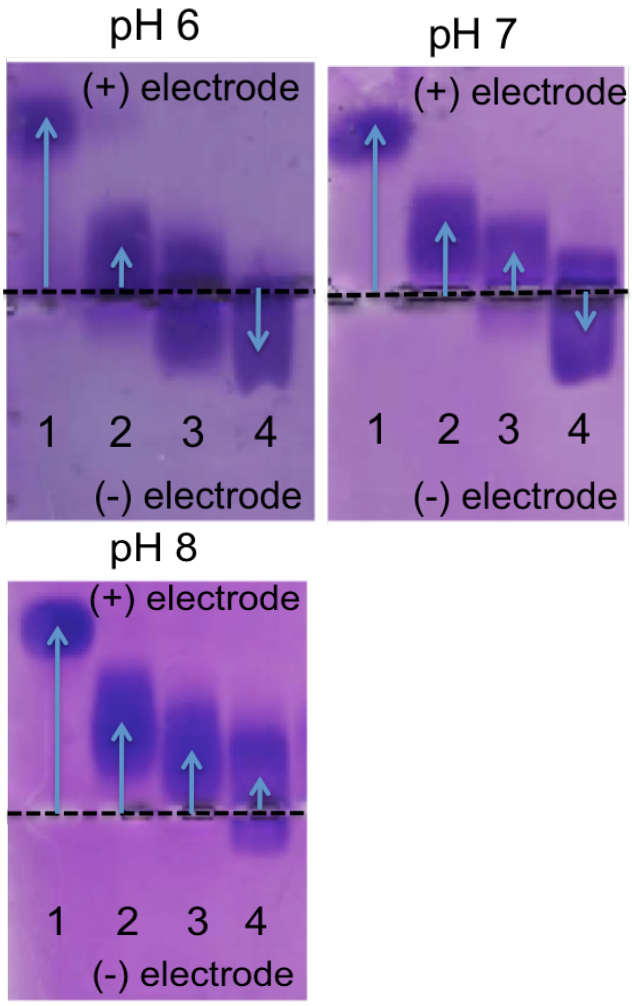

Figure 1.4. Agarose gels of GO (lane 1) , GO-Lysine (lane 2) , GO-NH_4Cl (lane 3) and GO-TETA (lane 4) in 40 mM Tris acetate, gels were run at specific pHs, as indicated.When pI of the protein equals to the pH of the running buffer, protein does not move out of the well, which are located in the middle of the gel. Mid point of each protein band as indicated was taken as the distance migrated in the agarose gel. Distance and charge relationship of the modified GO derivatives, relative to the distance and charge of unmodified GO, were estimated using imageJ 1.46r software from NIH and average charge at pH 7 was tabulated in **Table 1.3**

The pI values of GO conjugates obtained from agarose gel electrophoresis were confirmed by plotting the net charge on the GO derivative as a function of the pH. The pI of each conjugate was extracted from the y intercept of the linear plot, which signifies the net charge on the conjugate is zero. The observed pI value of GO (3.75) is in agreement agreed with the reported value of 3.9 (**Figure 1.5**).

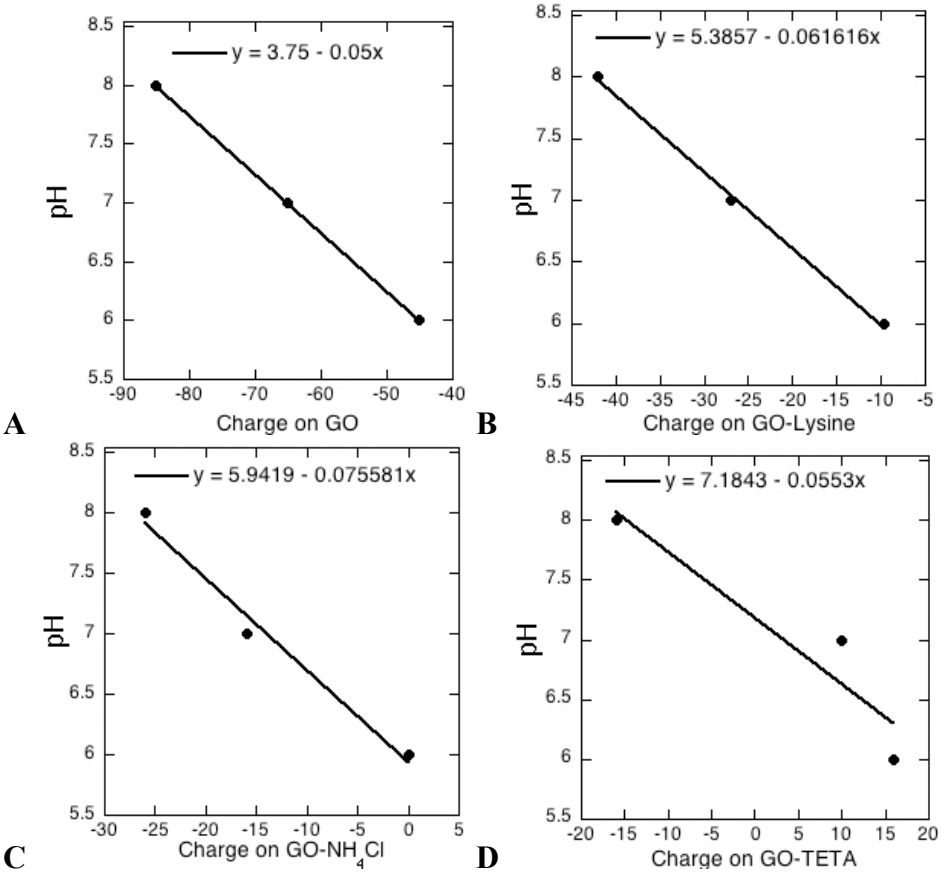

Figure 1.5. Plot of pH vs charge of (A) GO, (B) GO-Lysine, (C) GO-NH_4Cl and (D) GO-TETA. The Y-intercept of each is the corresponding isoelectric point (pI).

The net charge on each sample, as estimated above, was used to calculate the number of COOH groups that have been modified, in each case. For example, GO-L-lysine had a net charge of -27, reduced from -65, due to the covalent linking of L-lysine to the COOH groups of GO. According to the known pKa values of L-Lysine (2.2, 10.53), both its amine and COOH groups will be ionized and hence, each L-lysine attachment would lower the charge by one unit. Thus, charge reduction from -65 to -27 would require the reaction of 38 COOH groups (65-27=38) with L-Lysine. Similarly, the number of COOH groups modified by the attachment of NH_3 and TETA were determined using corresponding pKa values of ammonia (7) and TETA (3.37, 6.62, 9.09, 9.69) to be 50 and 30, respectively (**Table 1.3**). The number of COOH groups modified by TETA, obtained from gel electrophoresis was cross checked by the Cu(II) titration method. TETA that was left behind after the reaction was separated by dialysis and titrated with Cu(II). From the absorbance of the TETA-Cu complex at 260 nm and a previously determined calibration graph, the amount of unreacted TETA has been estimated. The value obtained from Cu(II) titration is 31 ± 6 which is comparable to 30, the value obtained from the gel electrophoresis.

Table 1.3 Isoelectric points, net charge at pH 7 and the number of carboxylic acid groups modified for each modified GO sample.

Sample	Isoelectric point (pI)	Enzyme charge at pH 7	Number of COOH groups modified
GO	3.9	-65	0
GO-100mM L-lysine	5.4	-27	38 ± 4
GO-100 mM NH_4Cl	5.9	-16	50 ± 6
GO-20 mM TETA	7.2	+10	30 ± 6

The chemically modified enzymes were further examined by SDS PAGE to make sure that the chemical modification did not produce significant amounts of enzyme-enzyme cross links.

1.4.2.2. SDS PAGE: Chemical modification with multifunctional amines such as L-lysine, TETA, or PEI could result in the crosslinking of two or more enzyme molecules, and hence, the reaction mixture has been examined by SDS PAGE to examine the extent of crosslinking, if any (**Figure 1.6**). Lane one in each gel contained the molecular weight markers in kD, lane 2 contained unmodified enzyme, and lanes 3-6 contained enzymes modified with TETA, PEI, NH_4Cl and L-lysine, respectively. Modified GO, for example, indicated predominantly the monomeric form. There has been some cross linking in specific cases, but extent of crosslinking has been minimal.

A. GO modification

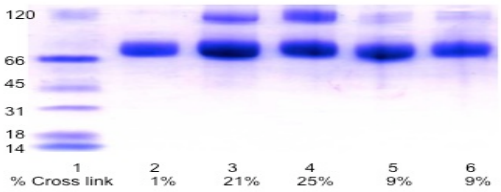

B. Hb modification

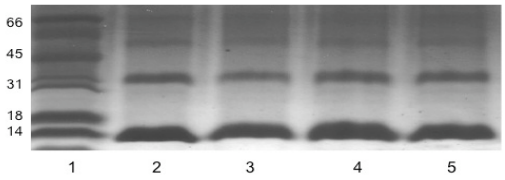

C. CA modification

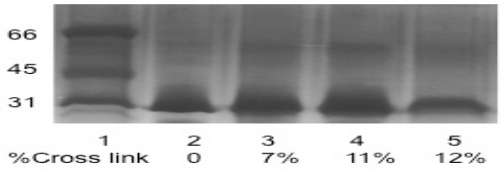

Figure 1.6. SDS PAGE of **A.** the modified glucose oxidase. Lane, 1 is the molecular weight marker and lane 2 is unmodified glucose oxidase. Lanes 3 to 6 are glucose oxidase samples modified with TETA, PEI, NH_4Cl and L-lysine, respectively. The extent of crosslinking in each of these lanes is indicated under the gel; **B**. modified hemoglobin, Lane 1 is the molecular weight marker and lane 2 is unmodified hemoglobin. Lanes 3 to 5 are modified carbonic anhydrase, synthesized using L-lysine, TETA and NH_4Cl, respectively; **C**. modified carbonic anhydrase, Lane 1 is the molecular weight marker and lane 2 is unmodified carbonic anhydrase. Lanes 3 to 5 are modified carbonic anhydrase, synthesized using L-lysine, TETA and NH_4Cl, respectively.

1.4.2.3 CD Studies: The CD spectra in the deep UV region (190-250 nm) of enzymes are characteristic of their secondary structure,[36] and significant decreases in the intensities of these CD bands or shifts in the peak positions would indicate of loss of secondary structure, and secondary structure is critical to maintain biological activities of modified enzymes.

The CD spectra of GO modified with NH_3, TETA and PEI are shown in **Figure 1.7**, and they are comparable to the CD spectrum of unmodified GO (black line) recorded under the same conditions of concentration, path length, buffer and pH. These data clearly show that there have been no significant changes in the secondary structure of modified GO.

Similarly, the CD spectra of modified CA and Hb samples are compared with those of the corresponding unmodified proteins (**Figure 1.8**), and the spectral shape and intensities at 210 and 222 nm are comparable. The molar ellipticities of the samples are collected in **Table 1.4** for comparison. The data show that careful, controlled chemical modification can be nearly benign. Next, we examined activities of modified enzymes to evaluate the extent of their activity retention despite these small changes in the CD spectra.

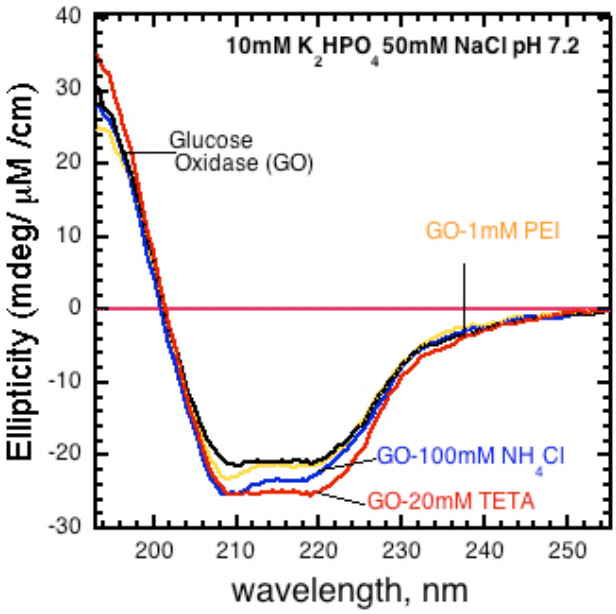

Figure 1.7. The far UV CD spectra of (**A)** glucose oxidase (black line) before and after modification with 20 mM TETA (red line), 100 mM NH_4Cl (blue line) and 1 mM PEI (Green line); and note that the CD spectra of modified GO are similar to that of the corresponding GO, which indicates retention of native-like structure to a significant extent.

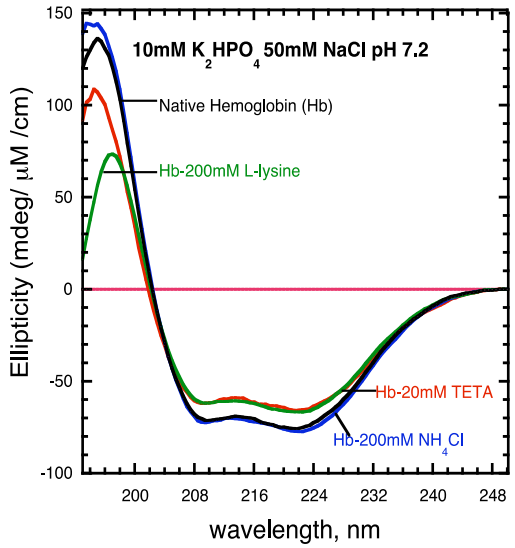

A.Hb

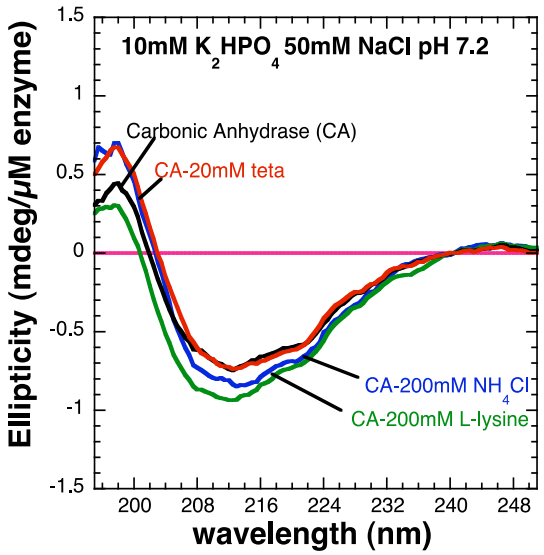

B.CA

Figure 1.8. Far UV CD spectra of **A**. carbonic anhydrase and **B**. hemoglobin before and after modification with 20 mM TETA (red line), 200 mM NH_4Cl (blue line) and 200 mM L-lysine (Green line) recorded in 10 mM K_2HPO_4 50 mM NaCl pH 7.2 buffer. Note that in all cases, the CD spectra of modified enzymes have significant overlaps with those of the corresponding unmodified ones.

Table 1.4. Molar ellipticities (per μM per cm) of natural and modified enzymes. Enzymes used (4 μM) were in K_2HPO_4 (10 mM) NaCl (10 mM) pH 7.2 buffer.

Enzyme/Amine Used	Unmodified	NH_4Cl	TETA	PEI	L-Lysine
Glucose oxidase					
208 nm	-21	-25	-25	-23	NA
210 nm	-20	-21	-24	-20.6	
Hemoglobin					
208 nm	-70	-70	-60.7	NA	-60.7
220 nm	-74	-77	-65		-65
Carbonic anhydrase					
197 nm	8.6	13.7	13.5	NA	6.0
212 nm	-14.6	-16.3	-14.7		-18.5

1.4.2.4.Activity Studies: The activities of natural and modified GO samples are monitored using glucose as the substrate (**Figure 1.9A**). Addition of glucose to a mixture of GO, HRP and guaiacol in phosphate resulted in rapid generation of the oxidation product, which has characteristic absorption maximum at 470 nm. The data show the facile oxidation of guaiacol by hydrogen peroxide catalyzed by HRP, where hydrogen peroxide has been produced by the catalytic oxidation of glucose by ambient oxygen, catalyzed by GO.

The initial rates of substrate conversion to the products by GO, Hb and CA and their derivatives were extracted from the kinetic traces of activities. Only in the case of amine modified Hb, the activity is decreased significantly. In all other cases, activities are comparable to those of the unmodified enzymes. Thus, chemically modified samples were characterized by a number of methods and the data show that modification was nearly benign to alter the net charge without significantly altering native-like structure or biological activities.

1.4.3 Evaluation of Enzyme Stability as a Function of pI values: This small set of enzymes was used to test the hypothesis that enzyme stability is directly related to enzyme charge by two distinct approaches.

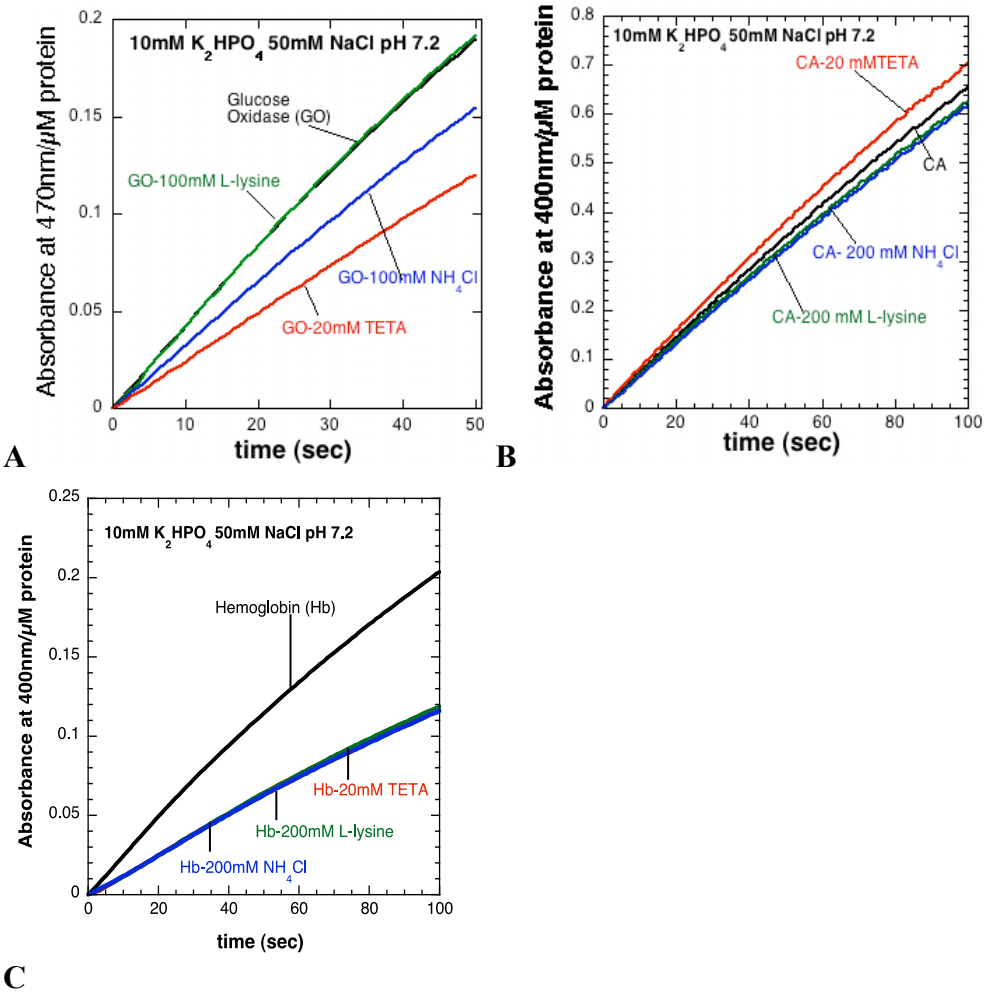

Figure 1.9. Comparison of activities of: **A**. GO **B. CA** and **C.** Hb before and after chemical modification. Activities were monitored using 1 μM protein solution in 10 mM K_2HPO_4 50 mM NaCl pH 7.2 buffer in room temperature according to the procedure explained in experimental section. The particular amines used for the modification are as marked in the graph.

1.4.3.1.Storage stability*:* Storage stabilities of enzymes are usually low, and they often require to be stored under refrigerated conditions. To check for improvements in enzyme stabilities predicted by the above hypothesis, we examined activities of our samples after storing them at 30 ˚C pH 7.2, phosphate buffer, for extended periods of time. Specific activity vs storage time was plotted for each sample (**Figure 1.10**) and time taken to reduce the activity by half (half life) has been estimated from these plots.

The half lives of modified GO samples, for example, are plotted as a function of their isoelectric points which showed substantial improvement, as the pI increased from 4 to ~7 **(Figure 1.11)**. The stabilities have been monitored for nearly 350 h. Note that maximum storage stability was achieved for GO-TETA derivative, with a pI of ~7, among all the GO-derivatives. The increase is measured as $(\tau-\tau_o/\tau_o)$ >500% where τ_o is half life of unmodified enzyme and τ is the maximum half life of the modified enzymes. The observed trend is GO-TETA > GO-L-lysine > GO-L-Lysine >> GO For example, GO lost 50 % of its initial activity after 50 h and all the modified GO samples indicated half lives >250 h. The lowest stability was noted with GO which has a pI of 4 as well as the highest charge at pH 7. The highest half life was observed with TETA modified GO, with a pI of ~7 and least amount of charge at pH 7. Therefore, GO-TETA had the lowest net charge and the longest half life with a 500% increase in half life over the unmodified GO.

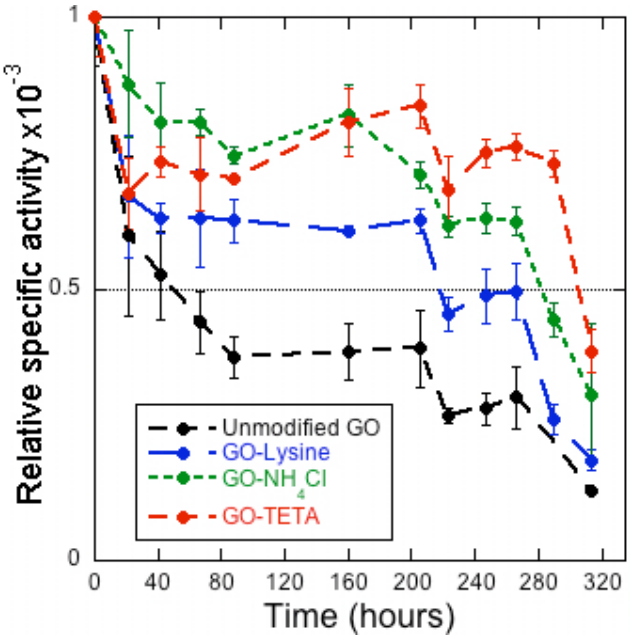

Figure 1.10: The plot of relative specific activities (Relative to the initial activity) of unmodified and modified glucose oxidase vs time in hours . Time taken for the relative specific activity to be half was take as the half life of each sample. Note that the half life of unmodified GO is around 50 hrs and all the modified GOs have half life above 160 hours.

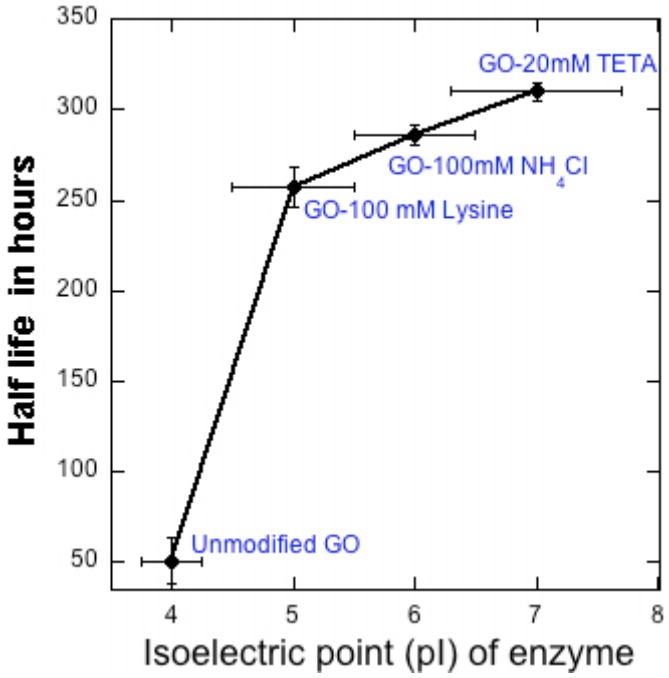

Figure 1.11: The plot of half life in hours vs isoelectric point of GO and modified GO. Note that the half life of unmodified GO is around 50 h and highest half life was >300 h, >500% improvement.

Improvements in storage half lives were also observed with Hb derivatives when compared to that of Hb (**Table 1.5**). Stabilities are in the order Hb-L-Lysine > Hb-NH_3 > Hb-TETA > Hb over a range of 57 for Hb (pI 6.5) to 73 h for Hb-L-Lysine (pI of ~7.5). The maximum increase in half life for Hb derivatives is ~28%, not as much as in the case of GO derivatives (>500%). In contrast, all CA derivatives indicated storage half lives that are essentially the same, within our experimental error. The plots of half life vs isoelectric points of Hb and CA derivatives are shown in **Figure 1.12** for comparison.

Table 1.5: Half-lives of chemically modified and unmodified CA, Hb and GO in h. Enzymes used (1 μM) were in K_2HPO_4 (10 mM) NaCl (10 mM) pH 7.2 buffer. Enzymes were stored at 30 ^{0}C water bath and measure the activity at room temperature.

Enzyme/Amine Used	Unmodified	NH_4Cl	TETA	L-Lysine
Glucose oxidase	51 ± 12	286 ± 5	310 ± 5	257 ± 11
Hemoglobin	57 ± 0.3	70 ± 0.1	60 ± 0.1	73 ± 0.2
Carbonic anhydrase	45 ± 0.1	46 ± 0.1	47 ±1	46 ±0.1

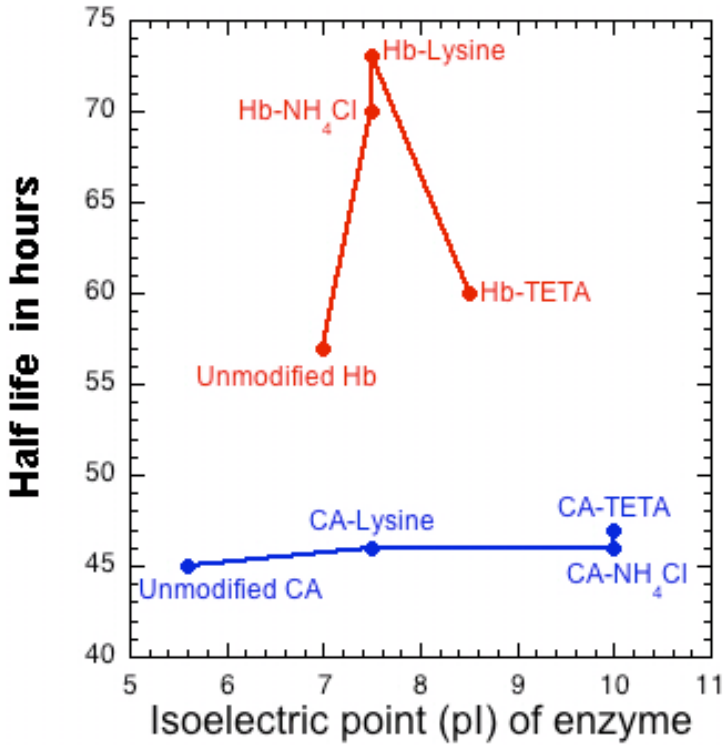

Figure 1.12: The plot of half life vs isoelectric point of hemoglobin and carbonic anhydrase. Note that the highest half life among hemoglobin samples were observed with lysine modified Hb which has pI around 7.5. Amine modified carbonic anhydrase samples do not show any correlation between the half life and isoelectric point.

These data clearly show that the general trend of increase in stabilities of all derivatives is: GO-derivatives >>> Hb-derivatives > CA-derivatives. Overall, the data show that half lives of both GO and Hb derivatives increased by modification, and these roughly correlated with the extent of reduction in the net negative charge of these molecules. Encouraged by these data, we next examined the thermal stabilities of the bioconjugates by differential scanning calorimetry for further insight.

***1.4.3.2 Thermodynamic stability**:*

Differential scanning calorimetry is a direct method to determine the denaturation temperature (T_m) and the corresponding enthalpy of denaturation (ΔH), even when the thermal transitions are not reversible. Comparison of DSC thermograms of GO and modified GO are shown in **Figure 1.13**. Thermograms of modified GO are consistently shifted to higher temperatures by ~7˚C, when compared to that of GO (black line). For example, the peak transition temperatures (Tm) for these derivatives increased from 63 ˚C for GO to 70 ˚C for GO-NH_3. These changes are nominal but they are in the right direction, and all three derivatives indicated higher Tm values than the unmodified GO.

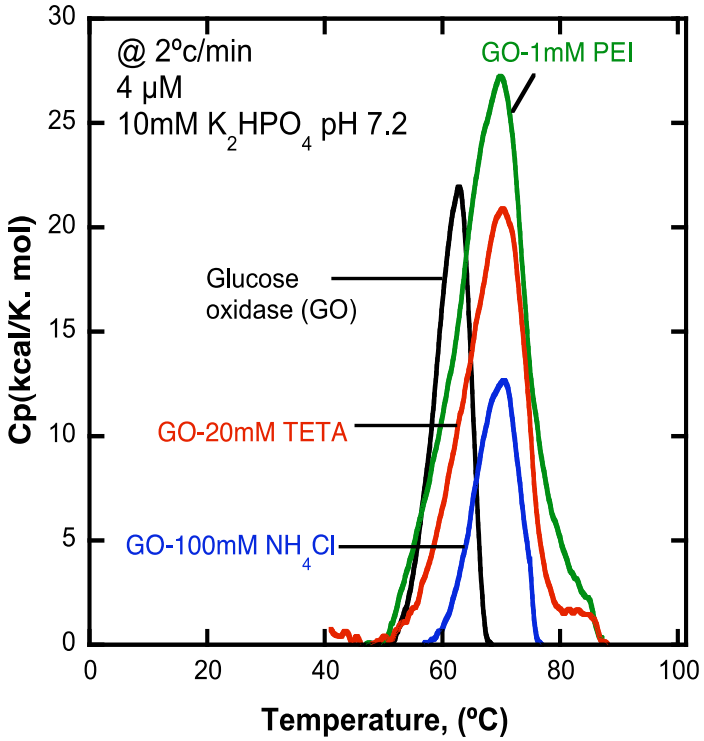

Figure 1.13. Thermograms of modified GO, recorded in 10 mM K_2HPO_4 pH 7.2, at a scan rate of 2 ˚C/min. GO (black), GO-TETA (red), GO-NH_3 (blue) and GO-PEI (green).

The DSC thermograms of Hb and CA derivatives were also recorded to test the influence of chemical modification on thermal stabilities (**Figure 1.14**). The peak transition temperatures for Hb-derivatives and CA-derivatives remained essentially the same as those of the corresponding unmodified proteins (**Table 1**). Thus, the storage half lives are much more sensitive to enzyme modification than the denaturation temperatures.

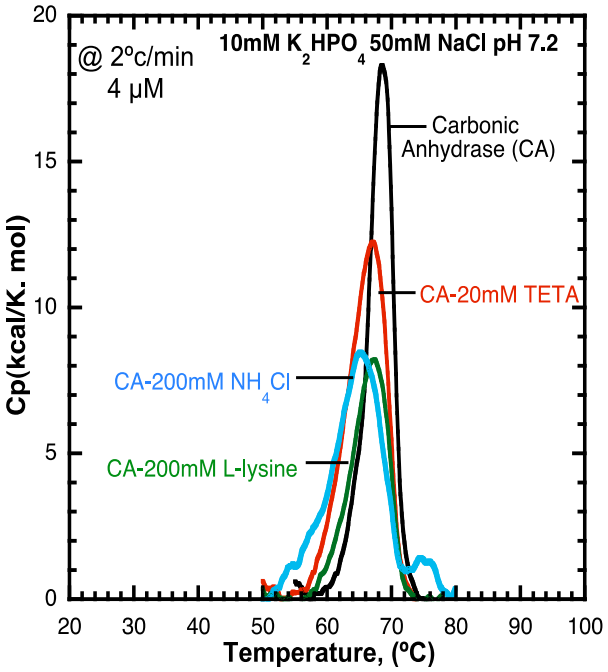

A. CA

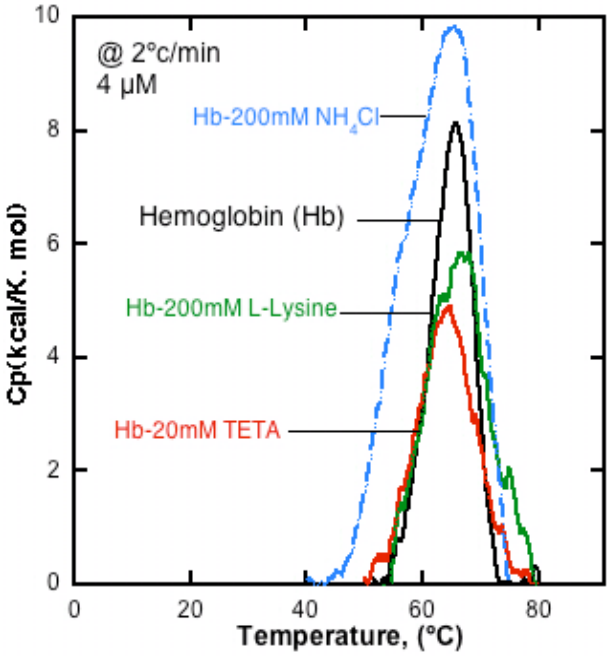

B. Hb

Figure 1.14. Molar heat capacity profile of CA (**A**) and hemoglobin **(B)**, unmodified (black), modified with TETA (red), NH_4Cl (blue) and L-lysine (green) in corresponding buffers at a scan rate of 2 ˚C/min.

The DSC curves were further analyzed to estimate the integrated area under the curve (ΔH), and the corresponding enthalpies of denaturation ($\Delta H_{denaturation}$) are collected in **Table 1.6**. The denaturation enthalpies of the bioconjugates are comparable to those of the unmodified enzymes or larger, in specific cases. With TETA-modified GO, for example, the denaturation enthalpy increased substantially, while in case of TETA-modified Hb the lowest value has been noted. In all other cases, the differences between the modified and unmodified enzymes are not substantial.

Table 1.6. Enthalpy of denaturation ($\Delta H_{denaturation}$ in kcal/mol) and denaturation temperatures (in parenthesis/˚K) of unmodified and modified enzymes. GO and CA samples (4 μM) were in K_2HPO_4 (10 mM) NaCl (10 mM) pH 7.2 while Hb samples (4 μM) have been examined in K_2HPO_4 (10 mM).

Enzyme /Modifier	Unmodified	NH_4Cl	TETA	L-Lysine	PEI
Glucose Oxidase	221 (63 ± 1.0)	170 ± 46 (70 ± 1.1)	332 ± 46 (69 ± 1.0)	NA	330 ± 112 (69 ± 1.0)
Hemoglobin	74 (66 ± 0.14)	87 (65 ± 0.3)	60 (64 ± 1.0)	78 (66 ± 1.3)	NA
Carbonic Anhydrase	92 (69 ± 1.4)	88 (65 ± 2.0)	84 ± 18 (67 ± 0.35)	59 (67 ± 1.0)	NA

1.5 Discussion

Chemically engineered enzymes can provide a simple method to modify their surface residues, alter enzyme-water interface, and in turn, alter their structure, activities and stabilities. But the extents of these changes are not well documented. A clear understanding of the basis for these changes at the molecular level will be a major break through in obtaining control over types and extents of modifications required for the desired outcomes. The main focus in the area of chemical modification of enzymes, however, has been largely limited to the applications of the modified enzymes but not their stability or the underlying causes for their altered behavior.[38,39] In the current study, we have systematically altered the enzyme surface residues with increasing numbers of amines carrying increasing numbers of amine groups and examined their influence on key properties of modified enzymes. Carboxyl conversion to amides resulted in the elevation of enzyme pI values, and this is due to the removal of negative charge of each carboxyl group by converting it to the corresponding amide. Furthermore, in many cases, there are additional basic nitrogens which can be protonated at neutral pH, further reducing the net negative charge on the enzyme. Therefore, the increase in the pI depended on the amine used as well as the extent of modification carried out. Thus, enzymes with desired pI values can be readily obtained by choosing the appropriate amine and by stopping the reaction at the desired stage of charge reduction. Thus, enzyme charge at a given pH can be exquisitely controlled depending on the reaction conditions used.

The chemical modifications carried out are mild enough not to cause any significant structural changes in the enzymes, and structure retention is essential for the biological activities of the modified enzymes. Consistent with this idea, activity

studies show that essentially all modified enzymes retain their activity above 80% of the corresponding unmodified enzymes, except in the case of Hb-L-lysine, which retained about 60% activity. Note that both GO-NH_3 and CA-TETA indicated activities that are slightly greater than the corresponding unmodified enzymes.

Most significant feature of modified enzymes is that the storage stability has been improved substantially, particularly in the case of GO derivatives. The stabilities correlated strongly with the isoelectric points of the derivatives, and highest stability is achieved when the pI equals to the pH of the buffer medium used for measuring the stabilities. This implies that the stability is inversely correlate with the charge on the enzyme molecule and highest stability is obtained when the charge is close to zero. Thus, under these conditions, the electrostatic contribution for the unwinding of the protein is close to zero, and hence its contribution to denaturation is minimized. This physical insight is significant, and guided our design the reaction conditions to adjust the net charge on the derivatives.

In the case of Hb nd CA the influence of chemical modification is not as pronounced as in the case of GO, and this is because the net charge on the unmodified molecules is quite small. This is also indicated by the number of carboxyl groups present in Hb and CA which are much less than those of GO. Thus, the electrostatic contributions to the unfolding free energy of these enzymes are not significant at neutral pH. Nevertheless, the stabilities of these derivatives also showed small but definite improvements. Based on these observations, we predict that stabilities of Hb and CA derivatives at pH values far from the pI values of the unmodified proteins will be substantially better than the corresponding unmodified proteins. This hypothesis will be tested in future studies.

In the case of GO, the peak denaturation temperatures are distinctly improved but in the case of both Hb and CA they are not significantly different from those of the corresponding unmodified proteins, as explained above. One interesting observation was that a plot of T_m vs half life of chemically modified derivatives (**Figure 1.15**) indicated a strong correlation for GO derivatives but those of Hb and CA did not show any such correlation. GO-derivatives showed an increase in half lives as well as melting temperature (T_m) and T_m is a good measure of their half life, *vice versa*, which is quite useful for optimizing thermal or solution stability of GO without compromising its activity.

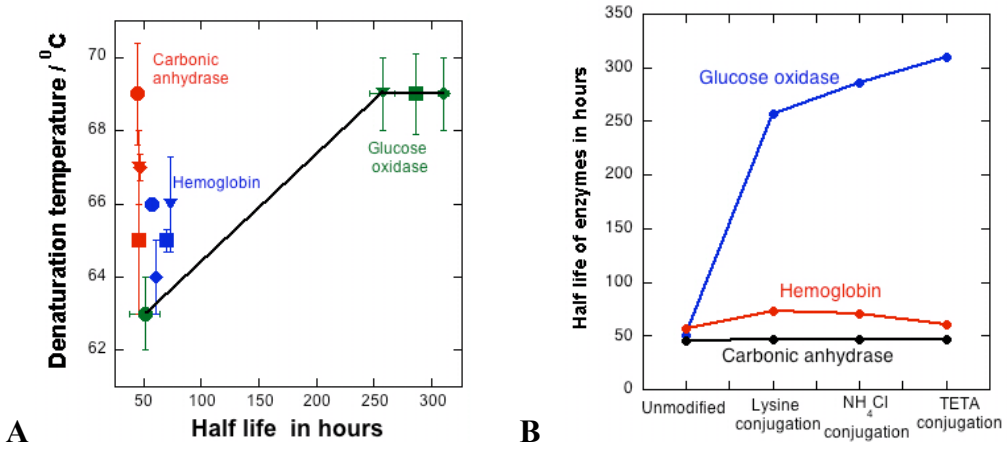

Figure 1.15. (A) .Plot of denaturation temperatures (T_m/°C) of GO, CA and Hb derivatives vs their corresponding half lives (● Unmodified enzyme, ■ NH_4Cl derivative, ◆ TETA derivative, ▼ Lysine derivative). Unmodified and modified derivatives of GO show a clear correlation between the denaturation temperature and half life while CA and Hb derivatives don't show any such correlation. **(B) .** The plot of half life of enzyme vs corresponding amine conjugation of each enzyme. The plot indicates higher half life with modified glucose oxidase which has 120 acidic amino acids. Hemoglobin and carbonic anhydrase, which contains 60 and 30 acidic amino acids respectively, does not show a significant increase in half life.

Additional insight into the stability was gained by correlating the increase in stability and number of carboxylic groups in the enzyme (**Figure 1.15B**). Glucose oxidase with 120 aspartic and glutamic acid residues shows the highest storage stability. The observation clearly demonstrates the strong correlation of increase in stability vs number of carboxyl groups for each substituent, and greater number of carboxyl groups provides a greater opportunity for charge neutralization by chemical modification. In addition, carboxyl modification with polyamines provide additional opportunities for ion pairing with the surface carboxyl groups, further enhancing the stability of the native state. Since carboxyl-carboxyl repulsion energy (ΔG_{repl}) is expected to increase with increasing numbers of carboxyl groups, the above trend indicates that enzymes with the largest number of carboxyl groups provide the greatest opportunities for increasing stability via chemical modification of these groups.

Stability increases also depended on the type of ligand used for modification, and this is expected. For example, reaction with ammonia would neutralize the negative charge due to amidation of the carboxyl groups while reaction with TETA would provide additional basic sites for protonation leading to further charge reduction. On the other hand, reaction of each COOH group with L-Lysine would effectively reduce the negative charge by one unit but would decorate the enzyme with zwitter ionic groups which do not favor enzyme aggregation.

Increase in stability of GO and Hb can be explained based on the electrophoretic mobilities. For example, when the excess charge on the enzyme is neutralized by chemical modification, contribution of ΔG_{repl} toward the denaturation

free energy is minimized, thereby increasing the overall stability. The stability measured at pH 7.2 can be explained based on the mobilities of samples in agarose gels at this pH, and this provided a simple method to predict stabilities of modified enzymes. The phenomenon is clearly visible when the half life is plotted against isoelectric point **(Figure 1.12)**. The maximum stability was observed when the negative charge on glucose oxidase is completely neutralized by making ΔG_{repl} equals to zero. The effect of charge neutralization on storage stability is prominent when the unmodified protein has a higher negative or positive charge at the pH where the stability was measured. In the case of hemoglobin and carbonic anhydrase the effect is low as they have isoelectric points closer to 7. Based on the above argument, we can assume that the chemical modification can improve the storage stability of hemoglobin and carbonic anhydrase at low and high pHs. The new sight provides a handle to increase the storage stability of chemically modified enzymes at desired pHs by neutralizing the charge on the surface of the enzyme at the desired pH. Given the above insights into the chemical modification and its influence on the deactivation pathways, we predict that current model provides an excellent handle to improve enzyme stability and half lives via a chemical route.

1.6 Conclusions

Although chemical modification of enzymes is known for some time, there has been no systematic evaluation of the influence of the chemical modification on key properties of the modified enzymes, nor there is a systematic study of how side chains of increased numbers of amine functions would influence the resulting bioconjugates. A general strategy is described here to systematically control the pI of a small set of enzymes by chemical conjugation without compromising their structure or biological activities.

A small set of amines with increasing number of positive charges per chain are used successfully, and all the samples examined indicated attributes that are comparable to those of the corresponding unmodified enzymes. Modification with this small set of ligands show that key properties of the enzyme are essentially independent of the amine used. The pI has been controlled systematically by increasing the number of basic groups present in the ligand. This resulted in the production of highly positively charged enzymes (at pH 7) without compromising their secondary structure, stabilities or activities.

We conclude that chemical modification, when done carefully under controlled conditions, is a viable method to modulate net charge on enzymes without considerable loss in their structure, activity, or stability. This modulation can in turn be used to control enzyme-DNA or enzyme-solid interactions, which will be reported in future studies. Chemical modification, therefore, provides a powerful handle to control enzyme properties, and in specific instances, there have been increases in activity and stability, which are attractive for biocatalytic applications or fundamental studies of chemically modified enzymes.

Chapter 2 : Chemical Modification of Protein Using Poly(acrylic acid)

2.1 Abstract

Synthesis, characterization and evaluation of a novel polymer-protein conjugate is reported here. Covalent conjugation of high molecular weight poly(acrylic acid) (PAA) to the lysine amino groups of hemoglobin (Hb) resulted in covalent conjugation of hemoglobin to PAA (Hb-PAA conjugate), as confirmed by dialysis and electrophoresis studies. Retention of native-like structure of Hb in Hb-PAA was established from Soret absorption, circular dichroism studies as well as the redox activity of the iron center in Hb-PAA. The peroxidase-like activities of Hb-PAA conjugate further confirmed the retention of Hb structure and biological activity. Thermal denaturation of the conjugate was investigated by differential scanning calorimetry and steam sterilization studies. The Hb-PAA conjugate indicated improved denaturation temperature (T_d) when compared to that of the unmodified Hb. One astonishing observation was that polymer conjugation enhanced Hb-PAA storage stability at room temperature significantly. After 120 hours of storage at room temperature, for example, Hb-PAA retained 90% of its initial activity, while Hb retained <60% of its original activity, under identical conditions. Our conjugate demonstrates the key role of polymers in enhancing protein stability via a very simple, efficient and general route. Protein-polymer networks with increased shelf life can be produced quickly and economically by this approach for a wide variety of applications.

2.2 Introduction

Soft hybrid materials that are biologically functional, yet possess high mechanical strength and remain inert, are important for applications in biocatalysis, sensing, design of components for artificial organs and biomarker detection.[40,41] Examples of these soft hybrid materials include novel protein-polymer covalent conjugates, which combine the impressive biological activities of proteins with the tailorable structures and properties of synthetic polymers.[42] Currently, there are two approaches to achieve this goal: a) covalent conjugation of the polymer at particular sites on the protein[43,44] and b) random conjugation where the protein-polymer conjugation is not at specific sites.[45] Both approaches aim to synthesize protein-polymer conjugates that protect the hierarchical structures and biological activities of proteins[46,47,48,49] Polymers have specific, controllable properties such as mechanical strength, biocompatibility, and tailorability of functional groups. The combined influence of polymer properties and their conjugation to proteins can be exploited so that protein properties such as precipitation, unfolding or degradation, can be altered in a controlled manner.[49]

The wide availability of synthetic polymerization techniques allows for the preparation of polymers with tunable functionality, molecular weight, cytotoxicity, biocompatibility or biodegradability and ability to form nanoscopic structures.[50,51,52,53] The structure, composition and properties of the polymers also determine their applications. For example, one of the most commonly used polymers for protein conjugation is poly(ethylene glycol) (PEG), which has been attached to numerous proteins such as human glucocorticoid receptor, superoxidase dismutase and interferons.[42] While PEG has attracted much attention for conjugation with proteins, other polymers with interesting and highly desired properties are yet to be investigated.

Depending on the desired applications, polymers can tailored for biocompatibility, biodegradability, physical properties and nanoscale structures such that physical properties of protein-polymer conjugates can be controlled systematically.

The protein chosen for the current study, hemoglobin (Hb), has been used to develop artificial oxygen carriers and biosensors.[54,55] Hb is a tetrameric globular protein,[56] responsible for oxygen transport in the blood, and several approaches are being tested to use Hb as an artificial blood substitute. Attachment of PEG[57] , liposome encapsulation [58] and entrapment in vesicles[59] are some examples. Hb also has a high binding affinity for toxic gases such as nitric oxide and carbon monoxide[60] and Hb sensors currently use liquid crystalline surfactant films, gold colloidal particles[61] or polymer films. However, some limitations with protein-based sensors are their short shelf life and lack of long-term stability.[62]

Here, we report a polymer network crosslinked with Hb where the lysine amino groups of Hb are covalently attached to the carboxyl functional group of poly(acrylic acid, PAA) resulting in a crosslinked polymer-Hb network. Crosslinked hydrophilic polymers that utilize PAA are Carbopols®, which are being tested for protein delivery[63] , controlled release[64] and other biomedical applications. We have chosen to use 450 kDa PAA, which is known to have reduced cytotoxicity compared to lower molecular weight PAA.[41] The use of high molecular weight PAA allows for easy processability compared to traditional sensor materials such as metal oxides and solid electrolytes. [65,66,67,68,69] The Hb-PAA system described here indicated retention of its biological activity, protein secondary structure, and long shelf life compared to unmodified hemoglobin. The details of our investigations are described below.

2.3 Experimental Details

2.3.1 Materials.

Poly(acrylic acid) (450,000 MW) and 1-ethyl-3-(3-dimethyl aminopropyl) carbodiimide hydrochloride (EDC), bovine met-hemoglobin, and 2-methoxyphenol were obtained from Sigma Aldrich. Phosphate buffered saline (10 mM PBS, 0.137M NaCl) pH 7.4 or 7.2 was used for preparing protein solutions.

2.3.2 Conjugate Synthesis.

PAA (137.2 mg, 3.05×10^{-4} mmol, 450,000 MW) was dissolved in distilled water (20 ml) and brought to a pH of 7.0 with concentrated NaOH. EDC (51.8 mg, 2.70×10^{-1} mmol) dissolved in de-ionized (DI) water (5 ml) was then added and the solution placed in an ice bath for 15 min. Hb (65.8 mg, 1.03×10^{-3} mmol) dissolved in PBS (phosphate buffered saline) (10 mM, pH 7.4, 5 ml) was added slowly with stirring. Additional PBS (20 ml) was added to adjust the PAA weight percent to 0.2%. The solution was then allowed to stir overnight while reaching room temperature and dialyzed (100k cut-off) for several days. The dialysate was monitored by UV-Vis for Hb, which indicated no release of Hb from the bag. In a blank run, when Hb was not conjugated to the polymer, large portions of Hb was released from the bag, thus confirming the conclusion that EDC coupling was nearly 100% efficient in conjugating the protein to the polymer.

2.3.3 Native Gel Electrophoresis.

Native agarose gels were prepared by dissolving agarose (0.5% w/v) (Sigma electrophoresis grade) in a hot solution of tris acetate (40 mM, pH 6.5). The gel was run in a horizontal gel electrophoresis apparatus (Gibco model 200, Life Technologies Inc,

MD) using tris acetate (40 mM pH 6.5) as the running buffer. Samples were loaded into the gel with loading buffer (50 % v/v glycerol and 0.01% m/m bromophenol blue) and electrophoresis carried out for 30 min at 100 mV at room temperature. The gel was stained overnight with 10% v/v acetic acid, 0.02% m/m Coomassie blue and then destained with 10% v/v acetic acid for an additional night. The gel was photographed using a Molecular Imager Gel Doc XR System.

2.3.4 TEM

Transmission electron microscopy (TEM) was used to examine the morphology of the Hb-PAA conjugate, Hb and PAA mixture (Hb/PAA), Hb and PAA. The images were obtained with a Tecnai T12 instrument operating at an accelerating voltage of 120 kV. Solutions of Hb-PAA, Hb/PAA and PAA were diluted to 0.1 mg/mL based on PAA concentration. The Hb solution was diluted to 0.1 mg/mL Hb. A drop of each solution was deposited on a copper grid covered with Fomvar film. Excess solution was blotted away with a piece of filter paper to leave a thin layer of solution on the grid. The sample was left to dry in air, and then stained with ruthenium tetroxide for 30 min. Digital images were collected and presented as is.

2.3.5 CD Spectra.

Far UV spectra of unmodified Hb, Hb-PAA and Hb/PAA were recorded using Jasco 710 spectropolarimeter. Each sample (2 μM) was in K_2HPO_4 (10 mM) pH 7.2 buffer and the buffer spectrum was subtracted during processing. Step resolution was kept at 0.2 nm/data point and bandwidth and sensitivity were 1 nm and 20 millidegrees, respectively. Each protein sample was scanned from 190 nm to 260 nm and scan speed

was maintained at 50 nm/min. Average of four accumulations was recorded using 0.05 cm pathlength cuvette. Each sample was scanned from 350 to 450 nm and the scan speed was 50 nm/min. Pathlength used was 1 cm and eight accumulations were averaged to get each spectrum. These same parameters were also used to record far UV CD spectra, except for shorter pathlengths or lower protein concentrations, as stated in specific cases.

2.3.6 Catalytic Activity Measurements.

Peroxidase-like activity of Hb was used to compare the activity of Hb-PAA, Hb/PAA and Hb. Substrate, O-methoxyphenol (2.5 mM) and the oxidant, H_2O_2 (1 mM) were added to the protein solution (0.5 μM Hb in K_2HPO_4 (10 mM) pH 7.2 buffer). Oxidized product formation was observed by measuring the absorbance at 470 nm as a function of time in the kinetics mode, using HP 8453 diode array spectrophotometer.[70] From the plot of absorbance vs. time, initial activities and specific activities were calculated and the values of Hb, Hb-PAA and Hb/PAA compared.

2.3.7 Redox Activities.

Redox activity of Hb was tested by using sodium dithionite for the reduction of Fe(III) to Fe(II) and sodium ferricyanide to oxidize Fe(II) to Fe(III). Sodium dithionate was added to solutions of Hb (1 μM) and Hb-PAA (1 μM) and the absorbance spectra recorded. Similarly, the oxidation of Fe(II) to Fe(III) was monitored by recording the Soret absorbance after the addition of sodium ferricyanide (20 μM). The spectra of the untreated, reduced and the oxidized samples were scaled, corrected for the dilutions and overlaid for comparison.

2.3.8 Differential Scanning Calorimetry.

DSC thermograms were recorded using a 6100 Nano II differential scanning calorimeter (Calorimetry Sciences Corporation, CSC Utah) by following a previously reported method from this laboratory[71] All samples were degassed at least for 5 min prior to loading into the calorimeter, and cells were filled without air bubbles. Constant pressure of 3 atm was applied to the calorimeter to prevent solvent evaporation during the thermal scan. During buffer versus buffer scan, both cells were loaded with buffer (10 mM K_2HPO_4 pH 7.2), equilibrated for 10 min at 20°C and scanned from 20 to 100°C at a scan rate of 2°C/ min. Once both heating and cooling scans were completed for buffer versus buffer system, the sample cell was emptied, washed and filled with the desired protein solution (4 μM Hb). Heating and cooling scans were recorded using parameters that were previously used with buffer versus buffer scan. The nanocalorimeter was interfaced to a personal computer (IBM compatible) and during data processing, background scan or the buffer vs. buffer scan was subtracted from the sample scan. Each scan was normalized with respect to hemoglobin concentration in the sample. A second heating cycle of the sample was used to check for reversibility of the thermal denaturation. Model independent parameters, such as peak transition temperature (T_m) and $\Delta H_{denaturation}$ (area under the curve) were calculated for each sample.

2.3.9 Steam Sterilization Studies.

Solutions of Hb, Hb-PAA and Hb/PAA were autoclaved using SI-120 scientific isothermal sterilizer (Steric corporation, PA). Samples were heated to 120°C at 15 psi for 45 min in the sterilizer and cooled down to room temperature for 1 h. Activity

studies and CD studies were carried out with the samples at room temperature, using the above-mentioned procedures.

2.3.10 Shelf-life Studies.

Storage stabilities of Hb, Hb-PAA and Hb/PAA were measured by monitoring the peroxidase-like activity of the heme protein as a function of storage at room temperature. Samples were withdrawn periodically, and activities have been measured using the procedure described above. Specific activities of samples were calculated, data normalized with respect to their corresponding initial activities, and relative specific activities thus obtained have been plotted as a function of storage time.

2.4 Results

2.4.1 Conjugate design and synthesis.

The covalent attachment of PAA to Hb was carried out at pH 7.4, and at this pH the polymer was known to exist in an extended conformation due to its ionized carboxyl groups[72] The reaction contained 0.2 % wt PAA and remained homogenous during synthesis. Conjugation of the protein to the polymer was confirmed by dialysis studies. The dialysate was monitored for Hb by monitoring absorbance due to the Soret band at 406 nm, which showed no release of Hb from Hb-PAA reaction mixture. Hb-PAA samples, thus purified by dialysis, were investigated by UV-Vis spectroscopy by monitoring the heme Soret band (**Figure 2.1**). The Soret band of unmodified Hb indicated a peak maximum at 406 nm (**Figure 2.1, blue line**), which overlapped well with the Soret band of Hb-PAA conjugate (**Figure 2.1, red line**). The absorption spectrum of the physical mixture of Hb/PAA (same concentrations as above, **Figure 2.1**, 406 nm λ max, green line), indicated a small decrease in intensity. The important observation is that both the peak position as well as the extinction coefficients of Hb and Hb-PAA at 406 nm are identical and the data suggests that the heme environment is not influenced by the covalent conjugation of lysine side chains of Hb with the carboxyl groups of PAA. Gel electrophoresis was also used to confirm attachment of Hb to PAA. Distinct differences in the net charge and mobilities of Hb, Hb-PAA and Hb/PAA are clearly visible in the gel (**Figure 2.2**). Hb and Hb/PAA both showed bands moving towards the cathode while Hb-PAA, which is highly negatively charged at pH 6.5, moved towards the anode.

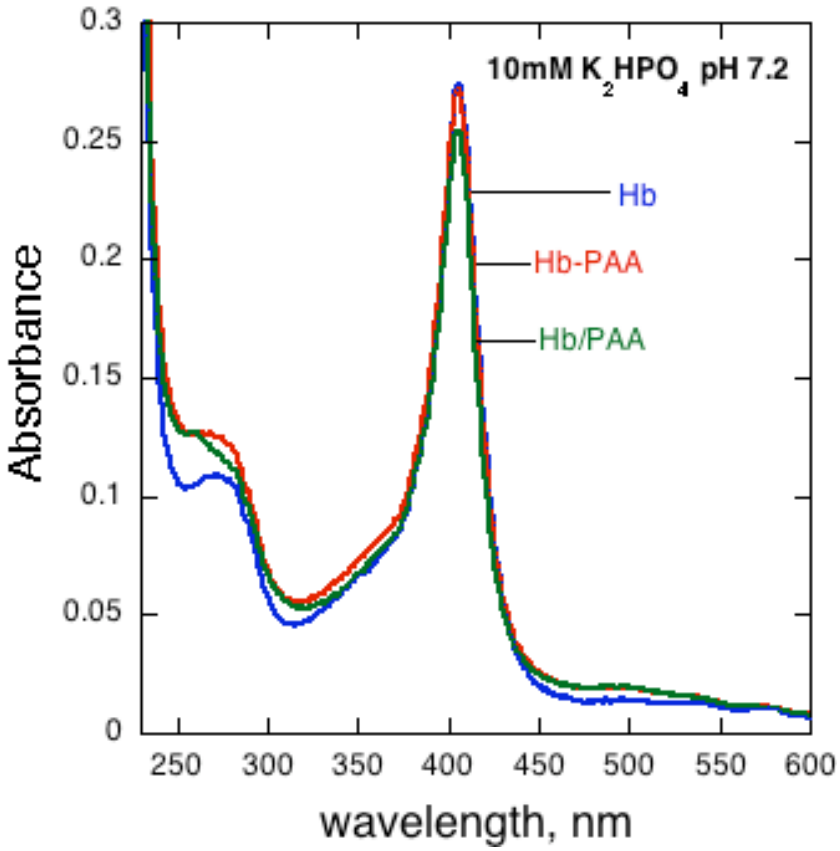

Figure 2.1 Absorption spectra of Hb, Hb-PAA and Hb/PAA (1 μM protein) recorded in phosphate buffer (10 mM K_2 HPO_4 pH 7.2, 1 cm pathlength). The Soret bands of Hb (blue line) and Hb-PAA (red line) are nearly superimposable while that of Hb/PAA mixture (green line) indicated minor decrease in Soret band intensity.

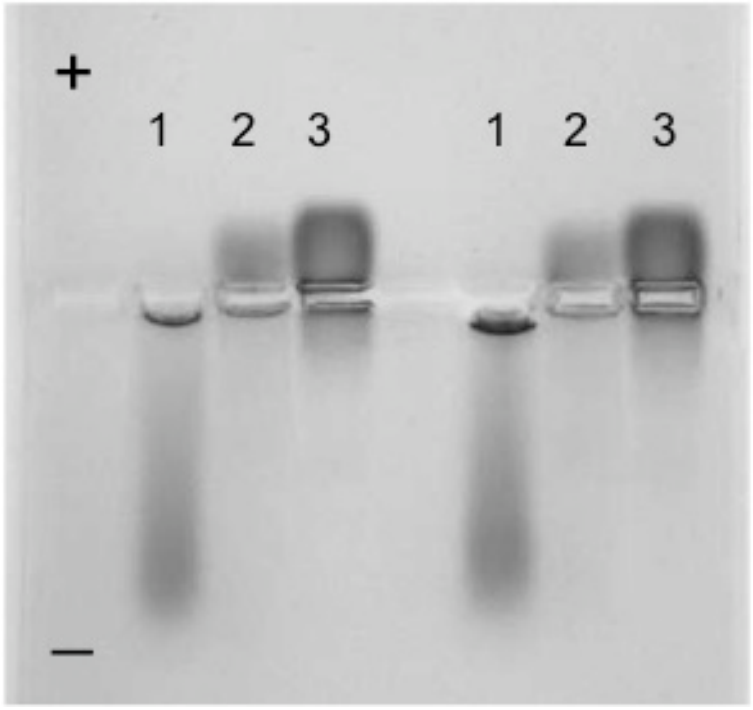

Figure 2.2 Gel electrophoresis image of agarose gel run at pH 6.5 tris acetate buffer, Hb-PAA conjugate (1), Hb/PAA mixture (2) and Hb (3).

2.4.2 Conjugate morphology.

The TEM image of Hb-PAA conjugate showed a porous network structure and not spherical particles (**Figure 2.3a**). The formation of fibrous network structure indicates that Hb and PAA are cross-linked randomly. Visible precipitate formation or flocculation is not observed and therefore a lightly cross-linked homogeneous solvent swollen network is proposed. As expected, the RuO_4 did not preferentially stain either PAA or Hb but stained the conjugate as a whole (**Figure 2.3a**). The TEM of Hb/PAA also showed fibrous structure (**Figure 2.3b**) while the TEM image of Hb showed large spherical aggregates as well as smaller particles. PAA at pH 7 showed the formation of spherical aggregates (**Figure 2.3c and 2.3d**, respectively).

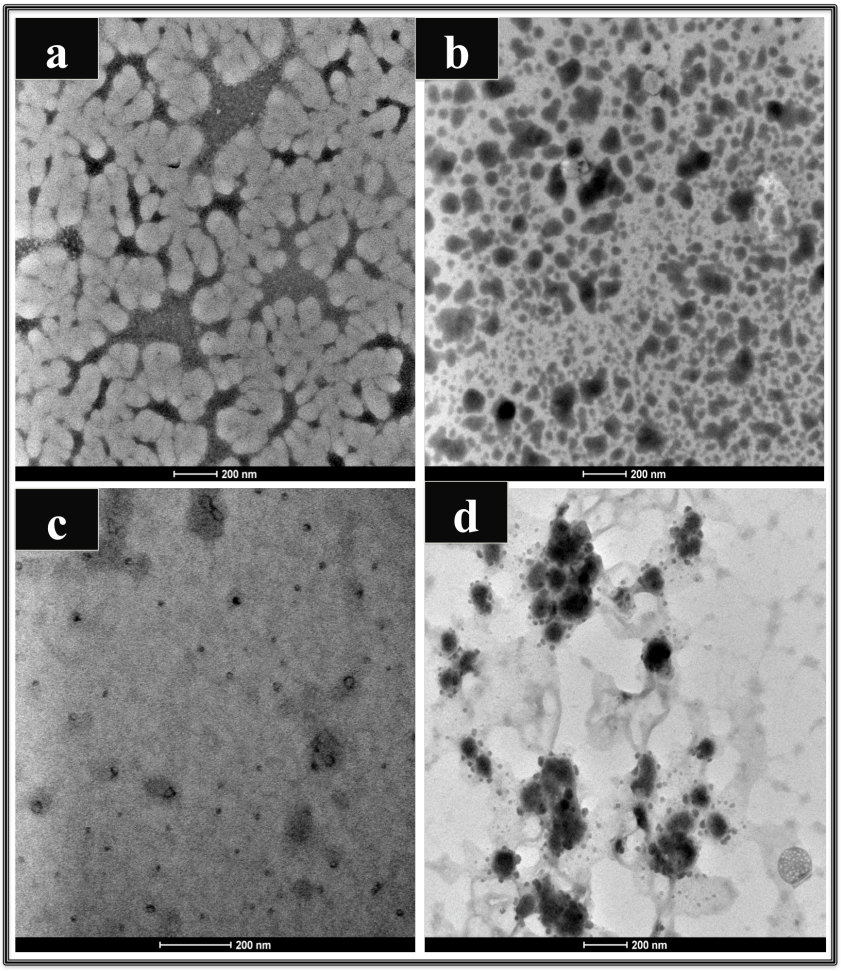

Figure 2.3 TEM images of (a) Hb-PAA (0.2 wt% PAA) (b) Hb/PAA (0.2 wt% PAA) (c) Hb and (d) PAA (0.2 wt% PAA), stained by RuO_4.

2.4.3 CD Spectra.

Changes in protein secondary structure due to covalent conjugation were assessed by comparing the UV-CD spectra of the conjugate with that of the unmodified Hb (**Figure 2.4a**). The UV-CD spectra are highly sensitive to the changes in protein secondary structure and they serve as excellent probes to examine protein structure[73]. The CD spectrum of unmodified Hb indicated a strong maximum at 190 nm and double minima at 208 nm and 222 nm (**Figure 2.4a, blue line**) and this is nearly the same as that of the Hb-PAA (**Figure 2.4a, red line**), recorded under the same conditions of buffer, concentration and pathlength[74]. The UV-CD of Hb/PAA (**Figure 2.4a**, **green line**), recorded under the same conditions as above, also indicated CD spectrum that is similar to that of the native Hb. In light of only minor differences noted between the spectrum of the conjugate and that of Hb, we conclude that the secondary structure of the protein has been retained to a large extent.

The Soret CD of the Hb-PAA conjugate, which is a sensitive measure of the asymmetry of the heme environment in hemoglobin, was also examined (**Figure 2.4b**) to evaluate the changes in the heme environment, if any. The Soret CD spectra of Hb (blue line) and Hb-PAA (red line) are similar, as in the case of the UV CD spectra, and the peak positions remained unchanged, which implies that heme coordination environment in the conjugate is well preserved and very similar to that of the unmodified Hb. The physical mixture of Hb and PAA indicated a minor decrease in the intensity of the Soret CD but not substantially different from that of the Hb. Encouraged by these CD data, we tested the redox activity of the heme prosthetic group in Hb-PAA. Retention of the redox

activity would be essential for biological or sensor applications of the protein-polymer conjugates.

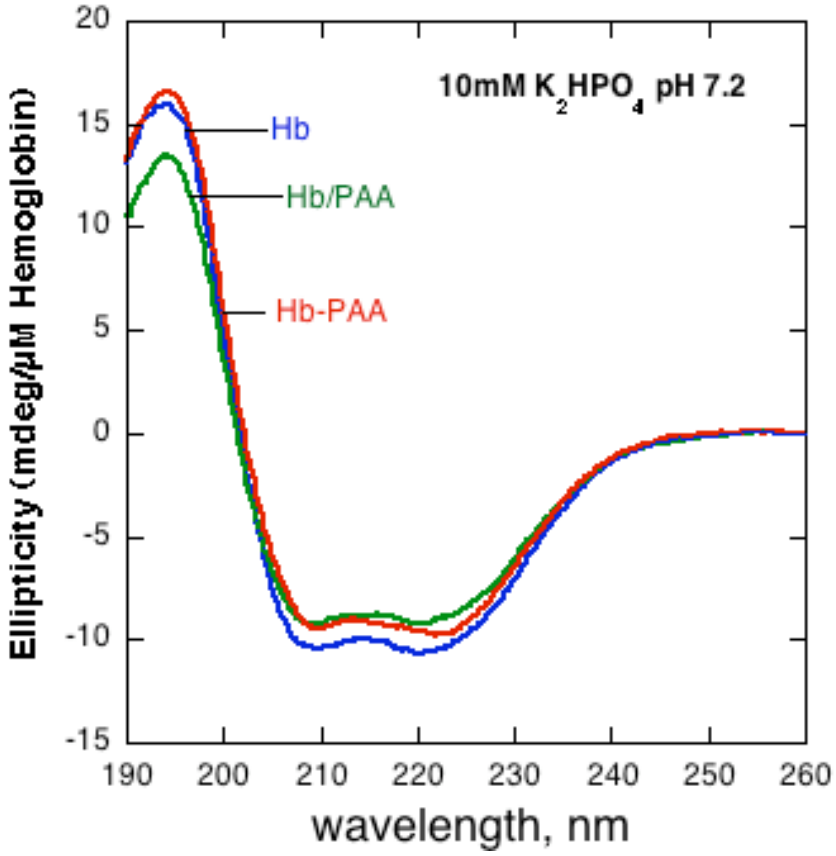

a

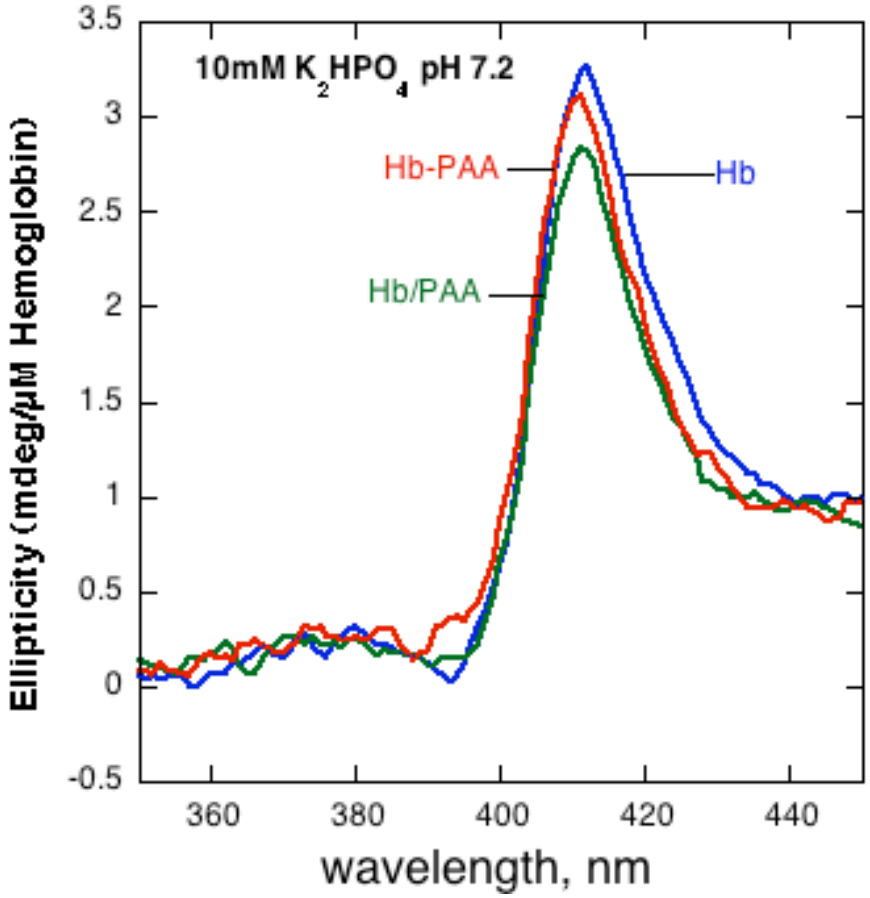

b

Figure 2.4. Far UV CD spectra (**Figure 2.4a**) of unmodified Hb (black line) and Hb-PAA conjugate (red line), as well as those of a physical mixture of Hb and PAA (green line). All three samples contained same amount of Hb (4 μM protein in 10 mM K_2HPO_4 pH 7.2 buffer). Soret CD (**Figure 2.4b**) of Hb and Hb-PAA (4 μM protein in 10 mM K_2HPO_4 pH 7.2 buffer). Soret CD peak position of the conjugate is the same as that of Hb.

2.4.4 Redox Activity of Hb-PAA.

The Fe(III) center in met-hemoglobin undergoes efficient redox chemistry. Maintaining the Hb Fe(II) state under physiological conditions is critical for its biological activity. The Fe(II) form of Hb, for example, is capable of binding dioxygen while the Fe(III) form cannot, and therefore, the production of Fe(II) form of Hb-PAA is essential for practical applications. Addition of sodium dithionite reduces the Fe(III) form of Hb to the Fe(II) form, and the Soret band shifts concomitantly to the red.[75] If the reduction is reversible, then the addition of sodium ferricyanide to the Fe(II) form of Hb reverts the heme to the Fe(III) state with a concomitant blue shift of the Soret band back to 406 nm.[75] Therefore, we examined the redox activities of Hb and Hb-PAA (**Figure 2.5**). Reduction of the Fe(III) form of Hb (red line) to the corresponding Fe(II) form (green line) by the addition of dithionite resulted in a small red shift in the Soret band while the addition of ferricyanide to the Fe(II) form indicated the reversal of the Soret position to its initial position (blue line). Similarly, the addition of dithionite to Hb-PAA (**Figure 2.5b**) indicated a large red shift (green line) while the addition of ferricyanide to the Fe(II) form reverted the peak back to 406 nm (blue dashed line). The Fe(II) form of Hb-PAA showed a larger red shift than Hb and reasons for this are not immediately clear, but the spectral data clearly show that the Fe(III) form of the conjugate is reduced by dithionite, reversibly, and ferricyanide is capable of oxidizing the Fe(II) form of the conjugate. Thus, Hb-PAA retained its redox activity, and covalent conjugation with the polymer did not inhibit this key property of Hb.

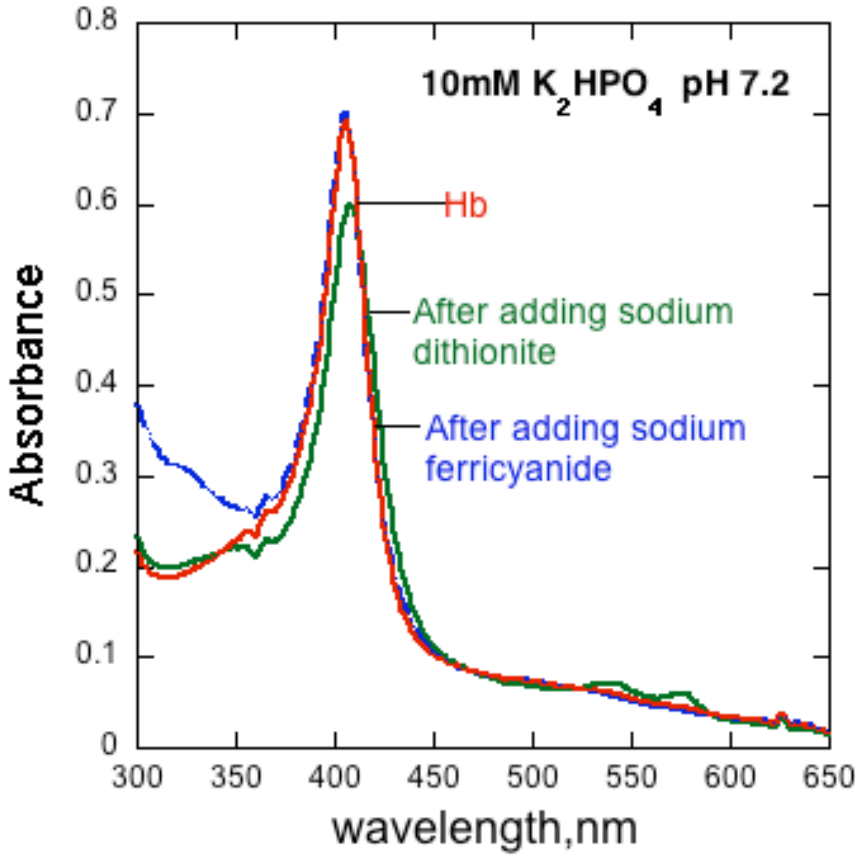
10mM K2HPO4 pH 7.2
Hb
After adding sodium dithionite
After adding sodium ferricyanide
Absorbance
wavelength,nm
0.8
0.7
0.6
0.5
0.4
0.3
0.2
0.1
0
300
350
400
450
500
550
600
650

a

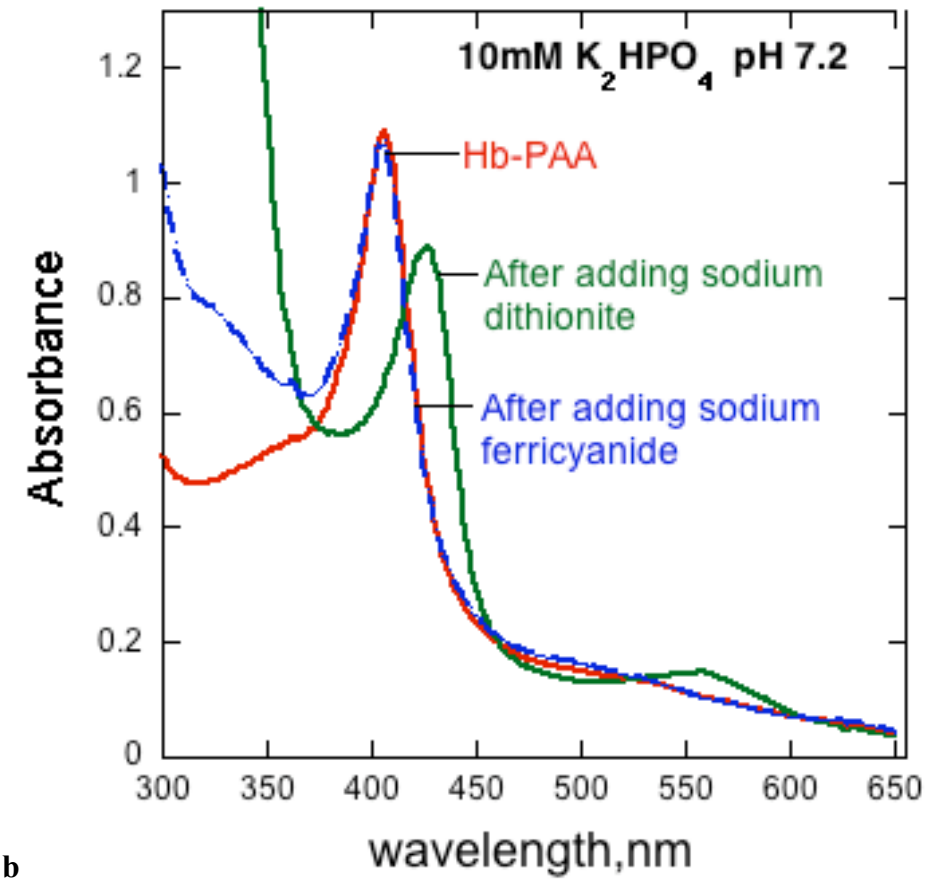

b

Figure 2.5. Redox activities of Hb (**Figure 2.5a**) and Hb-PAA conjugate (**Figure 2.5b**) (1 μM protein in 10 mM K_2HPO_4 pH 7.2 buffer) as indicated by the Soret absorption bands, upon the addition of sodium dithionite and sodium ferricyanide (20 μM). Redox activity of the heme moiety is retained in Hb-PAA conjugate.

2.4.5 Peroxidase-like Activity of Hb-PAA Conjugate.

Although Hb is not an enzyme, Hb can catalyze the oxidation of lipids and phenolic derivatives while using H_2O_2 as the oxidant. Oxidation of 2-methoxyphenol, for example, by Hb in the presence of H_2O_2 produces a deep purple color due to the formation of dimeric and higher aggregates of the phenol which has an absorption maximum at 470 nm.[76] The catalytic activities of Hb-PAA, Hb/PAA and Hb, under the same conditions of concentration, buffer, pH, and temperature, are compared in **Figure 2.6**. The addition of H_2O_2 to the mixture of the biocatalyst and 2-methoxyphenol immediately produced the colored product, and increase in absorbance at 470 nm was monitored as a function of time (**Figure 2.6**). The catalytic activity of Hb-PAA (red line) is nearly the same as that of Hb (blue line) and Hb/PAA (green line).

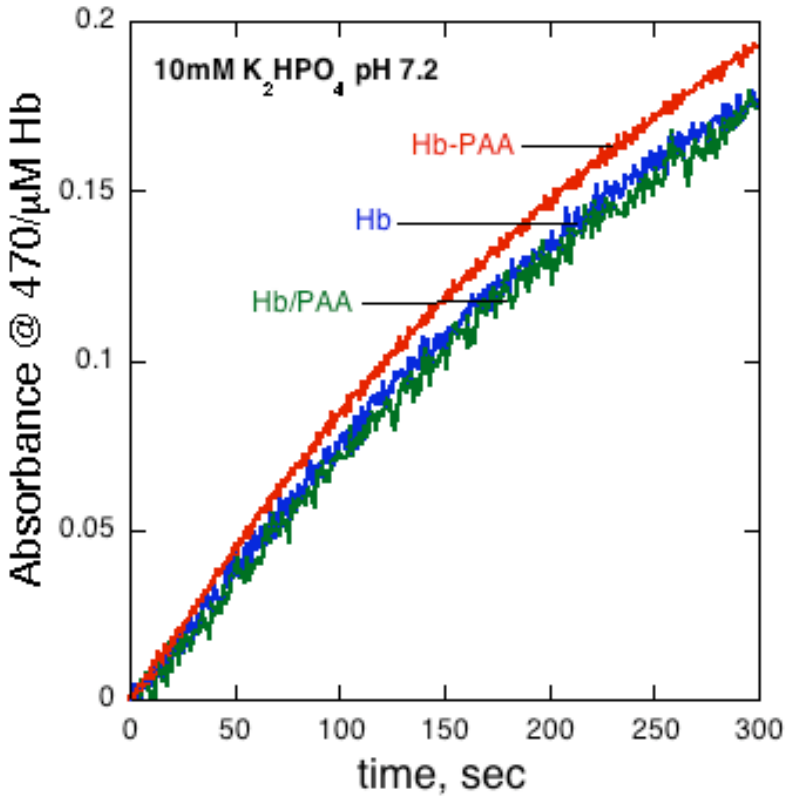

Figure 2.6 The peroxidase-like activity of Hb, Hb-PAA and Hb/PAA (1 μM protein) by the addition of 2-methoxyphenol (2.5 mM) and H_2O_2 (1 mM) as monitored by following the absorbance of the product at 470 nm (10 mM K_2HPO_4 pH 7.2 buffer at room temperature). Activity of Hb-PAA (red line) is almost the same as that of Hb (blue line) or Hb/PAA mixture (green line). Activities were normalized to the concentration of Hb in each sample. Conjugation of the polymer with the protein did not alter Hb activity.

2.4.6 Differential Scanning Calorimetry.

The influence of polymer conjugation on protein stability was evaluated by recording the DSC thermograms of Hb, Hb-PAA and Hb/PAA (**Figure 2.7**). The thermograms show that the conjugate (red line) begins to denature at 40˚C with a peak maximum of 65˚C and continues to denature up to 105˚C. This can be compared to Hb, which denatures over the range of 50-70˚C. The Hb/PAA mix shows a peak, which is much broader and centered around 65˚C (**Table 2.1**). The integrated area under the curve is the corresponding enthalpy of denaturation and there was a significant difference in the enthalpy values obtained for Hb, Hb-PAA and Hb/PAA (**Table 2.1**). Hb and PAA had denaturation enthalpies of 90 and 760 kcal/mol, respectively. The Hb-PAA conjugate, on the other hand, showed a significantly higher ΔH (1558 kcal/mol), which is greater than that of Hb/PAA (399 kcal/mol). The value is higher than the sum of the enthalpies of Hb and PAA by ~700 kcal/mol. Such a substantial increase in the denaturation enthalpy is a welcome change and can be exploited to improve the thermal stability of the polymer conjugate. Hence, the storage stability of the conjugate, at room temperature, is expected to be significantly better than that of the parent Hb. First, we examined the stability of the protein-polymer conjugate toward sterilization with steam, which is a simple and efficient way to sanitize biomaterials for practical applications.[77]

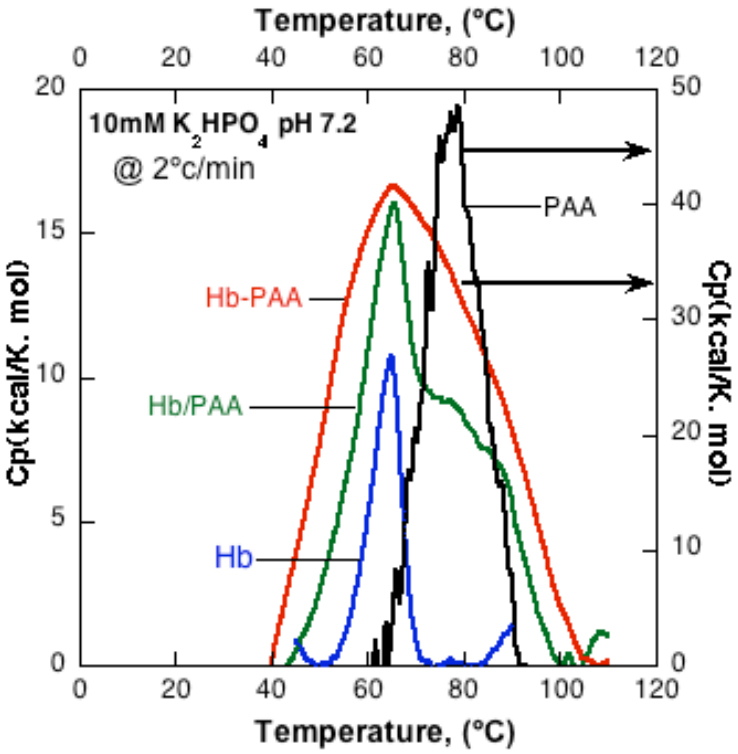

Figure 2.7 The DSC thermograms of Hb, PAA, Hb-PAA and Hb/PAA. The molar heat capacity profiles of Hb (8 μM protein, blue line), PAA (4.4 μM, black line), Hb/PAA (8 μM protein, 4.4 μM PAA, green line), and Hb-PAA (8 μM protein, 4.4 μM PAA, red line) recorded in 10 mM K_2HPO_4 pH 7.2 buffer at a scan rate of 2 ˚C /min. The quantitative values of the corresponding thermodynamic parameters are listed in Table 1.

Table 2.1 Denaturation temperatures and ΔH values for Hb, Hb-PAA, Hb/PAA and PAA in 10 mM K_2HPO_4 pH 7.2 buffer, at a scan rate of 2 ˚C /min.

Sample	**ΔH /kcal/mol**	**T_m/ ˚C**
Hemoglobin	90	65
Hb-PAA conjugate	1559	65
Hb/PAA mix	399	65
PAA	760	79

2.4.7 Steam sterilization data.

The effect of high temperature sterilization of the conjugate on its structure and biological activity was investigated by subjecting the samples to steam sterilization. The ability to sterilize a material can influence its potential use as a biomaterial. Samples of Hb, Hb-PAA and Hb/PAA were heated to 120˚C at 15 psi, for 45 min. After cooling the sample to room temperature, the peroxidase-like activity of each sample has been monitored, as described earlier. The activities of all of the samples decreased after steam sterilization, which is a commonly observed trend.[78] The data shows that the decrease in activity is consistent for all three samples (**Figure 2.8**).

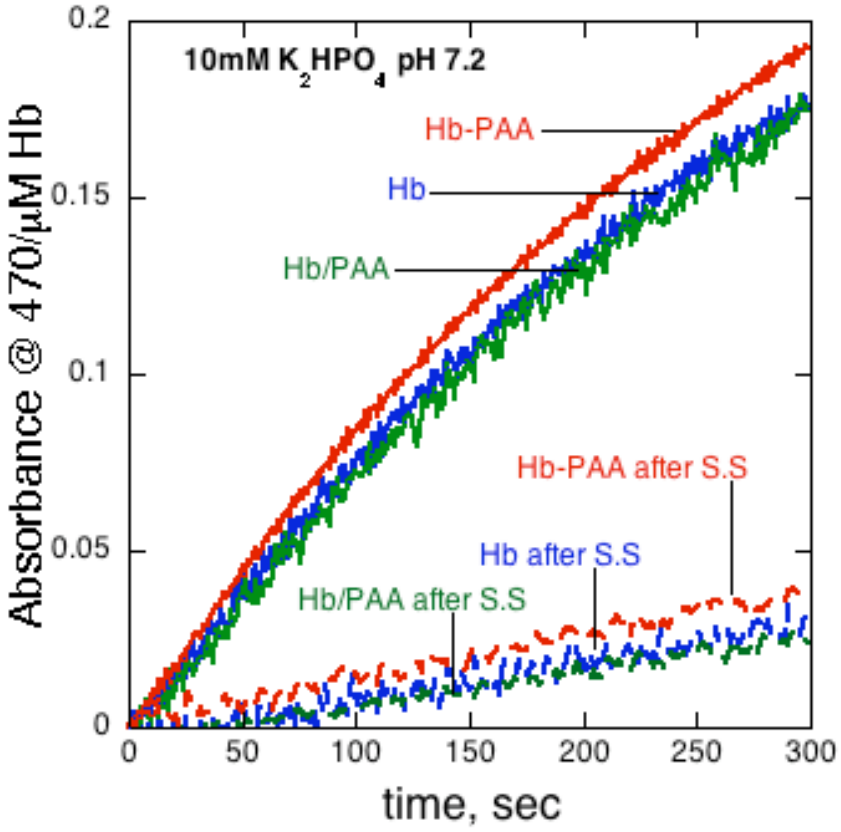

Figure 2.8 Peroxidase activities after steam sterilization and cooling to room temperature. Activities were measured with with1 mM H_2O_2 and 2.5 mM 2-methoxyphenol in 10 mM K_2HPO_4 pH 7.2 buffer, at room temperature. The data has been normalized to the concentration of Hb in each sample. Activity of Hb-PAA (broken red line) after steam sterilization is similar to the activities of Hb (broken blue line) and Hb/PAA (broken green line). There are no measureable differences among the three samples.

2.4.8 pH responsiveness.

The conjugation of PAA to Hb is expected to enhance the pH-responsiveness and Hb-PAA presented an excellent opportunity to test this hypothesis. The effect of pH was investigated by monitoring the Soret peak as a function of pH (**Figure 2.9, blue line, pH 7 to 11**). As the pH was raised from pH 8.1 to 9.5, the Soret peak of Hb-PAA shifted from 406 to 410 nm. Upon lowering the pH by the addition of acid, the Soret peak shifted back to 406 nm, and the two curves showed significant overlap with a good degree of reversibility. The reversibility of this transition was compared to that of Hb.[79] The two transitions look very similar but that of the Hb-PAA appears in a narrower range of pH when compared to that of Hb. This decrease in the pH range, and the resulting sharpening of the response, is likely due to the polymer network binding the subunits of Hb together. Thus far, the conjugate indicated properties that are very similar to that of the parent Hb and only minor improvements are noted with the conjugate, if any.

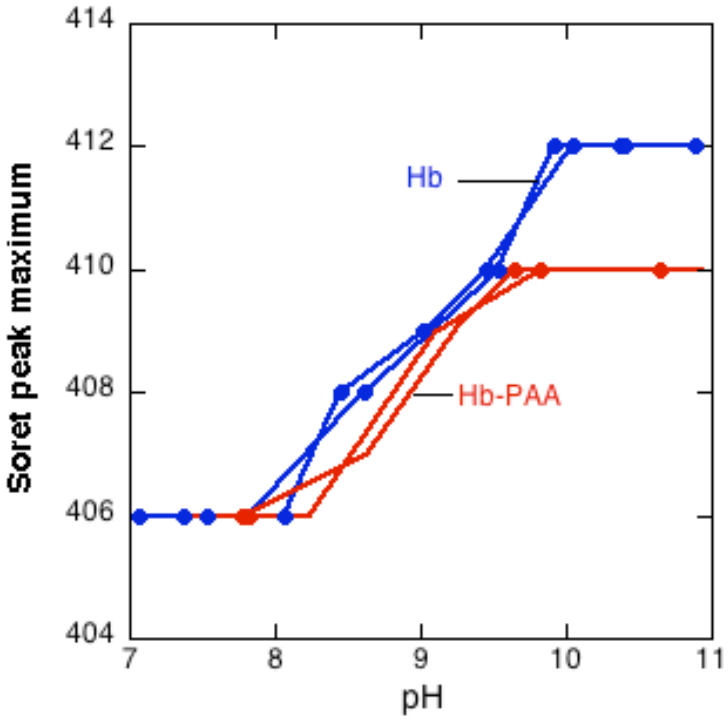

Figure 2.9. The effect of pH on heme Soret peak from pH 7 to 11, (Hb (blue line) Hb-PAA (red line), 4.4μM PAA, 8μM Hb in PBS pH 7.4 buffer at 25°C). The peak shifted from 406 nm to higher values upon addition of NaOH and the transition was reversible with little or no hysteresis.

2.4.9 Shelf Life.

Since proteins are designed to function in the well-controlled biological environment, solution stability of a protein rapidly decreases over time when stored at room temperature. Current state-of-the-art biocatalysts for large scale applications do not retain their catalytic activity at room temperature over extended periods of time, and this is a major barrier for practical applications in biocatalysis, biosensor fabrication or for use as biomaterials. Bioconjugation of enzymes is a known method to improve its room temperature stability or shelf life.[80] To test, if conjugation of Hb to PAA improved its shelf life, specific activities of Hb, Hb-PAA and Hb/PAA samples that were stored at room temperature, have been measured as a function of time (Figure 2.10). This investigation successfully showed that PAA acts as a protection shell for Hb while allowing for the retention of catalytic activity. Hb-PAA and Hb/PAA retained 90% of their initial activities even after room temperature storage for 120 h. Activity of native Hb decreased rapidly, compared to conjugate and the physical mixture, and after 120 h of storage only 60% of activity was retained. The study implies that conjugation or addition of PAA improves the retention of catalytic efficiency of protein over time allowing for proteins or enzymes to be stored at room temperature for long periods of time with little or virtually no loss in activity.

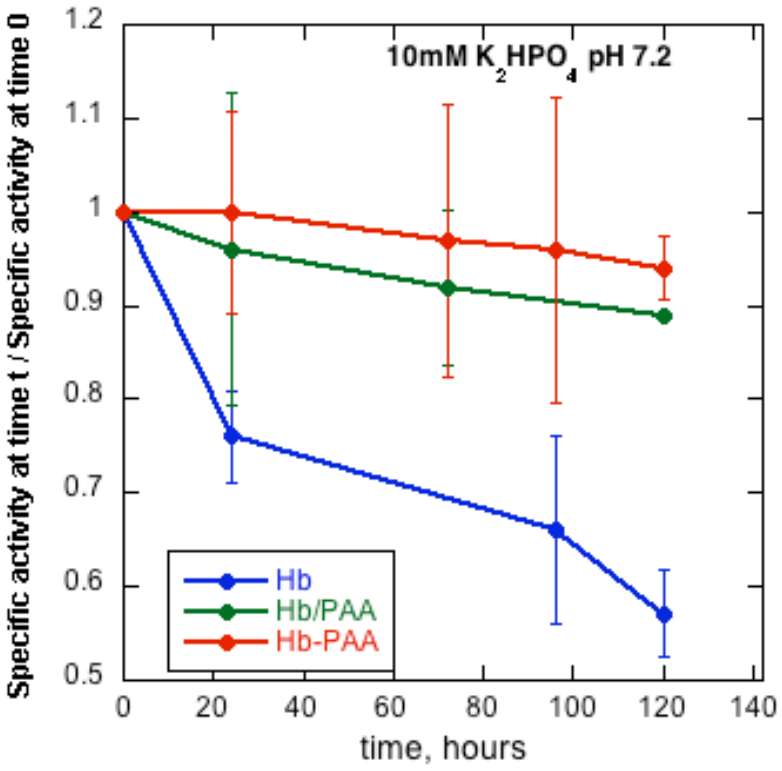

Figure 2.10 Change in specific activity of the Hb-PAA as a function of time. Specific activities of Hb (*blue line*), Hb/PAA mix (*green line*) and Hb-PAA conjugate (*red line*) are compared, as a function of time. 1 mM H_2O_2 and 2.5 mM 2-methoxyphenol in 10 mM K_2HPO_4 pH 7.2 were used to measure the peroxidase-like activities of the samples. Specific activity at time t was divided by specific activity at time 0 to compare the three sets of data.

2.5 Discussion

Our synthesis of the Hb-PAA conjugate was quick, facile, efficient, and scalable. PAA of high molecular weight was the polymer of choice due to its large number of attachment points (COOH), mechanical characteristics, decreased cytotoxicity and scaffold potential.[41,81,82] The use of carbodiimide coupling in phosphate buffer allowed for complete conjugation of hemoglobin to PAA. The complete attachment was confirmed by the absence of the release of Hb from Hb-PAA in dialysis studies, and from the absence of free Hb in gel electrophoresis studies. The Hb-PAA conjugate, though lightly cross-linked, remains homogenously dispersed in solution, and this feature makes the solution-based characterization of this conjugate possible.

Table 2.2 Viscosities at a shear rate of 1.0 (1/s) for 0.2 wt% PAA and Hb-PAA in PBS. The PAA concentration is 0.2 wt% is the Hb-PAA sample.

Sample	Viscosity (Pa s)
PAA 450k	7.82×10^{-3}
Hb-PAA	0.023

The TEM and viscosity (Table 2.2) aided in confirming the prescence of a lightly cross-linked network. The extensive characterization of the conjugate showed that despite multiple covalent attachments to Hb, there is no significant difference in heme environment, helical content and peroxidase-like activity of the conjugate in comparison to the unmodified Hb. The activity of Hb-PAA was found to be slightly higher than that

of Hb and Hb/PAA. The retention of structure protein structure was further confirmed by the reversibility of the Soret peak characteristics upon reduction and oxidation of the iron center. The thermal denaturation of Hb occurs at 64.9°C, and this value is very close to that of the Hb-PAA conjugate, although the range of denaturation and enthalpy value was significantly increased. The conjugation of Hb to PAA leads to an increase in $\Delta H_{denaturation}$ of ~700 kcal/mol. The increase in denaturation enthalpy implies an increase in thermal stability of conjugate over unmodified Hb and Hb/PAA mixture. Steam sterilization followed by activity measurements show that the conjugate retained only a slightly higher percent activity compared to Hb and Hb/PAA. In contrast to thermal denaturation, the pH-induced denaturation was shown to be completely reversible for the conjugate as well as the free Hb but the denaturation of the conjugate occurred over a narrower pH range than that of Hb. Investigations into the room temperature stability showed interesting results.

The shelf life of Hb-PAA was investigated by monitoring the activity of the conjugate after storing the samples at room temperature for increased lengths of time. This study conducted over a period of 120 h showed a dramatic loss in activity of Hb (<60%). After just 20 h, Hb activity dropped by 25% while Hb-PAA showed no apparent decrease. Hb-PAA did show a loss of less than 10% after 120 h storage at room temperature, while that of Hb dropped by >40%. This dramatic retention of activity of the conjugate can be attributed to the presence of PAA chains that prevent the protein from denaturation, followed by aggregation. There was no visible aggregation observed in the Hb-PAA solution , which was not the case for Hb solution.

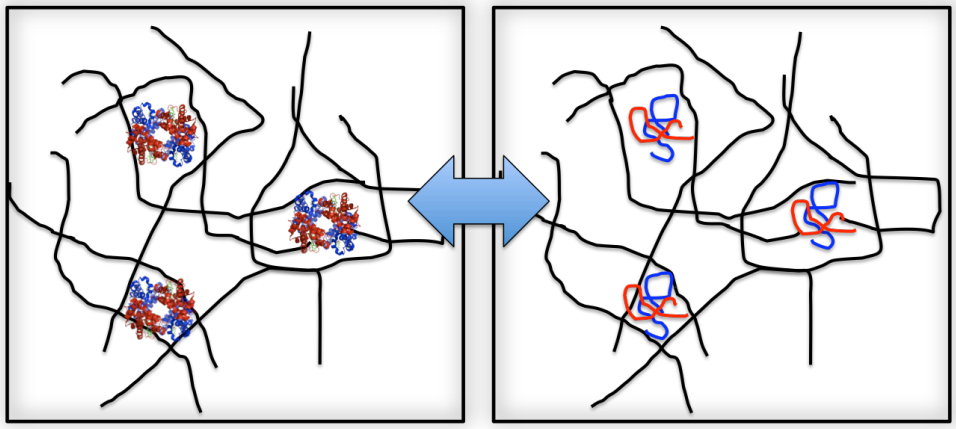

Scheme 2.1 Proposed Hb-PAA network structure. Black lines represent the PAA chains with Hb (blue and red objects) covalently attached. The cartoon on the left shows the sample at room temperature with Hb in its native state, and the one on the right represents the conjugate above the denaturation temperature of Hb. The double-headed arrow represents reversibility of this transition under thermal or pH cycling.

The protein-polymer material we have presented here, Hb-PAA, has properties and characteristics that make it a good candidate for biomedical and sensing applications[82]. Most of the investigations of Hb conjugates have been targeted towards improving in vivo circulation times and oxygen binding capacity for applications as blood substitutes.[83,84] However, to exploit unique properties of Hb conjugates in other applications, it is imperative to design methods to protect the 3D structure of Hb and to investigate its catalytic efficiency and shelf life when stored under ambient conditions. Our ability to prepare Hb-PAA conjugates that remain solvent-swollen can be exploited to cast films, which retain catalytic efficiency and prolonged shelf life, and they would be extremely important for sensing applications. Covalent conjugation is preferred over physical interaction-based systems because the covalent bonding would prevent protein or catalyst from leaching out of the conjugate, thereby resulting in lowered catalytic activity. Another advantage of our system is that by attaching high-molecular-weight polymer to a protein, the processability and range of physical properties of the protein as a material is broadened significantly. The Hb-polymer conjugate system, demonstrated here, may be expanded to investigate the effect of other biocompatible or biodegradable polymers as well as other proteins or enzymes.

2.6 Conclusion

Here, we have shown that Hb can be covalently attached to polyacrylic acid without having any significant detriment to the structure and activity of the protein. The heme environment remains unaffected by the multiple PAA attachment points as shown by Soret absorption, peroxidase-like activity and redox activity. Thermal studies showed that the conjugation significantly increased the denaturation enthalpy. The room temperature stability of the solution was the most noteworthy result of this study. The stability of the protein in solution was extensively increased due to the covalent attachment of PAA chains. This work has demonstrated a facile approach to improving Hb stability, and our approach can be further expanded for use with other proteins or polymers.

Reprinted (adapted) with permission from Thilakarathne,V.; Briand, V.A.; Zhou,Y.; Kasi, R.M; Kumar, C.V. Protein Polymer Conjugates: Improving the stability of Hemoglobin with Poly(acrylic acid). *Langmuir* **2011**, 27, 7663-7671.

Chapter 3 : Tuning protein/polymer interaction by controlled chemical modification

3.1 Abstract

Protein-polymer interactions play a very important role in a number of applications, but details of these interactions are not fully understood. Chemical modification was introduced here to tune protein-polymer interactions in a systematic manner, where met-hemoglobin (Hb) and poly(acrylic acid) (PAA) served as a model system. Under similar conditions of pH and ionic strength, the influence of protein charge on Hb/PAA interaction was studied using chemically modified Hb by isothermal titration calorimetry (ITC). A small fraction of COOH groups of Hb was amidated with triethylenetetraamine (TETA) or ammonium chloride to produce the corresponding charge ladders of Hb-TETA and Hb-Ammonia derivatives, respectively. All the Hb/PAA complexes produced here are bioactive, entirely soluble in water, and indicated the retention of Hb structure to a significant extent. Binding of Hb to PAA was exothermic ($\Delta H<0$) and Hb-TETA charge ladder indicated decrease of ΔH from -8 ± 0.2 to -89 ± 4 kcal/mol, at a rate of -3.8 kcal/mol per unit charge introduced via modification. Hb-Ammonia charge ladder, in contrast, decrease of ΔH from -8 ± 0.2 to -17 ± 1.5 kcal/mol, at much slower rate of -1.0 kcal/mol per unit charge. Thus, the amine used for the modification played a strong role in tuning Hb/PAA interactions, even after correcting for the charge, synergistically. Charge clustering may be responsible for this synergy and this interesting observation may be exploited to construct protein/polymer platforms for advanced biomacromolecular applications.

3.2 Introduction

Controlling protein/polymer interactions is vital for the construction of protein-polymer hybrid scaffolding platforms for biocatalytic, biosensing and biomedical applications. Many of the protein/polymer platforms use protein immobilization with polymers via layer-by-layer method[85,86,87,88] covalent bonding, precipitation[89,90,91,92] or encapsulation.[93,94,95]

Protein-polymer interactions, for example, are important in the development of biocompatible, stable, inexpensive and sterile drug delivery systems.[96] Biotherapeutics such as peptides, proteins and nucleic acids are susceptible to degradation or denaturation in the biological milieu,[97] and polymeric multilayer capsules have been used to protect these sensitive biologics.[98,99,100] Vast numbers of multilayer assemblies were fabricated by alternative deposition of oppositely charged polymers, where the polymer-protein interactions play crucial roles in the assembly formation and stability.[101] On a similar account, polyelectrolyte based microgels, hydrogels and interpenetrating polymer networks allowed uptake and delivery of biotheraputics.[102,103]

Molecular interactions play a significant role in the design and construction of these platforms, and understanding the contributions of specific molecular segments to these interactions can facilitate better design of materials for the above applications.[104] Our understanding of molecular signatures and thermodynamics of the protein/polymer interactions are rudimentary, despite several important studies.[105,106,107,108,109] The goal of the present work is to perturb the protein-polymer interactions precisely and gain insight into the details of these interactions by ITC studies. Very few thermodynamic studies provide a detailed analysis of contributions of each interactive force toward protein/polymer complex formation.[110] This gap in knowledge is because of the

complexity of separating these interactions and limited availability of rational approaches to control them in a predictable manner.

Use of different proteins to factor out specific contributions to these interactions, for example, would make the study complicated since each protein has its own structure with different kinds of amino acid residues decorating its surface. These amino acid residues play a major role in defining the hydrophobic and charged patches on the protein surfaces.[111] As a step forward, in this paper, we introduce protein chemical modification as a rational route to introduce specific interactions at the protein-polymer interface and study their influence quantitatively. Chemical modification is a powerful tool to introduce specific molecular segments on protein surfaces,[112] but it has not been used to control protein/polymer interactions in a systematic manner. This latter outcome could be quite useful in the design of novel functional biomacromolecules with defined, predictable properties.

Earlier studies from our group showed that protein charge plays a significant role in defining the protein/solid interactions and we hypothesized that protein charge controls the binding enthalpies in a predictable manner.[113],[114] Along these lines, we now test the hypothesis that binding of proteins to charged polymer molecules (polyions) would also depend on protein charge and that chemical modification of the protein can serve as a predictable tool to probe these interactions in a systematic manner by calorimetric methods. Poly(acrylic acid) (PAA), a water-soluble, negatively charged, polymer and met-hemoglobin (Hb) have been chosen as a model system. Previously, cross-linking of Hb with PAA was shown not to perturb Hb structure or it's peroxidase-like activity.[115] Surprisingly, PAA conjugation improved Hb shelf life. Therefore, understanding the

nature of Hb/PAA interactions will be interesting, and it may provide rational approaches to produce functional biomacromolecules with predictable properties.

Hb is negatively charged at pH 7, and its charge can be tuned by converting the carboxyl functions of aspartic and glutamic acid side chains to their corresponding amides. Replacing the negatively charged amino acid side chains, for example, with neutral or positively charged ones alters protein charge in a predictable manner. Control of Hb charge by chemical modification provided a simple method to gain further insight into Hb/PAA interactions.

The carboxyl groups of Hb, in the current study, are amidated with ammonia or triethylenetetramine (TETA) to produce the corresponding charge ladders. The extent of amidation, protein/polymer concentrations, ionic strength and pH are adjusted such that only soluble Hb/PAA complexes are produced.[116,117] This aspect is important because precipitation or insoluble complex formation introduces complications. Data show that the complex formation is exothermic and exothermicity increases with increasing protein charge. More interestingly ITC studies indicated that Hb-TETA/PAA interaction is much more enthalpically favorable than Hb-Ammonia/PAA interaction, even after correcting for the charge. This increase is over above that due to the binding of TETA itself to PAA, and thus, a strong synergistic effect has been established where the TETA s egment enhanced the binding enthalpies by anew mechanism.

3.3 Experimental methods

3.3.1 Materials:

Bovine met-hemoglobin (Hb), polyacrylic acid (PAA, 450, 000 MW), 1-ethyl-3-(3-dimethyl aminopropyl) carbodiimide hydrochloride (EDC), triethylenetetraamine (TETA), NH_4Cl, N-hydroxysuccinimide (NHS), ethanolamine and 2-methoxyphenol were purchased from Sigma Aldrich (St. Louis, MO). β-mercaptoethylamine hydrochloride was obtained from Fisher and used as received. Phosphate buffered saline (PBS, 10 mM phosphate 0.137 M NaCl) at pH 7.4 and 6.4 were used to prepare the solutions.

3.3.2 Isothermal titration calorimetry (ITC):

Energetics associated with Hb binding to PAA were measured using a nanocalorimeter (VP-ITC from Microcal Inc. Piscataway, NJ). PAA (450,000 MW) solution was prepared by dissolving 0.3 mg/ml or 0.03 wt% of PAA (0.7 μM) in distilled water and pH adjusted to 7.4. Hb (486 μM in PBS) and PAA samples were dialyzed against PBS pH 7.4 or PBS pH 6.4. Calorimeter was thermally equilibrated for one hour and dialyzed PAA was loaded into the calorimetric cell (1.4167 ml) while Hb solution has been loaded into the automated syringe. During the experiment, 6 μl aliquots of Hb solution were added in successive injections to PAA solution (0.7 μM) with 300 s intervals, and heat absorbed or released with each injection has been recorded.

The heats of dilution of the protein and the polymer were measured separately and subtracted from the titration data, analyzed by Origin software (v. 5.0, Microcal Inc., Piscataway, NJ). The heat released or absorbed (Q) during the titration is related to the molar heat of protein binding (ΔH), the volume of the sample cell (V_o), the initial concentration of the ligand (X_t), PAA concentration (M_t), the binding constant (K_b), and the number of binding sites (n) by equation 1.[118,119]

$$Q = \frac{nM_t \Delta H V_o}{2}\left[1 + \frac{X_t}{nM_t} + \frac{1}{nK_b M_t} - \sqrt{\left(1 + \frac{X_t}{nM_t} + \frac{1}{nK_b M_t}\right)^2 - \frac{4X_t}{nM_t}}\right]$$

The calorimetric data were fitted to a single set of non-interacting, identical binding sites model and K_b, n, ΔH and ΔS were extracted from best fits to the data to equation 1. The limitations of the above model to fully describe protein binding to various surfaces is well known, and hence, we proceeded to test the validity of the above binding enthalpies by using a direct method, described below. Each titration was performed three times and errors estimated from multiple measurements. Fits to each curve were performed multiple times with different initial values of K_b, n and ΔH to find the best fit, and the values of ΔS and ΔG calculated, using standard equations of thermodynamics.

3.3.3 Model independent method for the determination of binding enthalpies*:* Hb and PAA concentrations were adjusted such that when an aliquot of Hb solution was added to PAA solution, most of the protein binds to PAA to produce soluble protein/polymer complex. Four successive additions of 60 μl Hb solution (4 mg/ml 60 μM, in PBS pH 6.4) into the cell (PAA, 4 mg/ml in PBS pH 6.4) were done at intervals of 300 seconds

each. The injections were separated by 48 seconds of mixing time, at a stirrer speed of 300 rpm. Heat released or absorbed during the reaction time was recorded and the data have been corrected for the corresponding dilutions of Hb and PAA solutions. To factor out the enthalpy changes due to chemical modification, the binding enthalpies of TETA and NH_4Cl ligands (no protein) with PAA were also measured. Each measurement was repeated multiple times and the errors estimated from these.

3.3.4 Dynamic light scattering (DLS):

Hydrodynamic radius of Hb/PAA and Hb-TETA/PAA soluble complexes were measured using CoolBatch+ dynamic light scattering apparatus, where a Precision detector (Varian Inc.,) using a 0.5 x 0.5 cm^2 square cuvette and 658 nm excitation laser source at 90° geometry. Hb and Hb-TETA samples (60 μM) were diluted once and filtered with 0.2-micron filter (PVDF, 13 mm, Fisher Scientific) prior to the measurements. Hb/PAA and Hb-TETA/PAA, soluble complexes from the ITC chamber (8.7 μM protein and 7.7 μM PAA) were diluted 10x and filtered. All samples were equilibrated for 300 s at 26 °C and 5 repetitions with 60 accumulations were done at the same temperature. Precision Elucidate Version 1.1.0.9 was used to run the experiment and Deconvolve Version 5.5 was used to process the data.

3.3.5 Surface plasmon resonance studies for Hb binding to PAA:

Surface plasmon resonance (SPR) was performed using an SR7000DC dual channel flow SPR spectrometer from Reichert Analytical Instruments (Depew, NY) with a semi-automatic injection setup with 500 μL PEEK injection loop and Harvard Apparatus flow pump. The flow cell was setup with a Y-connector to facilitate parallel flow through the

sample and reference channels, at 25°C. The running buffer (PBS, 0.1M phosphate, 0.1M NaCl, 2.7 mM KCl) was thoroughly degassed before use. The data were analyzed using the Scrubber 2.0 software (BioLogic Software, Australia) and Kaleidagraph (Synergy Software, Reading PA).

The bare gold chips were obtained from Reichert (catlog # 13206060) and functionalized with 100 mM β-mercaptoethylamine hydrochloride in ethanol/water (80/20 v/v) mixture (**Scheme 3.1**). The chip was immersed in the solution, purged with nitrogen gas, sealed and equilibrated overnight (12 h) followed by rinsing with ethanol and drying in nitrogen flow. The aminothiol self-assembled monolayer (SAM) covered Au chips were used immediately to avoid oxidation.

The functionalized Au chip was mounted in the Reichert SPR flow cell and PAA was attached to the amine SAM by carbodiimide coupling (**Scheme 3.1**). The carboxylic acid groups of PAA (13.9 mM COOH groups, 1 mg PAA/mL) were activated by flowing a mixture of EDC (100 mM) and NHS (40 mM) over the SAM for 2000 s at a flow rate of 20 μL/min. The functionalized PAA surface was rinsed by washing with PBS buffer (50 uL/min flow rate) until the baseline remained constant. Any remaining activated PAA COOH groups were blocked by reaction with ethanolamine (1 M).

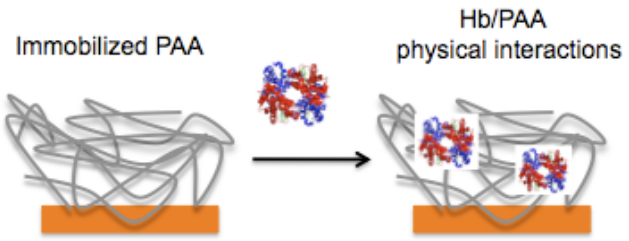

Scheme 3.1. PAA immobilized on SPR Au chip with Hb injections to determine Hb/PAA physical interactions.

Hb solutions (1 to 25 μM, as needed) were flowed over the PAA-coated Au chip for 300 s at a flow rate of 20 μL/min and the association/dissociation curves have been obtained in real time. These kinetic curves were fit to obtain the corresponding k_a and k_d values by Scrubber. The reference channel showed a significant amount of direct binding of Hb to the amine SAM and for this reason the reference curves were not subtracted from the corresponding sample channel curves. To re-cycle the chip, Hb bound to PAA-SAM was removed by injection of NaOH solution (pH 12.5) to wash Hb from the PAA layer on the Au chip and the regenerated polymer surface indicated consistent binding of Hb to PAA during the second and subsequent cycles of Hb binding. Multiple regeneration cycles were used to examine the binding at increasing concentrations of Hb, at a constant loading of PAA on the Au chip. Each measurement was repeated multiple times to obtain errors in the measurements.

3.3.6 Chemical modification of hemoglobin:

Aspartic and glutamic acid residues of Hb were modified by activating them with carbodiimide and by reaction with either ammonium chloride or TETA, by adopting reported methods.[120] Hb (4 mg/ml) dissolved in deionized water (DI) was stirred with the appropriate amine (pH adjusted to 5 or 7) for half an hour followed by the addition of EDC (10 mM). The reaction mixture was stirred for additional 4 h at room temperature and unreacted EDC, amine and byproducts were removed by dialysis against PBS buffer at pH 6.4.

The degree of modification, and therefore the net charge on the modified Hb, was controlled by adjusting the pH (5 or 7) or amine concentration (40 mM to 2.5 M), at a constant reaction time (4 hours, **Table 3.1**). Chemically modified Hb samples are

labeled as Hb-TETA40-7, where the derivative has been obtained by reacting TETA (40 mM) with Hb at pH 7.

Table 3.1. Optimum conditions for the synthesis of Hb derivatives (4 h reaction time).

Sample	Initial [amine] used for the reaction	[EDC]	pH of the reaction
Hb	-	-	-
Hb-TETA40-7	40 mM TETA	10 mM	7
Hb-TETA40-5	40 mM TETA	10 mM	5
Hb-TETA80-5	80 mM TETA	10 mM	5
Hb-TETA60-7	60 mM TETA	10 mM	7
Hb-TETA60-5	60 mM TETA	10 mM	5
Hb-$NH_3$400-5	400 mM NH_4Cl	10 mM	5
Hb-$NH_3$800-5	800 mM NH_4Cl	10 mM	5
Hb- $NH_3$1k-5	1 M NH_4Cl	10 mM	5
Hb-$NH_3$1.5k-5	1.5 M NH_4Cl	10 mM	5

3.3.7 Agarose gel electrophoresis:

Agarose gel electrophoresis was performed using horizontal gel electrophoresis apparatus (Gibco model 200, Life Technologies Inc, MD) and agarose (0.5 % w/w) in Tris acetate (40 mM) buffer. Modified Hb samples were loaded with 50% loading buffer (50% v/v glycerol and 0.01% w/w bromophenol blue). The running buffer was Tris acetate (40 mM) adjusted to specific pHs to determine the isoelectric points of the Hb-derivatives. Samples were spotted into wells placed at the middle of the gel, so that the protein could migrate towards the negative or the positive electrode, based on net charge. A potential of 100 V was applied for appropriate duration, gels were stained overnight with 10% v/v acetic acid, 0.02% w/w Coomassie blue, followed by destaining in 10% v/v acetic acid, overnight.

3.3.8 Circular dichroism measurements:

Structural changes of Hb, if any, upon chemical modification, as well as after complexation with PAA, were monitored using circular dichroism studies. Far UV and soret CD spectra of unmodified Hb, TETA modified Hb and PAA/Hb mixtues were recorded using Jasco 710 spectropolarimeter. Same concentrations of Hb and PAA used for ITC experiments were also used to for CD studies. All samples were in PBS pH 6.4 and the buffer scan was subtracted during processing. Step resolution was kept at 0.2 nm/data point and bandwidth and sensitivity were 1 nm and 20 millidegrees, respectively. When collecting far UV CD spectra each sample was scanned from 200 nm to 260 nm and scan speed was maintained at 50 nm/min. Average of four accumulations was recorded using 0.05 cm pathlength cuvette. For the soret CD spectra,

samples were scanned from 350 to 450 nm at a scan speed of 50 nm/min, 0,2 cm path length, and eight accumulations were averaged.

3.3.9 Hemoglobin peroxidase-like activity studies:

Peroxidase-like activity of Hb was used to compare the activities of Hb in the presence and absence of PAA. The substrate, O-methoxyphenol (5 mM) and the oxidant, H_2O_2 (0.5 mM) were added to the solution containing 1 μM Hb in PBS, pH 6.4. Absorbance at 470 nm, due to the product formation, was monitored as a function of time, using HP 8453 diode array spectrophotometer (Agilent Inc., Totowa NJ).[121] From the plots of absorbance vs. time, initial velocities and specific activities were calculated and the activities compared under the same conditions of pH, ionic strength, substrate concentration and temperature.

3.4 Results

The hypothesis that chemical modification of proteins serves as a convenient method to systematically modulate hemoglobin-PAA interactions has been tested here. Chemical modification with TETA, for example, served to probe the contributions of charge and TETA segments to these interactions which revealed strong synergy.

3.4.1 Energetics of Hb binding to PAA:

Using Hb as a model protein and PAA as a model polymer, we examined the binding of Hb to PAA to form a soluble complex, under a specific set of conditions by isothermal titration calorimetry (ITC). Exothermic binding of Hb to PAA, at pH 7.4 in PBS buffer, was demonstrated in **Figure 3.1**, and binding saturated at a Hb to PAA mole ratio of ~14.

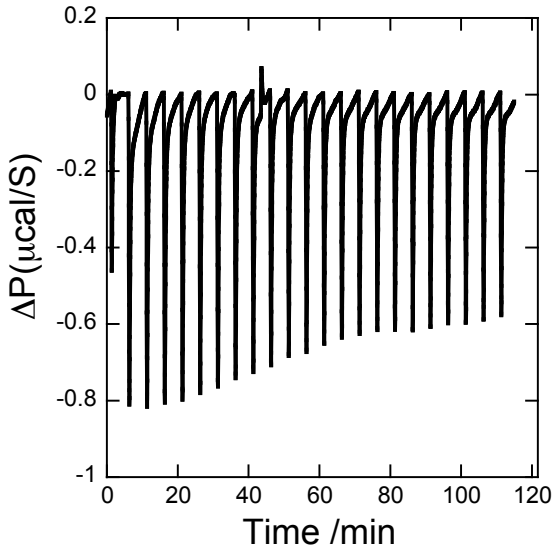

A

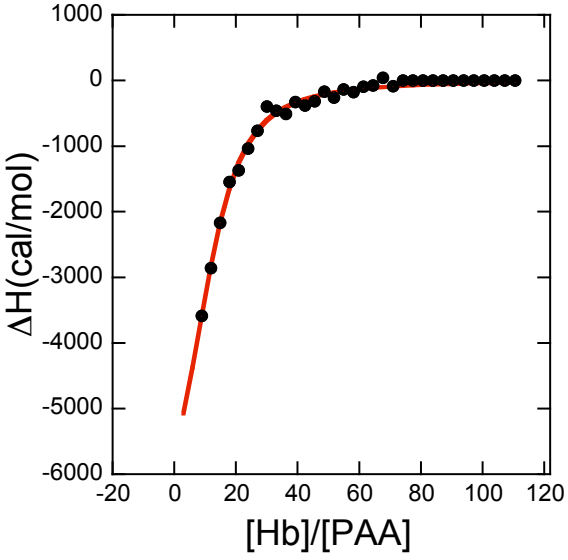

B

Figure 3.1. Titration of Hb (486 μM) with PAA (0.7 μM) in PBS, pH 7.4 at 25 ˚C. (A) Change in power vs time plot when PAA solution was titrated with Hb solution. (B) Enthalpy change vs [Hb]/[PAA] for titration. Red line is the best fit to the data, according to the single, identical, non-interacting binding site model. Best fit indicated a binding stoichiometry of 14 Hb per mole of PAA, binding constant of 3.2×10^5 M^{-1}, ΔH and ΔS values of -7.4 kcal/mol of Hb bound and 0.1715 cal/mol, respectively.

Enthalpy change associated with each addition of Hb solution to PAA solution was plotted as a function of the ratio of molar concentrations of Hb to PAA **(Figure 3.1B**, black dots), and the data were fitted to a single set of indistinguishable, non-interacting binding sites model (**Figure 3.1B,** red curve, using equation 1). The best fit to the data indicated K_b, ΔG, ΔH, ΔS and the binding stoichiometry to be $3.2\pm0.75 \times 10^5$ M^{-1}, -7.3± 0.95 kcal/mol, -7.4±0.2 kcal/mol, 0.17 cal/mol and 14 Hb molecules bound per each PAA molecule, respectively. Hb binding to PAA is exothermic, with significant affinity, and large loading on the polymer of 14:1 protein to polymer (monomer) mole ratio, and the binding is primarily enthalpy driven (-7.4±0.2 kcal/mol) but it is also entropy favored. The above single-site binding model assumes that there are no interactions between the bound protein molecules and that the binding sites on PAA are non-overlapping. Introduction of these assumptions simplifies data analysis but could introduce potential errors in the estimated parameters.[122,123] Hence, we have used a model-independent method to measure binding enthalpies, directly, and compared them with these values, as described later. The binding enthalpy determined above, is in good agreement with the values obtained from the direct measurement, described below.

3.4.2 SPR Studies:

Hb binding to PAA is also verified by SPR studies. PAA was immobilized on Au chip using the amino-thiol SAM and EDC coupling (**Scheme 3.1**), and from the SPR signal of 500 μRIU, and the conversion factor of one microRIU corresponds to 0,73 ng/mm^2 of mass,[124] we estimate that 365 ng of PAA was attached to one square millimeter. Using the known density of PAA,[125] we estimate an average polymer layer thickness of 300 nm and this is a lower limit on the PAA film thickness, as the polymer can swell substantially due to hydration as well as the pH of the medium. PAA film was used to monitor Hb binding by SPR. Flowing Hb solutions over the PAA surface in the sample channel resulted in huge SPR signal increases, while the reference channel indicated only weak signals. We monitored the on- and off-rates of Hb binding to the PAA SAM (**Figure 3.2**) and best fits to the data indicated on- and off-rate constants of $1.2x10^3$ $M^{-1}s^{-1}$ and $2.8x10^{-3}$ M^{-1}, respectively (5 μM, PBS, pH 7.2) to PAA film. The ratio of the on- to off-rate constants, the binding constant, is 7.1×10^5 M^{-1} and this value is comparable to that obtained from the ITC data, $3.2\pm0.7 \times 10^5$ M^{-1}. Therefore, the calorimetric and SPR measurements agree reasonably, and indicate substantial interaction of Hb with PAA but note that SPR cannot provide direct enthalpy measurements.

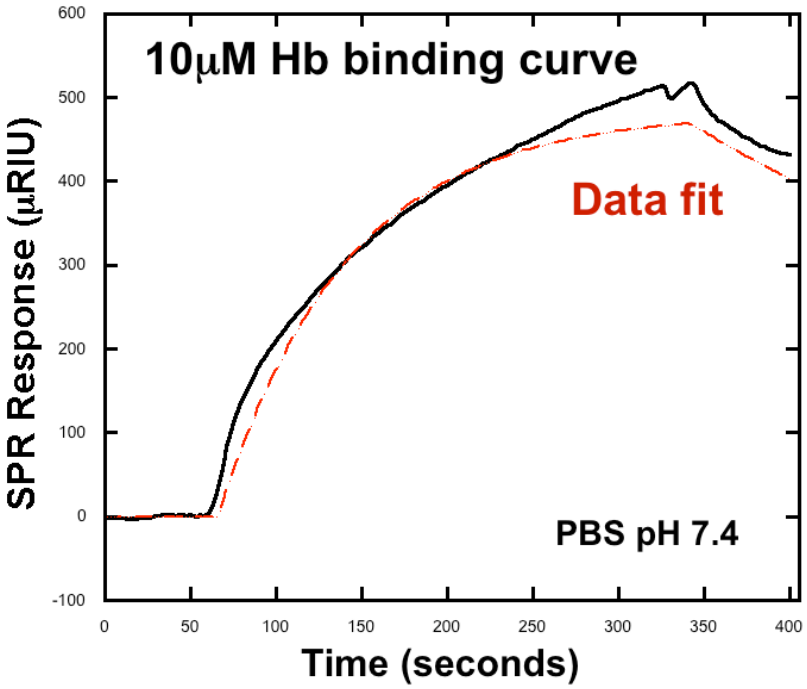

Figure 3.2. Hb association dissociation curve for 10μM Hb binding to PAA in PBS pH 7.4 (500μRIU PAA immobilized). (black – Hb binding curve, red- data fit by Scrubber software)

3.4.3 Chemical Modification:

Several factors could contribute to the observed Hb and PAA interactions, and chemical modification is a convenient tool to evaluate specific contributions to these interactions. For example, the conversion of the COOH groups of the aspartate and glutamate residues of Hb to the corresponding amides would neutralize at least one negative charge per COOH modified (**Scheme 3.2**). For example, amidation with TETA would lower the protein negative charge by the conversion of COOH groups to the corresponding amides, and additional charge neutralization can occur by the protonation of the basic nitrogens of TETA. Thus, chemical modification provided an appealing method to continuously tune net charge of Hb at constant pH and ionic strength, in a systematic and predictable manner.

Hb was reacted with increasing concentrations of TETA or NH_4Cl under specific conditions of pH, temperature, amine concentration and reaction time, using EDC chemistry **(Scheme 3.2)**. Nine different Hb-TETA and Hb-Ammonia derivatives were prepared successfully, and they have been purified by extensive dialysis to remove unreacted reagents and by-products. The progress of Hb modification has been monitored by agarose gel electrophoresis, described below.

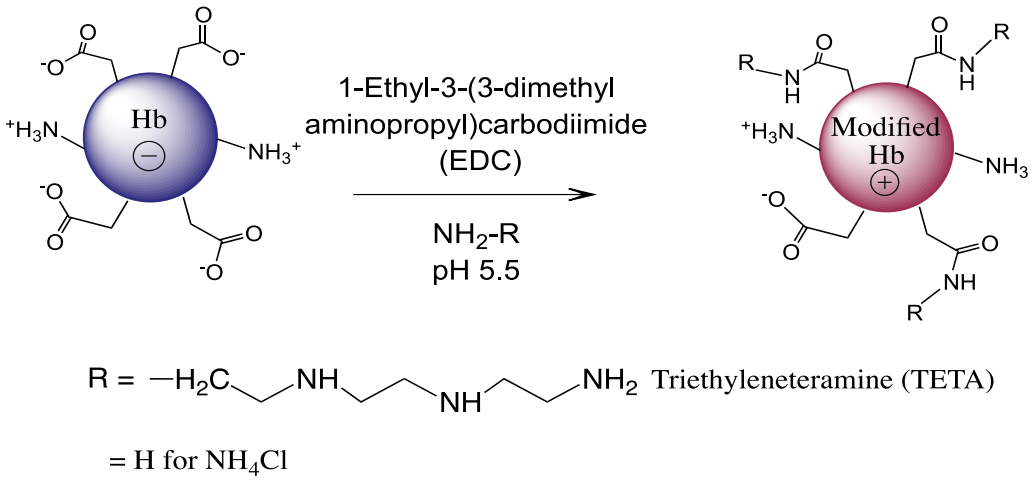

Scheme 3.2 : Chemical modification of Hb COOH groups via EDC chemistry.

3.4.4 Agarose gel electrophoresis:

Chemical modification altered the net charge on Hb, as monitored in agarose gels (**Figure 3.3**), and modified samples began to migrate toward the cathode. The samples were loaded into wells at the center of the gel, and Hb did not migrate out of the wells (lane 1, **Figure 3.3**). The isoelectric point (pI) of Hb is ~6.77[126] , at pH 7 Hb is nearly neutral, and hence, it did not move out of the well. As the extent of amidation increased with increasing TETA concentration, the net negative charge on the Hb-derivative decreased, or positive charge increased, and samples began to migrate towards the cathode (lanes 2-4, **Figure 3.3**). All the Hb-TETA samples migrated toward the cathode, directly proving that they bear net positive charge. Thus, Hb-TETA charge ladder consisting of Hb-TETA40-7, Hb-TETA40-5 and Hb-TETA80-5 are produced successfully.

The reaction of ammonia with Hb facilitated by EDC chemistry, under specific reaction conditions (**Table 3.1**), also resulted in a charge ladder of Hb-Ammonia derivatives (lanes 5-8). Note that these samples, although migrated toward the cathode, better than Hb, bore less positive charge when compared to those of the Hb-TETA derivatives. Nevertheless, Hb-Ammonia derivatives also indicated better mobilities than Hb.

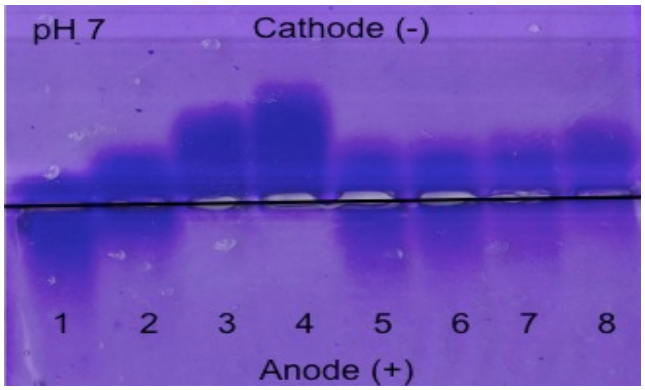

Figure 3.3. Agarose gel electrophoresis of Hb-TETA and Hb-Ammonia derivatives at pH 7 (samples spotted at the center of the gel). Lane 1 is Hb and lanes 2-4 are Hb-TETA40-7, Hb-TETA40-5 and Hb-TETA80-5, respectively, while lanes 5-8 are the Hb-Ammonia derivatives, Hb-Ammonia400-5, Hb-Ammonia800-5, Hb-Ammonia1k-5, Hb-Ammonia1.5k-5, respectively, produced under specific reaction conditions.

The electrophoresis data are consistent with progressive conversion of Hb to Hb-TETA or Hb-Ammonia derivatives with decreasing negative charge or increasing positive charge, as the case may be. Thus, chemical modification has successfully produced two different charge ladders of Hb-derivatives where the protein charge was controlled in a gradual and systematic manner.

3.4.5 Charge and isoelectric points of Hb charge ladders:

Since the mass difference between Hb and Hb-derivatives is negligible, migration distance of each band in the agarose gel is proportional to its charge.[127] Therefore, agarose gels were run at specific pH values (**Figure 3.4 & 3.5**) and at each pH, certain samples migrated toward the positive or negative electrode. Using the known charge of Hb[126] , charges of all Hb-derivatives were determined (**Table 3.2 & 3.3**).

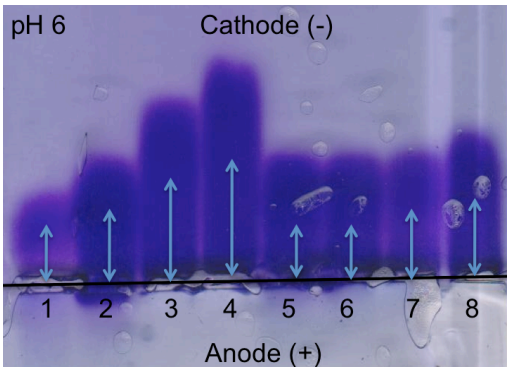

A

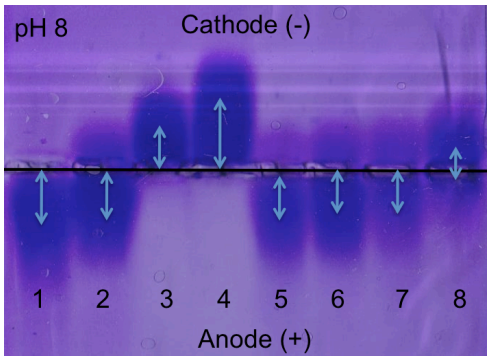

B

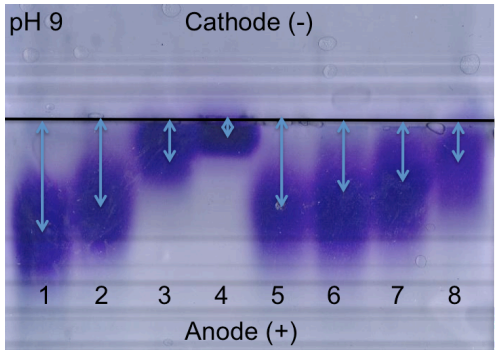

C

Figure 3.4. Agarose gels of chemically modified hemoglobin derivatives at pH 6, 8, and 9 (A through C respectively). Lane 1 in each gel is Hb and lanes 2, 3, & 4 are Hb-TETA40-7, Hb-TETA40-5 and Hb-TETA80-5 respectively. Lanes 5-8 are Hb-NH_4Cl400-5, Hb-NH_4Cl800-5, Hb-NH_4Cl1k-5, Hb-NH_4Cl1.5k-5, respectively. Mid point of each protein band as indicated was taken as the distance migrated in the agarose gel. Distance and charge relationship of the modified Hb derivatives, relative to the distance and charge of Hb, were calculated using imageJ 1.46r software from NIH and tabulated in **Table 3.2.**

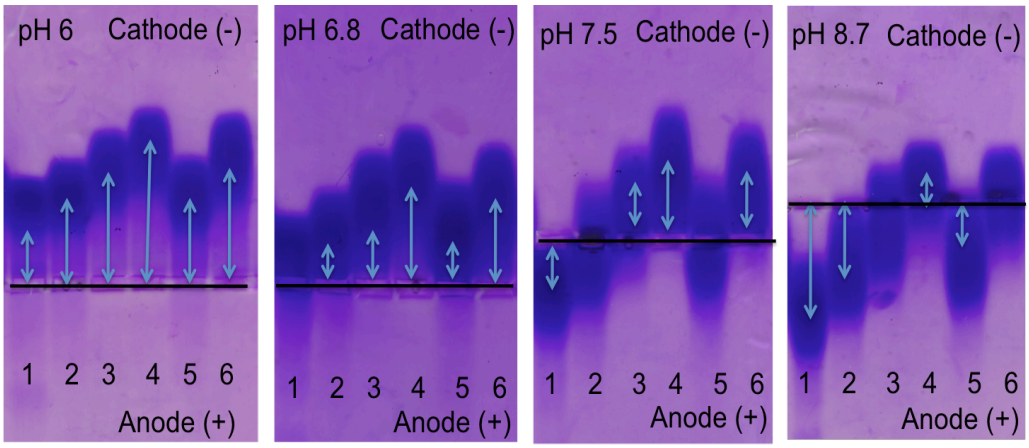

Figure 3.5. Agarose gels of chemically modified hemoglobin derivatives at pH 6, 6.8, 7.5 and 8.7. Lane 1 in each gel is Hb and lanes 2, 3, 4, 5and 6 are Hb-TETA40-7, Hb-TETA40-5 , Hb-TETA80-5, Hb-TETA60-7 and Hb-TETA60-7 respectively. Mid point of the protein band in lane 5 and 6 was taken as the distance migrated in the agarose gel. Distance and charge relationship of the modified Hb derivatives, relative to the distance and charge of Hb, were calculated using imageJ 1.46r software from NIH and tabulated in **Table 3.3**.

Table 3.2 Average charge of modified Hb were calculated from the distance charge relationship relative to the unmodified Hb.

Sample	Average charge at pH 6	Average charge at pH 8	Average charge at pH 9
Hb	+10	- 10	-20
Hb-TETA40-7	+15	-8.8	-15
Hb-TETA40-5	+21.6	+6.46	-6.2
Hb-TETA80-5	+26.6	+9.4	-3.1
Hb-$NH_3$400-5	+15	-8.2	-18.1
Hb-$NH_3$800-5	+15.4	-7.6	-16.9
Hb-$NH_3$1k-5	+15.8	-5.9	-11.2
Hb-$NH_3$1.5k-5	+18.3	+1.1	-8.1

Table 3.3 Average charge of modified Hb were calculated from the distance charge relationship relative to the unmodified Hb.

Sample	Average charge at pH 6	Average charge at pH 6.8	Average charge at pH 7.5	Average charge at pH 8.7
Hb-TETA60-7	+16.2	+ 10	0	-12.6
Hb-TETA60-5	+25	+ 15	+8	0

When pH of the running buffer is equal to the pI of the protein, net charge on the protein will be zero, and the sample will not move out of the loading well, under the influence of the applied electric field. Therefore, charge obtained from the band mobility of each sample was plotted as a function of pH, and from these plots we obtained the pH at which the charge on the protein is zero (pI value) (**Figure 3.6, Table 3.4**). The pI values of the samples, for example, increased from ~7 to ~9, with increased chemical modification, and chemical modification successfully resulted in the construction of Hb charge ladders.

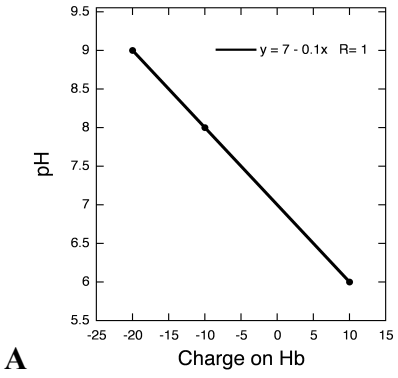
y = 7 - 0.1x R= 1
pH
Charge on Hb

A

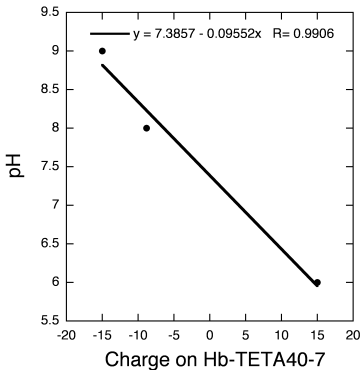
y = 7.3857 - 0.09552x R= 0.9906
pH
Charge on Hb-TETA40-7

B

C

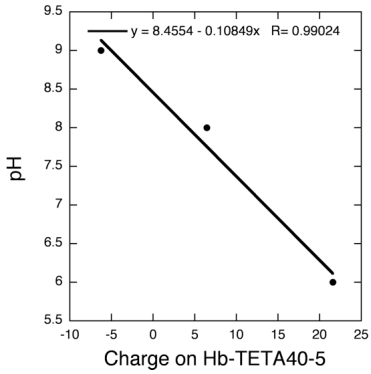
y = 8.4554 - 0.10849x R= 0.99024
pH
Charge on Hb-TETA40-5

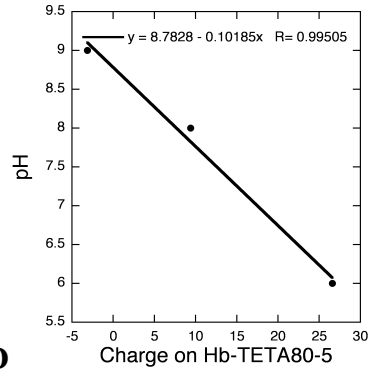
y = 8.7828 - 0.10185x R= 0.99505
pH
Charge on Hb-TETA80-5

D

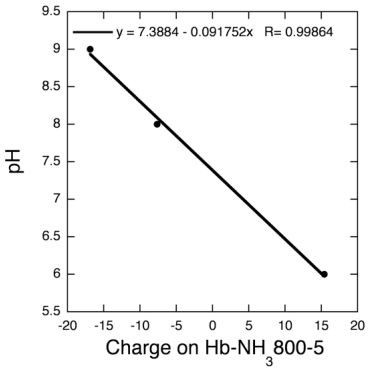
y = 7.3884 - 0.091752x R= 0.99864
pH
Charge on Hb-NH3 800-5

E

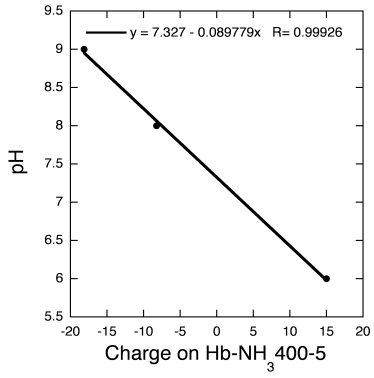
y = 7.327 - 0.089779x R= 0.99926
pH
Charge on Hb-NH3 400-5

F

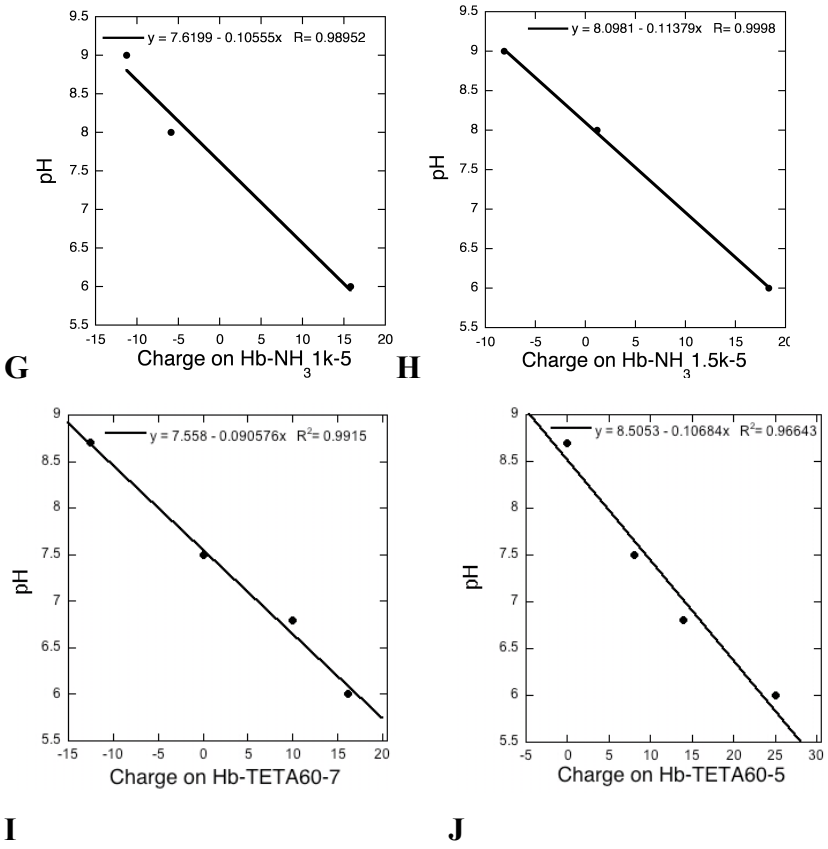

Figure 3.6. Plot of pH vs charge of Hb and Hb-TETA and Hb-NH_4Cl derivatives. Y Intercept of each curve was taken as the isoelectric point (pI). Charge of each derivative at pH 6.4 where ITC measurements were take were also extracted from the plot.

Table 3.4. Key properties of Hb-derivatives. The isoelectric points (pI), average charge at pH 6.4, and binding enthalpies (kcal/mol), in PBS, pH 6.4, at 25 ˚C.

Sample	pI	Charge at pH 6.4	ΔH (kcal/mol)
Hb	7	+6	-8 ± 0.2
Hb-TETA40-7	7.4	+10 ± 0.5	-45 ± 2
Hb-TETA40-5	8.4	+19 ± 1	-55 ± 3
Hb-TETA80-5	8.8	+23 ± 1	-89 ± 4
Hb-TETA60-7	7.5	+14 ± 0.5	-28.9 ± 4.1
Hb-TETA60-5	8.7	+22 ± 1	-68.04 ± 8.8
Hb-NH_4Cl400-5	7.3	+10 ± 0.5	-10 ± 0.9
Hb- NH_4Cl800-5		+10.8 ± 0.5	-14 ± 0.4
Hb- NH_4Cl1k-5		+11.6 ± 0.5	-16 ± 0.9
Hb- NH_4Cl1.5k-5		+15 ± 0.5	-17 ± 1.5

3.4.6 Circular dichroism studies:

In order to assess any distortions in secondary and tertiary structure of Hb in Hb-TETA derivatives due to chemical modification, circular dichroism spectra of the samples were compared with that of the unmodified Hb. The UV-CD spectra are highly sensitive to the changes in protein secondary structure and they serve as excellent probes to examine protein structure.[128] The UV CD spectra of Hb spectra has a strong peak maximum at 190 nm and double minima at 208 nm and 222 nm.[129] The CD spectra of Hb-TETA derivatives overlapped with that of the unmodified Hb, reordered under same conditions (**Figure 3.7**). Thus, the secondary structure of Hb has largely been retained after chemical modification with TETA. Similarly, the CD spectra of Hb-TETA derivatives reordered in the presence of PAA, showed that the spectra nearly well overlapped with that of Hb, except for a minor distortion in the case of Hb-TETA80-5/PAA (**Figure 3.8**). Hence, the majority of the samples, retained their structure after chemical modification and binding to PAA.

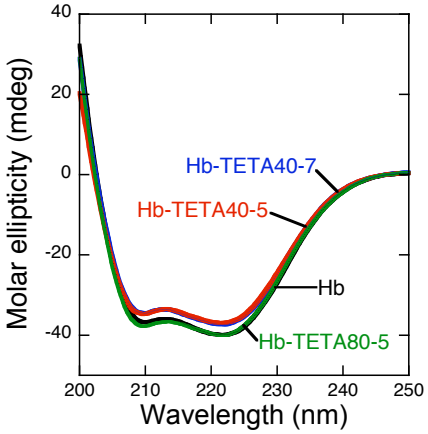

Figure 3.7. Far UV CD spectra of unmodified Hb (black line), Hb-TETA40-7 (Blue line), Hb-TETA40-5 (Red line) and Hb-TETA80-5 (Green line). All samples contained same amount of protein in PBS pH 6.4 buffer. Note that the peak positions and intensities of Hb did not change upon chemical modification.

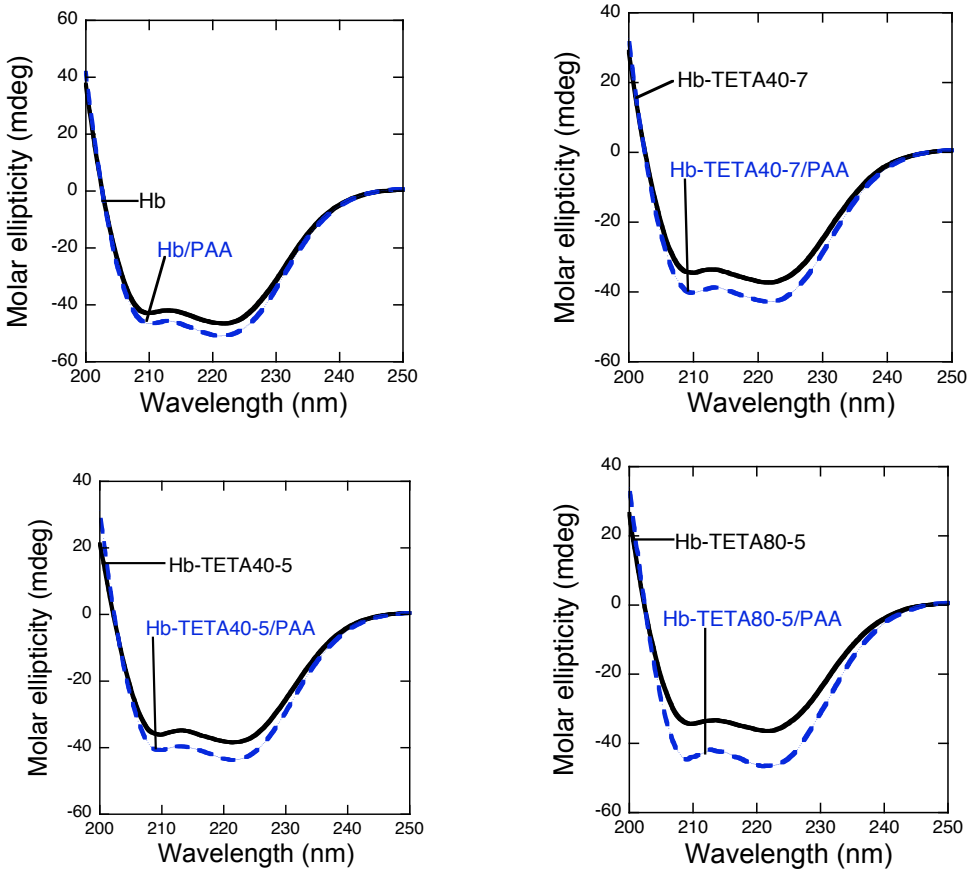

Figure 3.8. Far UV CD spectra of unmodified Hb and Hb-TETA derivatives in the absence (black line) and in the presence (Blue dash line) of PAA. All samples contained same amount of protein and PAA that was used for ITC measurements and were in PBS pH 6.4 buffer. CD spectra imply that there are no major distortions in protein secondary structure when bound to PAA.

We also examined the structure by recording the Soret CD, which is a sensitive measure of the asymmetry of the heme environment. The Soret CD spectra of the Hb-derivatives and their complexes with PAA (**Figure 3.9**). Since peak positions and intensities are the same, the heme coordination environment is well preserved when the protein was modified or modified protein was bound to PAA. Encouraged by the fact that PAA did not distort the structure of Hb or Hb-TETA derivatives to a significant extent, only minor changes noted, we proceeded to examine the binding enthalpies.

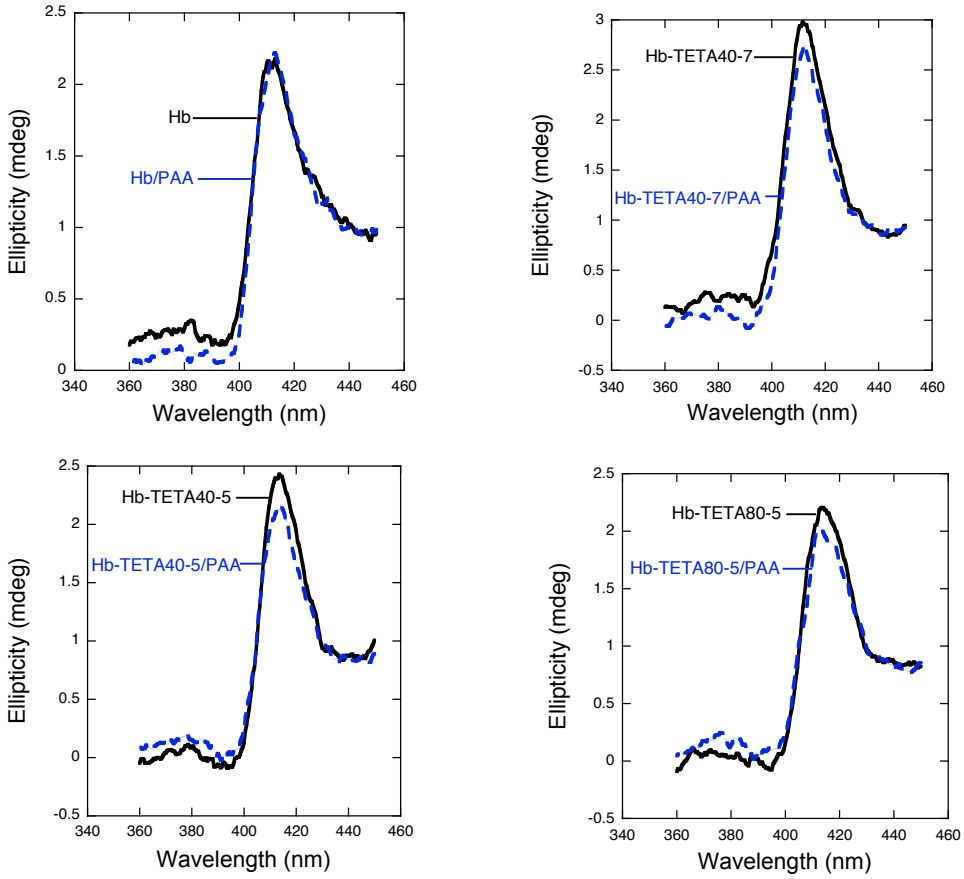

Figure 3.9. Soret CD spectra of unmodified Hb and Hb-TETA derivatives in the absence (black line) and in the presence (Blue dash line) of PAA. All samples contained same amount of protein and PAA that was used for ITC measurements and were in PBS pH 6.4 buffer.

3.4.7 Model-independent binding enthalpies:

As mentioned earlier, the estimation of the binding enthalpies from ITC curves using the model dependent method could introduce potential errors due to the tacit assumptions made in the model. Hence, we chose to measure the binding enthalpies of the Hb-derivatives with PAA, directly by the model independent method. The protein and polymer concentrations have been chosen such that each addition of the protein solution resulted in complete binding to PAA. The heat released or absorbed, under these conditions, was corrected for dilution, and the corresponding binding enthalpies evaluated.

The calorimetric curves representing the addition of Hb-TETA80-5 to PAA (black), Hb-TETA80-5 dilution (blue) and PAA dilution (red), in PBS at pH 6.4, are shown in **Figure 3.10 A**. The area under the peak for each injection (q) was used to calculate the binding enthalpy ($\Delta H_{Hb/PAA}$) and appropriate corrections have been made for the dilution enthalpies of the polymer (ΔH_{PAAdil}) and the protein (ΔH_{Hbdil}), using equation 2. The resulting, corrected binding enthalpies per mol of Hb-TETA80-5 bound to PAA (**Figure 3.10 B**) was extracted to be -89$\pm$4 kcal/mol (**Table 3.4)**.

$$\Delta H_{Interaction} = \Delta H_{Hb/PAA} - (\Delta H_{PAAdil} + \Delta H_{Hbdil}) \text{ ---------- (2)}$$

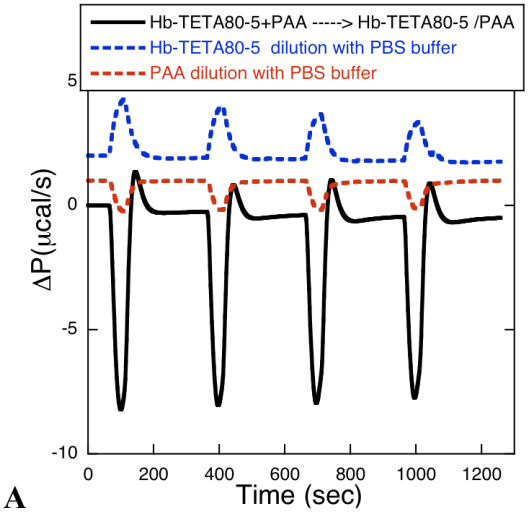

A

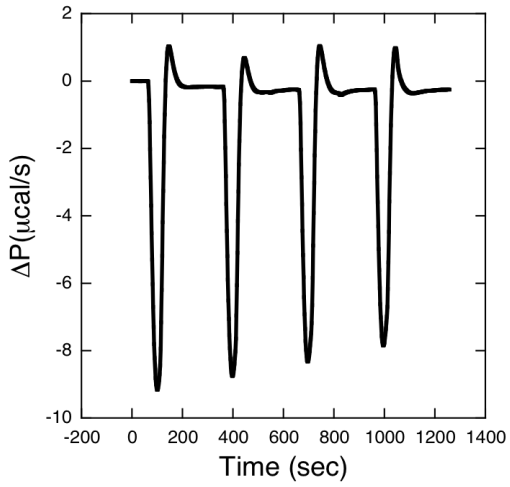

B

Figure 3.10. **A**. Change in power due to the addition of Hb-TETA80-5 (60 μM) to PAA (9 μM, polymer) (black curve), the dilution of Hb-TETA80-5 (60 μM) (blue curve), and dilution of PAA (9 μM) (red curve). **B**. Change in power due to the binding of Hb-TETA80-5 to PAA, after correcting for the dilutions of Hb-TETA80-5 and PAA (PBS, pH 6.4, 25 ˚C). These peaks were integrated to extract the corresponding ΔH values.

The binding enthalpies of Hb and all Hb-TETA derivatives were measured by this method, at pH 6.4, and their binding to PAA has been strongly exothermic. The binding enthalpies, measured under the same conditions of ionic strength, pH and temperature, varied from -45 to -89 kcal/mol (**Table 3.4**). The binding enthalpy of Hb measured by the titration method was -7.4±0.2 kcal/mol, which is in good agreement with the value obtained from direct method (-8.0±0.2 kcal/mol, Table 4.4). None of these protein/polymer complexes precipitated under these conditions, and proper corrections were done for dilution to obtain heat release due to protein interactions with PAA.

The Hb-TETA/PAA binding enthalpies are analyzed with respect to the protein charge, and plot of the binding enthalpies vs their charge was shown in **Figure 3.11** (blue dots). These showed a strong trend, and linear fit to the data had a slope of – 3.8 kcal/mol per unit charge. The steep, favorable, dependence of ΔH on protein charge, was observed with the TETA derivatives, and TETA modification substantially increased the binding exothermicity.

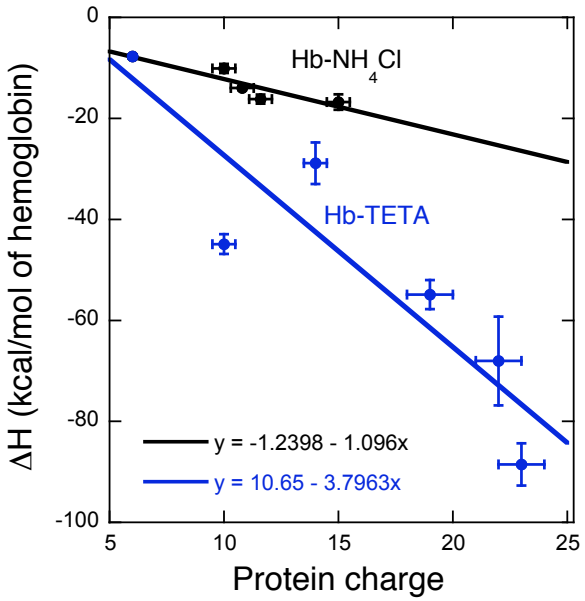

Figure 3.11. Binding enthalpies of Hb-TETA (blue dots) and Hb-Ammonia derivatives (black dots) (60 μM) to PAA (9 μM) as a function of their charge. Slopes of the linear fits to the TETA and ammonia derivatives are – 3.8 and -1.0 kcal/mol per unit charge, respectively (PBS, pH 6.4, 25 ˚C).

3.4.8 Binding enthalpies of the Hb-Ammonia derivatives:

Several factors contribute to the binding enthalpies measured above, and to separate the enthalpy contributions from protein charge vs the specific interactions of TETA side chains, we measured the binding enthalpies of similarly charged Hb-derivatives prepared from the chemical modification with ammonium chloride, rather than TETA. The TETA side chains may specific contributions to the binding enthalpies, and these have been evaluated using the Hb-Ammonia charge ladder.

The binding enthalpies of the members of the Hb-Ammonia charge ladder were obtained, under identical conditions of pH, ionic strength, and temperature as those of the TETA derivatives. Concentrations and the extent of modification have been adjusted such that all protein/PAA complexes were completely soluble and there has been no precipitation. The binding of this charge ladder was also exothermic, but the exothermicity increased much more slowly from -10 to -17 kcal/mol, while their charge varied over a range of +10 to +15 (**Table 3.4**), at the same pH, buffer and ionic strength. A plot of the binding enthalpies of the ammonia derivatives vs charge (black dots, **Figure 3.11**) was also linear but had a slope of -1 kcal/mol per unit charge. Magnitude of this slope is ~4 times smaller than that noted for the TETA derivatives. Therefore, it is clear that appending TETA to Hb has a strong synergistic effect to the binding enthalpies.

3.4.9 Activities of polymer-protein complexes:

The anomalous binding enthalpies of Hb-TETA derivatives could be due to extensive unwinding of the protein, before or after interaction with the oppositely charged PAA molecules. Therefore, we set out to assess the biological activities of the Hb-derivatives

and their complexes with PAA. Hb does not function as an enzyme in nature, but its peroxidase-like activity is well documented.[130] Therefore, the peroxidase-like activities have been determined, and compared, under the same conditions of pH, ionic strength, buffer and temperature.

The catalytic activities of Hb-TETA samples and Hb-TETA/PAA physical mixtures were determined using o-methoxyphenol as the substrate and H_2O_2 as the oxidant. Absorbance change at 470 nm due to product formation was monitored, as a function of time (**Figure 3.12**). All samples indicated a high degree of activity, and chemical modification did not inhibit their activities to a significant extent. Specific activities were determined from the initial rates of the activity curves, and these ranged from 0.74 to 0.94 per μM per s (**Table 3.5**).

The Hb-TETA derivatives also retained their activities after complexation with PAA, and these have been compared with those obtained in the absence of the polymer (**Figure 3.13**). The specific activities of the Hb-TETA/PAA complexes varied from 118 to 90% of that of Hb, and some of them improved slightly when compared to that of Hb. Therefore, neither chemical modification nor complexation with PAA had significant effect on the peroxidase-like activities of the Hb-TETA charge ladder.

The excess enthalpy change observed for Hb-TETA derivatives is not due to the distortion or denaturation, or precipitation of the protein-polymer complexes. It must be originating from intrinsic interactions between the modified protein and the polymer.

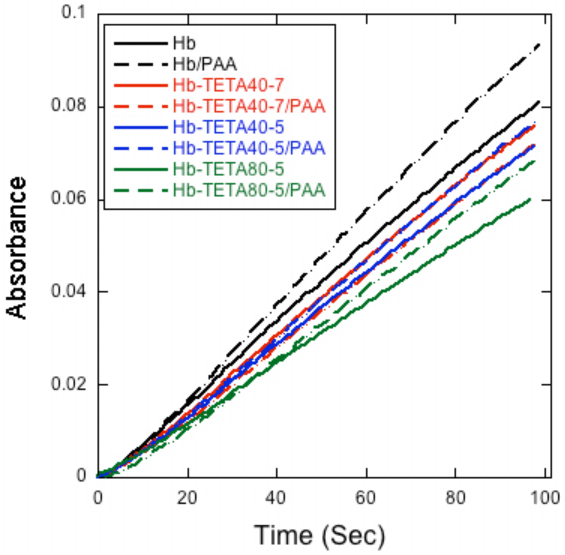

Figure 3.12. Comparison of activities of modified and unmodified Hb (1 μM) in the presence and absence of PAA (0.15 μM) in PBS buffer pH 6.4 at room temperature

Table 3.5 Specific activities of Hb-TETA derivatives and their complexes with PAA ($\mu M.s \times 10^3$)

Sample	Activities (proteins)	% Activity	Activities (protein/PAA complexes)	% Activity Retention
Hb	0.93 ± 0.06	100	1.08 ± 0.06	116 ± 6.4
Hb-TETA40-7	0.94 ± 0.028	100 ± 3	1.1 ± 0.02	118 ± 2.1
Hb-TETA40-5	0.89 ± 0.04	96 ± 4.3	0.91 ± 0.04	0.98 ± 4.3
Hb-TETA80-5	0.74 ± 0.01	80 ± 1.1	0.87 ± 0.02	0.93 ± 2.1

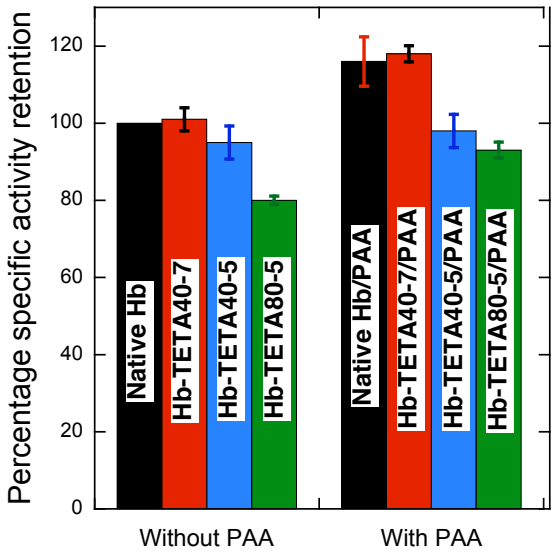

Figure 3.13. Relative activities of Hb-derivatives (1 μM) in the presence or absence of PAA (0.15 μM), with respect to that of Hb, in PBS, pH 6.4, at 25 ˚C.

3.5 Discussion

Unlike the interaction of a small, charged ligand with polymers, the interaction of proteins with polymers is more complicated. The presence of twenty different amino acid building blocks of the protein introduce various chemical and physical properties to the protein, and these make it a complex moiety to study. For example, the use of different proteins with specific charges to study the charge dependency on protein-polymer complex formation, at a particular pH, is complicated, since each protein has a unique way of folding which results in variability of the hydrophobic and charged patches on the protein surface.

Many factors could contribute to the formation of soluble protein/polymer complexes,[109,110,131] and electrostatic interactions have been implicated to play a major role.[117] Contributions of interactions other than electrostatic interactions is much less understood.[132] Hydrophobic interactions were shown to play a major role in the binding of bovine serum albumin (BSA) to hydrophobically modified PAA.[133] Gelation and precipitation of proteins by polymers are suggested to be due to hydrophobic interactions between proteins and polymers.[134,110,135] H-bonding and electrostatic interactions, hydration or dehydration or ion release or ion uptake were implicated in protein binding to inorganic polymeric materials.[113,114]

As a model system, here, we first examined the binding of Hb with a water-soluble weak polyelectrolyte, PAA (MW 450,000). Binding constant from data for Hb/PAA soluble complex formation is $3.2\pm0.7 \times 10^5\ M^{-1}$, which is in fair agreement with the binding constant obtained from SPR ($7.1 \times 10^5\ M^{-1}$). This value is similar to the binding constant observed with calf thymus DNA, anionic biopolymer, of $4.9 \times 10^5\ M^{-1}$, in Tris buffer at pH 7.0.[136] On the other hand, the binding constant of Hb with α-Zr(IV)

phosphate, anionic rigid, inorganic polymer, was reported to be 5.4×10^6 M^{-1}, an order of magnitude higher than observed with PAA.[137] Note that this solid is strongly negatively charged, one negative charge per 25 $Å^2$, and higher binding consistent with the idea that electrostatic interactions contribute substantially for Hb binding to its partners. In support of this notion, positively charged lysozyme was reported to bind to PAA with comparable affinities.[105]

From the observed stoichiometric ratio of 14:1, we propose that each Hb molecule occupies nearly 120 nm along the PAA chain, spanning 400 monomeric units, and that PAA wraps around the protein (beads-on-a-string model) due to favorable interactions with surface groups of the protein. The positively charged patches on Hb could interact favorably with the negatively charged carboxyl groups of PAA.

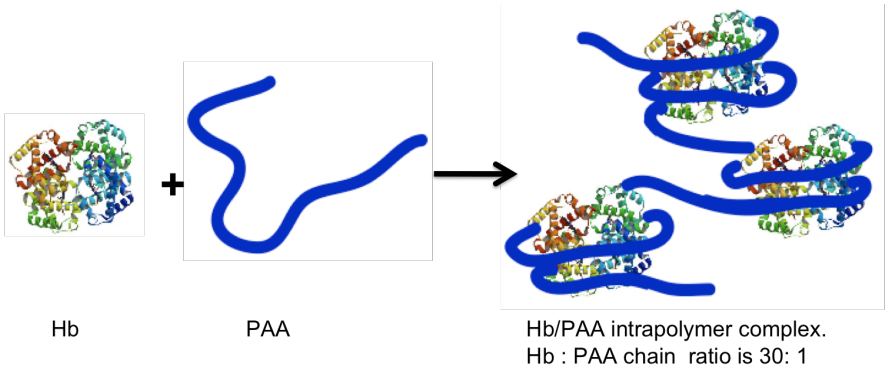

Scheme 3.3. Schematic representation of soluble intrapolymer complex formation between Hb and PAA.

According to the ITC data, the binding of Hb to PAA is exothermic (-7.4 kcal/mol, obtained at pH 7.4 in PBS) and the enthalpy change could be due to patches of positive charges on its surface despite its weak negative charge at pH 7.4 (pI ~7). When the pH was dropped to 6.4, the ΔH decreased from -7.4±0.2 to -8±0.4 kcal/mol, and this is consistent with the fact that Hb is slightly positively charged at pH 6.4 and greater electrostatic interactions contribute at lower pH. The binding of Hb to calf thymus DNA was weakly endothermic (ΔH=3.1 kcal/mol) at pH 7 in Tris buffer.[136] Along these lines, the binding of Hb to α-Zr(IV) phosphate was found to be strongly exothermic -24 kcal/mol, at pH 7.2, in phosphate buffer[114] due to the high charge density of this solid, as discussed earlier. The binding enthalpy for the interaction of strongly positively charged lysozyme to PAA (MW, 240,000) was reported to be -10 kcal/mol, at pH 5.5, and also supports the role of electrostatic interactions in its binding to PAA.[105] Thus, binding enthalpies or entropies differed in terms of the type of host material, pH, molecular weight of PAA and the buffer used for the studies. Therefore, we decided to chemically modify the net charge on Hb, and examine the trends in the binding parameters with PAA as a model polymer, under a consistent set of conditions to gain insight into the binding.

To evaluate the role of electrostatic interactions in these, at constant pH and ionic strength, without using different proteins or different host materials, we have prepared a number of Hb-derivatives of two separate charge ladders, TETA and ammonia. Note that modification of Hb with ammonium chloride would convert the glutamic or aspartic COOH groups to the corresponding CO-NH_2 groups, while reaction with TETA would produce CO-TETA groups on the protein. The basic nitrogens of TETA can be potentially protonated to produce additional positive charges. Therefore, these

differences are to be kept in mind in the interpretation of the observed data. At a given pH, the net charge on the protein is systematically varied to study its contribution to the binding interactions.

Hb modification with TETA resulted in the charge ladder (**Figure 3.3**), which indicated progressive decrease of binding enthalpies from -8±0.2 kcal/mol for Hb to -89±4 kcal/mol for Hb-TETA80-5 (**Figure 3.11**). The slope of the linear fit to these data indicated enthalpy decreases of -3.8 kcal/mol per unit charge. In contrast, the enthalpy decrease noted with the Hb-Ammonia ladder has been from -8±0.2 for Hb to -17+1.5 kcal/mol for Hb-Ammonia1.5k-5 with a slope of -1.0 kcal/mol per unit charge. The latter value is in good agreement with reported values for coulombic interactions, ΔH_{Ele} [105] but it is much smaller than noted for Hb-TETA charge ladder.

This discrepancy between the two sets of data could be attributed to additional contributions from the TETA ligand, such as hydrogen bonding with the amino groups and hydrophobic interactions from the ethyl segments of TETA (**Scheme 3.4**). To test this hypothesis, we have examined TETA binding to PAA by ITC, under identical conditions of pH, ionic strength and temperature. The binding of TETA to PAA was also exothermic with a ΔH of -2 kcal/mol per TETA. The estimated charge on TETA at pH 6.4 is +2, and hence, the ΔH per unit charge is -1.0 kcal/mol of charge on TETA, which is in good agreement with the ΔH value noted for the Hb-Ammonia derivatives but much lower than that of Hb-TETA derivatives (-3.8 kcal/mol charge).

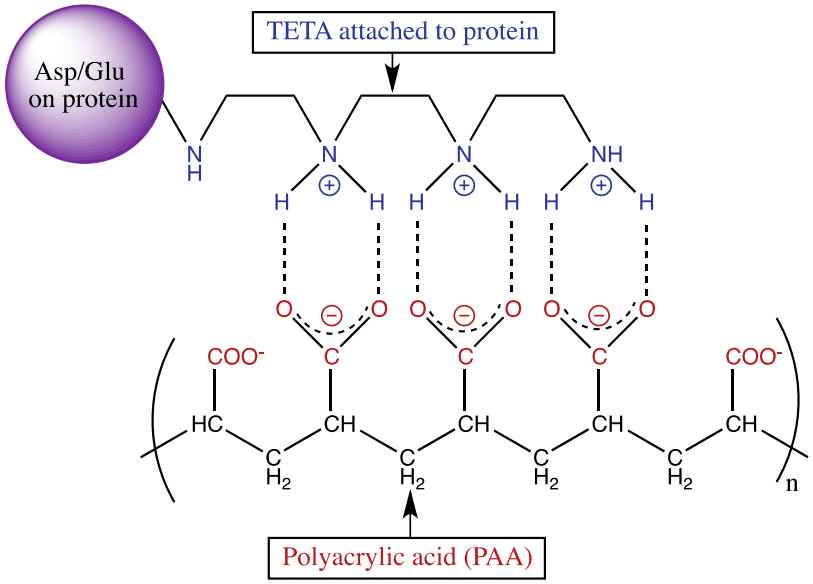

Scheme 3.4: Proposed hydrogen bond formation between TETA linked to Hb and PAA.

The dependence of binding enthalpies on protein charge observed here, is in good agreement with previous related work. Several key studies examined the interactions between oppositely charged peptides and polyelectrolyte microgels.[138,139,140] The strength of peptide-microgel interaction depended on the charge contrast between the peptide and the microgel. The binding and release kinetics of the peptide with the microgel depended directly on the net charge on the peptide as well as the microgel, and these are consistent with the current observations, despite the fact that two distinct approaches are being used. These previous data are in support of our current findings, in that the binding enthalpies gradually increase with increasing charge contrast, just as the on-off rates of the peptides increased with charge contrast. Unfortunately, these earlier studies did not quantify the relationship between the charge and binding enthalpies but related to the kinetics of association and release. Strong role of electrostatic contributions are clearly supported by thee studies and current data are consistent with earlier reports.

The difference between the binding enthalpies of the Hb-TETA and Hb-Ammonia derivatives (-3.8 vs -1 kcal/mol of charge) still needs to be explained. Increased substitution with TETA chains have greater chance to produce clusters of multiple charges by the close proximity of two or more TETA ligands on the protein surface. When these charges are separated by distances shorter than the Debye length (8 Å) at the ionic strength (150 mM ionic strength), they could function as a multivalent point charge, which can enhance the electrostatic interactions. This explanation is along the lines of previously reported peptide-microgel interactions where enhanced interactions due to charge-localization of charge clusters was invoked.[140] Clustering of charges along the TETA chain could function as a multivalent point charge, as opposed

to uniform distribution on the protein surface, and charges farther than Debye length would not substantially contribute to binding.

To make sure that observed excess enthalpy change (synergy) is not due to the unwinding of protein structure by PAA and subsequent enhanced interaction of the denatured protein with PAA, we proceeded to examine the secondary structures of the protein/PAA complexes. Unwinding of Hb by PAA will substantially decrease Hb secondary structure. However, we find that the CD spectra of the Hb/PAA complexes and their enzymatic activities are similar to Hb without PAA (**Figure 3.8).** Therefore, these structural changes are only minor, if any, and cannot account for the enhanced binding enthalpies of Hb-TETA derivatives.

If there are protein structure distortions that are not readily visible in the CD studies, they might influence its peroxidase-like activity. The peroxidase-like activities of the Hb-derivatives and their complexes with PAA are reasonably comparable to that of Hb (**Figure 3.13**). Interestingly, there have been small improvements in activities in specific cases, on binding to PAA. Therefore, it is unlikely that the excess binding enthalpies can be accounted for by the unwinding of the protein and its interaction with PAA. Neither chemical modification nor binding to PAA resulted in substantial loss of activity. Therefore, PAA-induced conformational changes in hemoglobin are minimal and cannot account for enhanced binding enthalpies. PAA conformational changes accompanying Hb binding, if any, are expected to be very small as the polymer adopts the conformations of a random coil.[141]

One other issue is that the conversion of the COOH groups on the protein surface to $CO\text{-}NH_2$, neutralizes the local negative charge and could alter the Hb/PAA contact points but may not necessarily involve the newly introduced $CO\text{-}NH_2$ groups in

the interaction, since these are polar but not charged. In contrast, TETA chains attached to Hb would favorably interact directly with COOH groups of PAA (**Scheme 3.4**) and this interaction could promote additional contacts with functional groups on the protein surface. These new interactions could potentially alter the points of contact between Hb and PAA. In simple terms, chemical modification alters the overall charge but it might also alter the points of contact between the protein and the polymer, and charge localization or clustering of TETA charges could enhance the interactions further. These aspects depend on the type and nature of chemical modification that has been carried out. Thus, controlled chemical modification provided a powerful new tool to alter binding enthalpies in a quantitative manner, without adversely affecting the biological activity, in a predictable, linear manner, in the charge range examined here. This powerful approach could be expanded to other systems, and it might be useful to fine-tune the protein-polymer interactions in a systematic manner via benign, controlled chemical modification of protein side chains.

3.6 Conclusions

The Hb and PAA interaction is weakly exothermic at pH 7 and the binding is mostly enthalpy driven but entropically favorable. Approximately, 14 Hb molecules associate with one PAA polymer chain, on an average, or occupy about 120 nm along the polymer backbone. One reason to form such discrete structures could be due to the extremely low concentrations of the polymer used here (0.7 μM). Regardless of the binding motif, discrete Hb-PAA complexes are produced, which are completely water-soluble and did not form macrogels or insoluble precipitates.

Carefully controlled chemical functionalization and consequent introduction of charge groups on Hb is a novel strategy to manipulate Hb interaction with PAA. Binding exothermicity has been substantially improved by chemical modification of the COOH groups of Hb with TETA, at a rate of -3.8 kcal/mol per unit charge. This provided a powerful approach to fine-tune the binding enthalpies, at least in this charge and concentration regions. In comparison, the binding enthalpies of the Hb-Ammonia charge ladder increased at a low rate of -1.0 kcal/mol per unit charge. We speculate that the excess exothermicity associated with the TETA derivatives as compared to that of the Hb-Ammonia derivatives can be due to changes in the contact points between the protein and the polymer, and possible localization of charge on protein surface with increased modification. The binding enthalpies of the Ammonia or the TETA derivatives can be predicted within the region examined here.

While chemical modification appeared to be a simple approach to factor out the electrostatic contributions to the protein-polymer interactions, it could potentially alter the protein-polymer contact points and hence, alter the strength/nature of these interactions further. Nevertheless, this synergy could be useful in tuning the binding

enthalpy in a systematic manner and the enthalpy change can be controlled by controlling the type and extent of modification used, under defined conditions. This type of ability to manipulate the molecular nature of protein/polymer interactions could be useful in designing novel protein/polymer hybrid materials for biomaterial and biotechnological applications.

Reprinted (adapted) with permission from Thilakarathne,V.K. ; Briand, V.A.; Kasi, R.M; Kumar, C.V. Tuning Hemoglobin-Poly(acrylic acid) interaction by Controlled Chemical Modification with Triethylenetetramine. *J.Phys.Chem.B.* **2012**, 116, 12783-12792.

Chapter 4 : Chemically Modified Protein/DNA Interaction Towards Fabrication of Bio-Solar Cells

4.1 Abstract

Solar energy is abundant, renewable and inexhaustible which would last over geologic time scales. However, successful design of an artificial light-harvesting complex is required for an efficient collection, capture and conversion of solar energy over a wide range of wavelength. We report here the successful construction of light gathering complexes consisting of multiple donor-acceptor dyes bound to protein-DNA complexes, in a self assembled manner. Our system consists of three distinct donors and an acceptor which absorb the wavelength range of 300-600 nm. Upon excitation of any one of the donor dyes, rapid energy transfer to the acceptor is noted which is followed by intense emission from the acceptor. Excitation spectra clearly show that each of the three donors transfer their excited state energy to the single acceptor. Steady state fluorescence study reveals an efficient step-wise energy transfer between the four chromophores used. These artificial light gathering complexes are unique, the first of their kind and facilitate our efforts toward the construction of bio-solar cells from proteins and nucleic acids.

4.2 Introduction

Higher depletion rate and adverse environmental impact of carbon-based fuels have raised the issue of development of long term, sustainable and green energy source to relinquish world's energy crisis[142]. Solar energy is abundant, sustainable and a renewable source, which has the highest potential to replace carbon-based fuels[143]. Major obstacle standing in the way of efficient solar energy conversion is the low energy density and broad spectral distribution of the solar source, which requires efficient energy capture over a wide range of wavelength. Photosynthetic systems in plants capture maximum amount of solar energy with the help of a set of pigments bound to well-organized non-covalent self-assembled protein complexes[144,145]. Inspired by this concept we designed a protein and DNA based artificial antenna complex to efficiently capture maximum amount of solar energy. Fabrication of robust artificial antenna complexes with higher energy transfer efficiencies that mimics what plant does is a challenging process. Several successful artificial antenna complexes were reported that used tobacco mosaic virus coat protein[146], dendrimers[147], DNA bundles[148] and DNA origami structures[149] as scaffolds for chromophores. Many of these methods involve tedious conjugation reactions, several purification steps and lack of solid-state applications. Our work stands out among reported strategies since we fabricate far more convenient, yet robust, self-assembled muti-choromophore system in solid state using biopolymers.

In order to capture solar energy, carefully selected donors and acceptors (four chromophores) were arranged in self-assembled DNA-protein hybrid materials. The provided close proximity of the scaffold for donor and acceptor chromophores promotes

Föster resonance energy transfer (FRET) process. Bovine serum albumin (BSA) is an excellent host for binding numerous chromophores[150,151], and in a similar manner; the double stranded DNA also can provide an opportunity to accommodate a number of donor and/or acceptor chromophores[152,153]. However BSA has no affinity for DNA at pH 7 due to charge repulsion and this problem was overcome in our laboratory by chemical modification of BSA using polyamines (**Scheme 4.1**).

Tightly bound DNA/cBSA complex was served as the scaffold to accommodate donors and acceptor chromophores. Our hypothesis is that reducing the Föster radius between donors and acceptors by non covalently assemble them in DNA/cBSA scaffold; energy transfer efficiency can be improved (**Scheme 4.2**). Previously published data from our group have shown that Donor/DNA/ cBSA/Acceptor quaternary system has increased the energy transfer efficiency compared to two dyes alone[154].

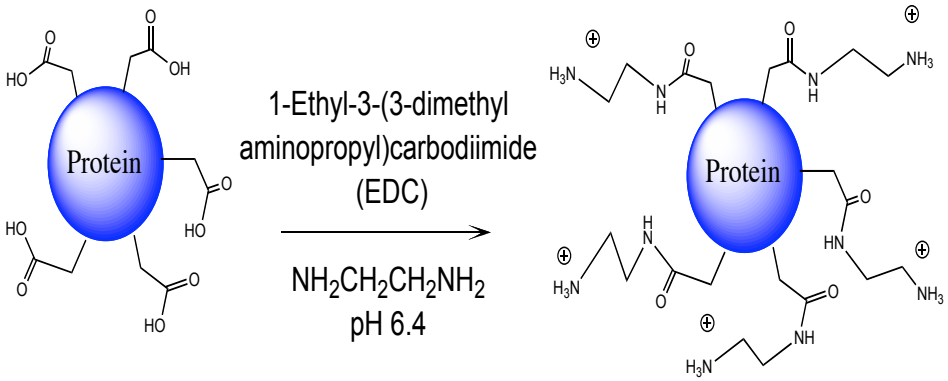

Scheme 4.1: Activation of carboxylic groups on the surface of BSA using water soluble carbodiimide followed by amidation using triethyleneteramine to produce the corresponding catinized BSA (cBSA).

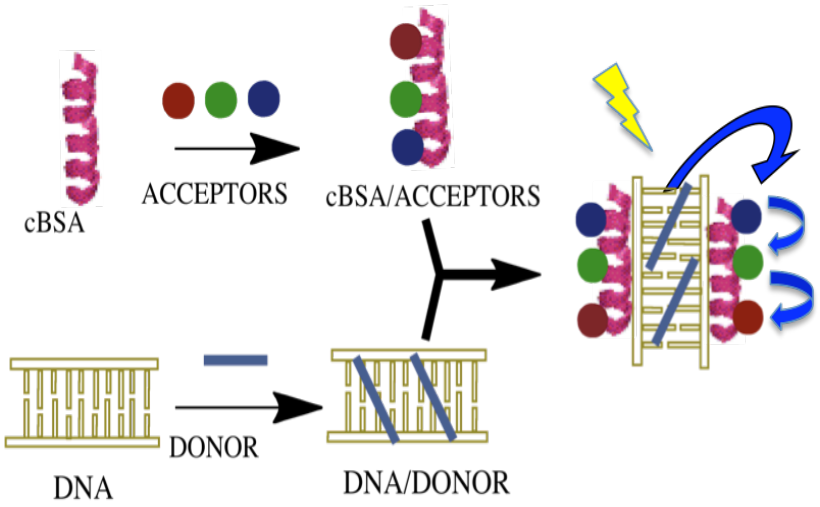

Scheme 4.2: Artificial antenna complex constrcuted from donors, acceptors , modified BSA (cBSA) and DNA.

Here we reported the design and construction of biomacromolecule based self-assembled artificial antenna complex that contains four chromophores, DNA and proteins. A unidirectional step-wise energy transfer cascade from initial donor chromohopre to primary and secondary acceptors and at the end to the ultimate acceptor was demonstrated using steady state fluorescence spectra analysis.

4.3 Experimental details

4.3.1 Materials

Bovine serum albumin was purchased from and fish sperm DNA sodium salt was purchased Amresco (Ohio) . Dyes used for the experiment, bisBenzimide H 33258 (Hoechst) and Fluorescein were purchased from sigma. Coumarin C540A was purchased from Exciton chemical CO.Inc (Ohio) and Rhodamine was from Eastam Kodak company NY. Glass cover slips with dimensions 22mmx22mm were purchased from Fisher Scientifics.

4.3.2 Synthesis of cationic bovine serum albumin (cBSA)

Aspartic and glutamic acid residues of BSA were modified by activating them with carbodiimide and by reaction with triethlenetetramine (TETA) , by adopting reported methods. BSA (1g) was dissolved in deionized water and stirred with 0.5 M TETA (pH adjusted to 5) for half an hour followed by addition of 50 mg of EDC. The reaction mixture was stirred for additional 4 hrs at room temperature and unreacted EDC, TETA and byproducts were removed by dialysis against 10 mM phosphate buffer at pH 7.2 .

TETA attached BSA (Cationized BSA or cBSA) was then concentrated using amicon tubes (20,000 MW)

4.3.3 Agarose gel electrophoresis

Agarose gel electrophoresis was used to determine the extent of chemical modification on TETA attched BSA. Agarose gel electrophoresis was performed using horizontal gel electrophoresis apparatus (Gibco model 200, Life Technologies Inc, MD) and agarose (0.5 % w/w) in tris acetate (40 mM) buffer at pH 7. Modified and unmodified BSA samples were loaded with 50 % loading buffer (50% v/v glycerol and 0.01% w/w bromophenol blue). Samples were spotted into wells placed in the middle of the gel , so that the protein could migrate towards the negative or the positive electrode, based on net charge. A potential of 100 V was applied for appropriate duration. Gel was stained over night with 10% v/v acetic acid and 0.02% w/w coomassie blue , followed by destaining in 10% v/v acetic acid overnight.

4.3.4 Fabrication of thin films using drop casting method.

Thin film of self-assembled cBSA/DNA/dye complex was constructed by preparing two separate solution of cBSA/Rhodamine/Fluorescein/C540A and DNA/Heochst solution and finally mixed both solutions together allowing dyes and macromolecules to arrange in self-assembled manner. Rhodamine in DI (40 μM) was added to cBSA solution (300 μM) in 10 mM phosphate buffer pH 7 and mixed well. After that Fluorescein (100 μM) in DI and C540A (125 μM) in DMF were added to the cBSA solution respectively. DMF content in the final complex should be less than 1% v/v. DNA/dye solution was prepared by adding Hoechst (100 μM) in DI to a DNA solution (800 μM) in 10 mM

phosphate buffer pH 7. cBSA/dye solution and DNA/dye solution that were prepared separately was then combined together and mixed well to arrange in a self-assembled cBSA/DNA/chromophores complex. Concentrations of dyes, cBSA and DNA mentioned above are the final concentrations of each in the self-assembled complex. Chromophore content of the final complex was kept below 5 % v/v. Once the self assembled complex was formed in the solution, 500 µl of the solution was taken and covered the surface of the 22mmx22mm glass coverslip and allowed to air dry overnight.

4.3.5 Absorption and steady state fluorescence measurements

Absorption spectra of each film on glass cover slip were reordered using HP 8453 diode array spectrophotometer. Steady state fluorescence spectra were collected using home-build fluorescence spectrophotometer using SLM-Aminco optics. The instrument is routinely calibrated prior to each experiment. Front phase accessory was used to collect emission and excitation spectra of thin films. During absorbance and steady state fluorescence experiments, glass cover slip was aligned in both instruments in such a way that the same area is exposed to both absorbance light beam and to the excitation beam in fluorescence.

4.3.6 High temperature stability

Protein/DNA/Dye films were incubated at 80 ^{0}C and absorbance and fluorescence spectra were collected after certain time intervals. Films were allowed to cool 2- 3 hours prior to take measurements.

4.4 Results and Discussion

4.4.1 Chemical modification of BSA

Bovine serum albumin used in this study has a pI of 5 and hence negatively charged at pH 7.2. At this pH, because of the charge repulsion BSA does not bind to DNA. Aspartic and glutamic acid residues on the surface of BSA were conjugated with triethylenetetraamine (TETA) using EDC mediated coupling reaction. Charge reversal of BSA was monitored using agarose gel electrophoresis, where protein was subjected to an electric field. Since the very low percentage of agarose was used (0.5%) distance migration in the native gel is proportional to the charge of the protein (**Figure 4.1**) and the effect of protein size is minimal. For example at pH 7, since unmodified BSA is negative charge it migrated towards positive electrode (**Figure 4.1 lane 1**). After chemically modified with TETA the protein migrated towards negative electrode which signifies charge reversal (**Figure 4.1 lane 2**). Hence chemically modified BSA would be denoted further as cationic BSA or cBSA.

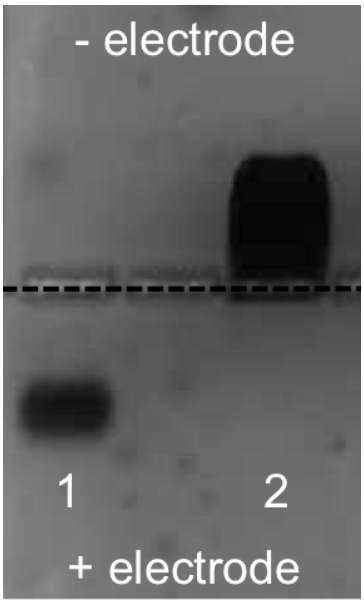

Figure 4.1: Agarose gel of unmodified BSA (lane 1) and BSA modified with TETA (cBSA) (lanes 2, 40 mM Tris acetate, gel run at pH 6) and samples were loaded into wells at the middle of the gel (dotted line).

4.4.2 Selection of chromophores

According to Föster energy transfer theory, efficient energy transfer between donor/acceptor pair, was observed upon fulfillment of following requirements[155].

1. Significant overlap between the donor emission and acceptor absorption in the frequency domain
2. Coulombic interaction between oscillation dipole moments of acceptor and excited donor
3. Separation of donor and acceptor (Föster radius)

Four chromophores that satisfy the required spectral overlap were chosen from commercially available organic chromophores. Hoechst ($\lambda_{max,Abs}$=340nm, $\lambda_{max,Em}$=440nm) is the donor in the system that binds specifically to DNA[156]. Coumarin 540A ($\lambda_{max,Abs}$=420nm, $\lambda_{max,Em}$=520nm) and Fluorescein ($\lambda_{max,Abs}$=490nm, $\lambda_{max,Em}$=510nm) are primary and secondary acceptors respectively while Rhodamine B ($\lambda_{max,Abs}$=550nm, $\lambda_{max,Em}$=575nm) is the ultimate acceptor. Rhodamine, Fluorescein and C540A are well known for binding to BSA[150,157,158]. Once the DNA/cBSA/Donors/Acceptors complex was formed in a self assembled manner close proximity of chromophores decrease the Föster radius and provided the ground to improve energy transfer efficiency. The self-assembled complex was then used to fabricate thin films on glass surface using drop casting method. Bovine serum albumin in the complex acts as a glue that stick the complex on to the glass surface. These thin films were used to perform absorbance and steady state experiments.

Selected chromophores capture solar energy from 300- 600 nm spectra region. According to the absorption and emission spectra, significant overlap was notable

between emission spectra of Hoechst (**Figure 4.2 blue dash line**) and absorbance spectra of C540A(**Figure 4.2 green solid line**). Similarly higher overlap integral was observed between C540A/Fluorescein pair and Fluorescein/Rhodamine chromophores pair (**Figure 4.2**). Spectral overlap was minimal between Hoechst/Fluorescein and C540A/Rhodamine dye pairs. These spectral features allow achieving unidirectional, stepwise energy transfer cascade between four chromophores bound to cBSA and DNA.

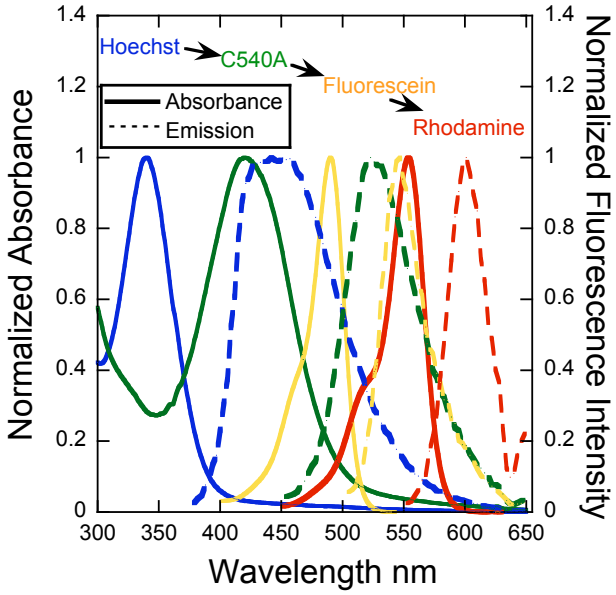

Figure 4.2 : Overlap of absorbance and emission spectra of the four chromophores used to make the artificial antenna complex. Abbreviations of dyes are ; **H** for Hoechst (Blue), **C** for C540A (Green), **F** for Fluorescein (yellow) and **R** for Rhodamine (red).

4.4.3 Steady state fluorescence study

The FRET between four-dye system was investigated using steady state fluorescence spectroscopy. Antenna complex was excited at the absorbance maxima of the initial donor Hoechst (λ=350 nm) where the ultimate acceptor, Rhodamine does not absorb significantly. The fluorescence spectra of four dyes with DNA and cBSA (**Figure 4.3 A** black line) shows a six fold increase in Rhodamine emission compared to Rhodamine only with DNA and cBSA (**Figure 4.3 A** blue dash line). More interestingly when intermediate primary or secondary acceptors are removed from the system, Rhodamine emission decreases and the corresponding donor quenching is also decreases. For example in the absence of C540A Hoechst emission was not quenched (**Figure 4.3 B** red line) and in the absence of Fluorescein C540 emission was not quenched (**Figure 4.3 B** green line).

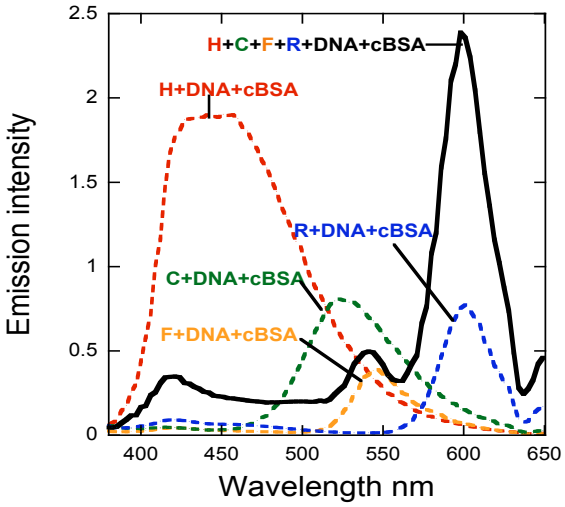

A

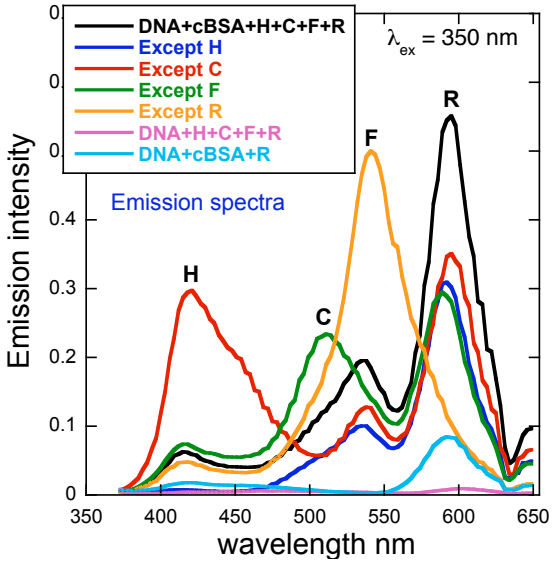

B

Figure 4.3 : Emission spectra of the self-assembled system showing the contribution of each chromophore to the energy transfer cascade. (Abbreviations of dyes are ; **H** for Hoechst, **C** for C540A, **F** for Fluorescein and **R** for Rhodamine). **A**) Note that the Hoechst emission was quenched and Rhodamine emission was increased in the presence of primary and secondary acceptors, C540 and Fluorescein respectively. **B**) Clear evidence of step-wise energy transfer cascade has shown since elimination of each intermediate results in decrease in Rhodamine emission and increase in corresponding donor emission.

In solid phase, molecular diffusion between donor molecules and acceptor molecules is prevented as they are fixed in rigid positions relative to each other. In such situations Perrin formulation is used to determine the quenching radius between donors and acceptors in a quenching spheres[155]. When donor chromophore and acceptor chromophore positioned within the quenching sphere, the acceptor molecule quenches the excited donor molecule emission. Any excited donor molecules resides out side the quenching sphere cannot be quenched by the acceptor molecule (**Scheme 4.3**). Hence quenching radius derived from Perrin formulation in solid state is comparable to the Föster radius discusses in Föster theory.

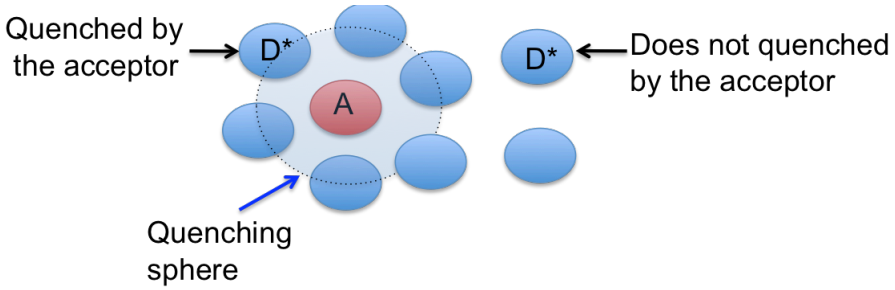

Scheme 4.3 Depiction of quenching sphere described in Perrin model that used to explain quenching phenomenon in solid-state systems.

Quenching radii of consecutive dye pair were extracted from the following Perrin equation (01)[155].

$$\ln \Phi_0/\Phi = VN[Q] \text{ ---------- Equation (01)}$$

Where Φ_0 and Φ are the quantum yield for donor emission in the absence and presence of acceptor, V is the volume of the quenching sphere; N is the Avogadro's number and [Q] is the concentration of the acceptor.

For example in order to determine the quenching radius between Fluorescein and Rhodamine , Rhodamine concentration was changed and emission spectra were collected (**Figure 4.4 A**). Note that the plot of ln ln Φ_0/Φ vs quencher concentration is linear which states that quenching phenomenon behaves according to Perrin model **(Figure 4.4 B & C)**.

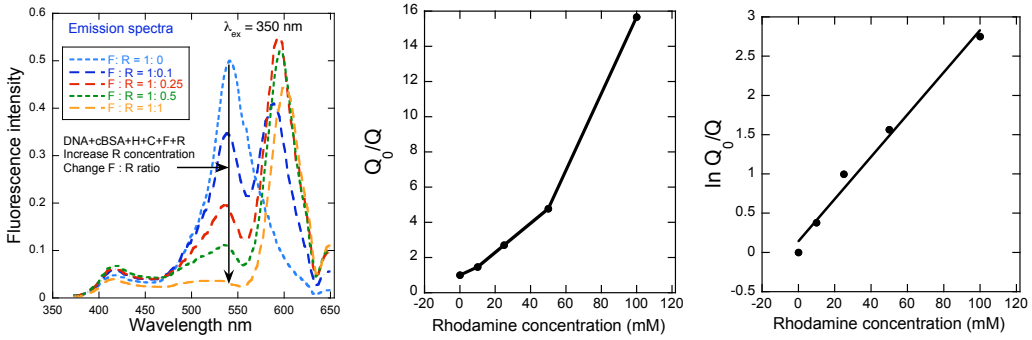

A **B** **C**

Figure 4.4. **A**) Increase in quenching of Fluorescein emission by increasing Rhodamine concentration. **B**) Plot of ln Φ_0/Φ vs quencher (Rhodamine) concentration. Note that the plot is non linear. **C**) Plot of ln Φ_0/Φ vs quencher (Rhodamine) concentration. Linear plot implies the quenching follows Perrin model.

Similarly quenching radius between Fluorescein and C540 was determined by changing Fluorescein concentration and radius between C540 and Hoechst was determined by changing C540 concentration (**Figure 4.5**).

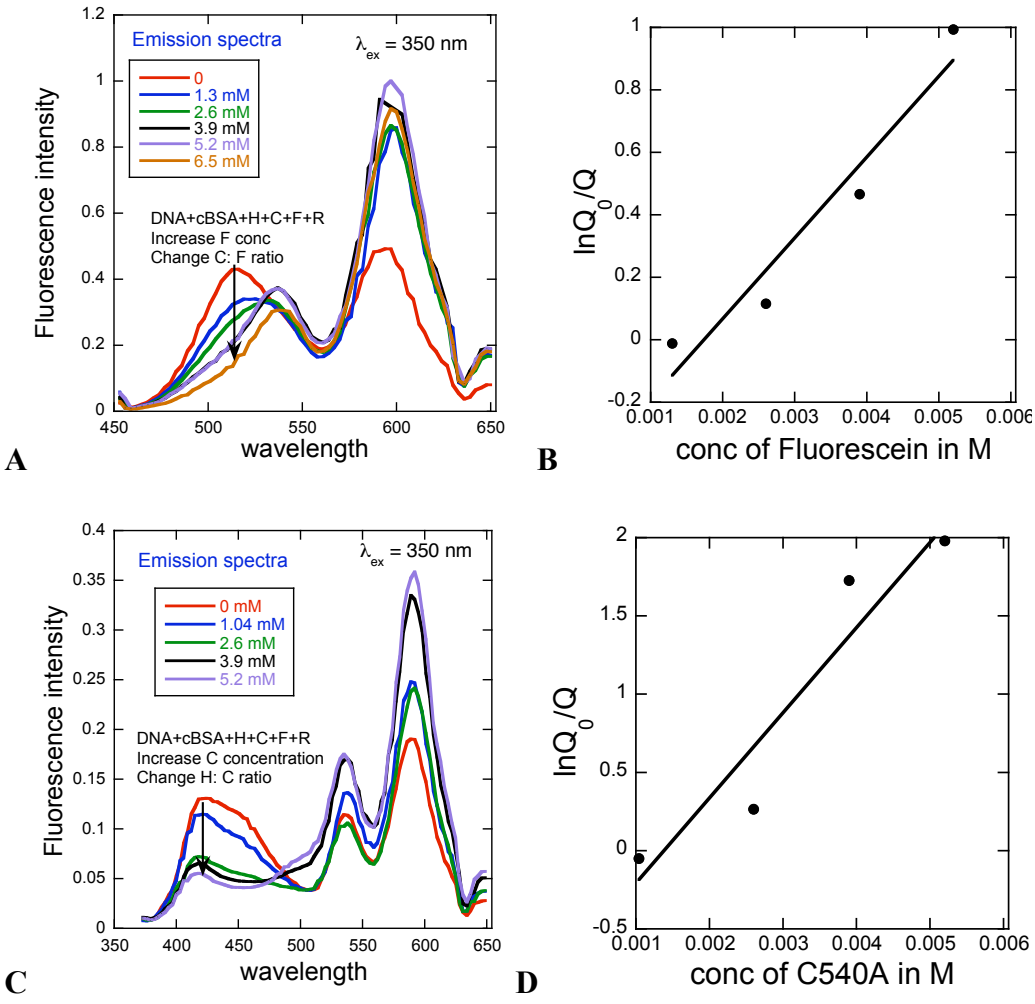

Figure 4.5 **A**) C540 emission was decreased concomitantly by increasing quencher (Fluorescein) concentration. **B**) Plot of ln Φ_0/Φ vs quencher (Fluorescein) concentration. Quenching radius between C540 and Fluorescein was extracted from this Perrin plot. **C**). Decrease of emission spectra of Hoechst due to the increase in C540 which as the immediate acceptor for Hoechst emission according spectra overlaps. **D**) Plot of ln Φ_0/Φ vs quencher (C540) concentration. Quenching radius between Hoechst and C540 was extracted from this Perrin plot.

Quenching radii between each chromophore pair, calculated from Perrin model were tabulated in **Table 4.1**. Those experimentally calculated radii are comparable to the known Föster radii between Fluorescein/Rhodamine pair (55 Å)[159] and Coumarin/Fluorescein pair (50 Å)[160].

Table 4.1 Quenching radii; extracted from Perrin plots.

Chromophore pairs	Quenching radius (Å)
Rhodamine - Fluorescein	57 .5 ± 1
Fluorescein – C540	44.6 ± 1.6
C540 - Hoechst	60.37 ± 2

Static quenching was further confirmed by the excitation spectra. Excitation spectra were collected by monitoring the emission at 650 nm, where only Rhodamine has a significant emission, while all three donors have no emission. Intensity ratio of excitation peak maxima corresponding to Hoechst at 360 nm (primary donor absorption maxima) and Rhodamine at 561 nm (ultimate acceptor absorption maxima) is proportional to the energy transfer efficiency. The plot of I_{360}/I_{561} as a function of each donor concentration showed that the energy transfer efficiency increases with donor concentration up to a certain concentration and then decreases (**Figure 4.6**).

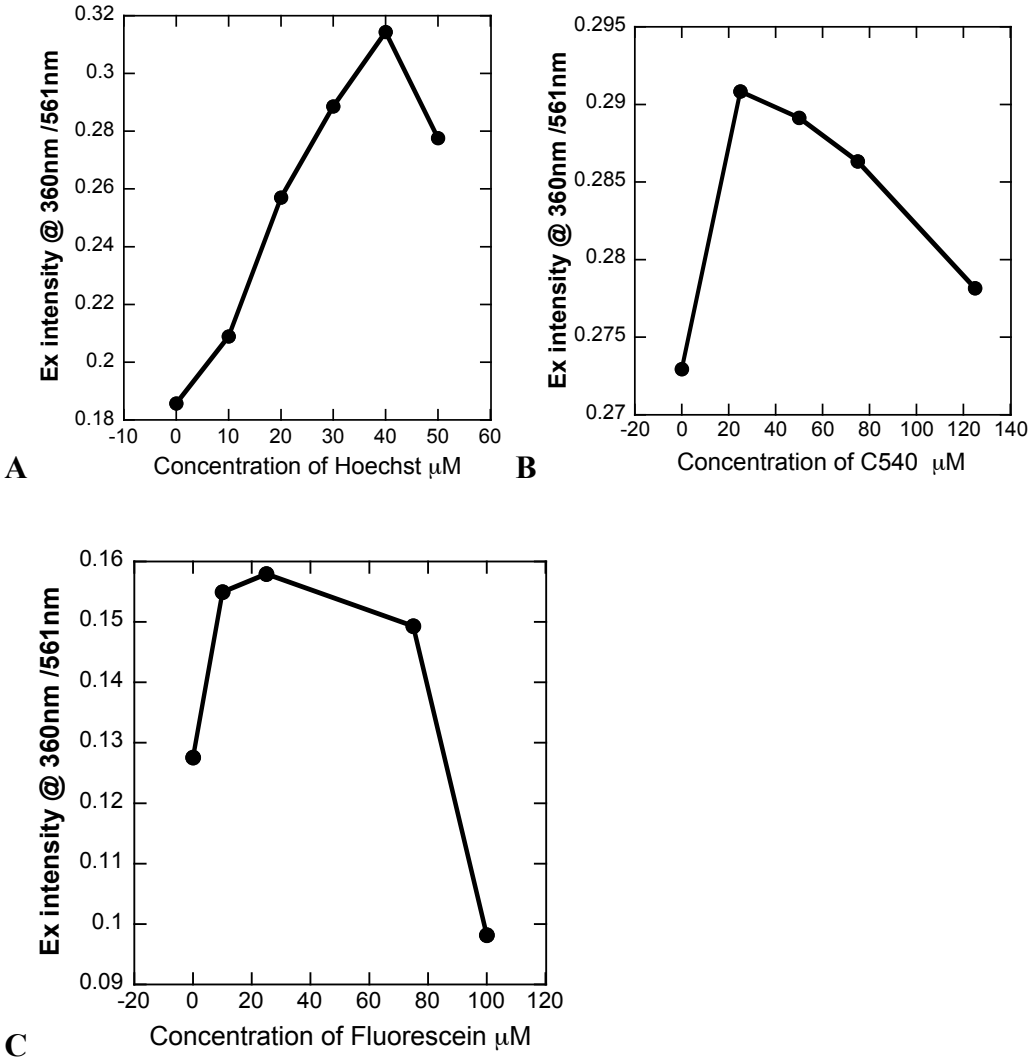

Figure 4.6 Energy transfer efficiency as a function of donor concentrations monitored using excitation spectra. Emission was monitored at 650 nm. A) Increase in concentration of Hoechst. B) Increase in concentration of C540A. C) Increase in concentration of Rhodamine.

The initial rapid increase in energy transfer is due to the accommodation of increasing number of donor molecules in the quenching sphere until it is saturated. Above that concentration free donors would absorb the light but cannot contributes to the energy transfer process since they are out of the quenching sphere and decrease the overall transfer efficiency.

When the complex was excited at 350 nm (absorbance maxima of Hoechst), a drastic quenching of Hoechst emission at 450 nm , Coumarin emission at 550 nm and Fluorescein emission at 550 nm was observed . At the same time strong emission increase at 600 nm characteristics to Rhodamine was also observed (**Figure 4.3**). From this quenching data FRET efficiency was calculated using following equation (02)[148].

$$E = 1 - \frac{I_{DA}/A_{DA}}{I_D/A_D} \qquad \text{---------- Equation (02)}$$

Where I_{DA} and I_D are integrated area of the donor emission with and without acceptor and A_{DA} and A_D are absorbances of donor with and without acceptor. Calculated energy transfer efficiencies (**Table 4.2**) further confirmed the step-wise energy transfer cascade, since the removal of one intermediate chromophore results in decrease in energy transfer efficiency. Overall 88% of ET efficiency was achieved by protein and DNA based multi chromophore antenna complex.

Table 4.2 : Energy transfer efficiency

System	Energy transfer efficiency
From H to all the acceptors	88 %
From H to F and R (without C)	63 %
From C to F and R	95 %
From C to R (without F)	48 %
From F to R	72 %

4.4.4 Morphology of protein/DNA/Dye films

Morphology of the protein-DNA-Dye film was observed using scanning electron microscopy. The SEM image shows well-defined patterns of protein-DNA scaffold that stretched across the film in micrometer scale (**Figure 4.7**). All the defined structures have similar dimensions with few micrometer gaps in between (**Figure 4.7**). This remarkable discovery of scaffolding pattern of protein and DNA would be a great advantage when pursuing device fabrication.

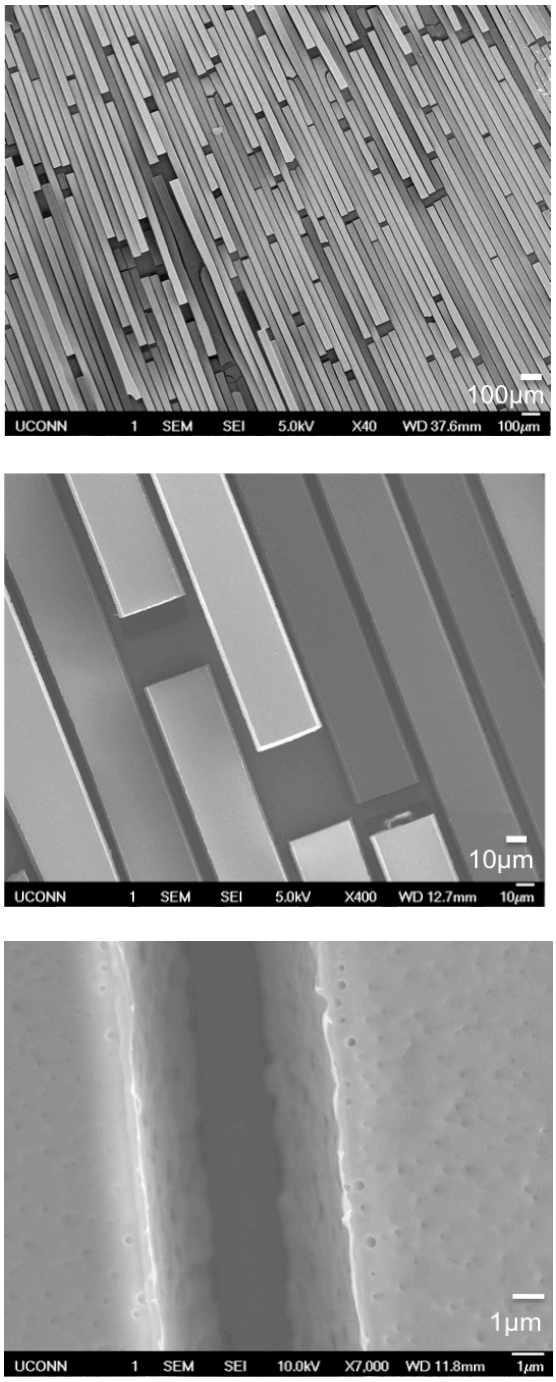

Figure 4.7 SEM image of protein-DNA-Dye film.

4.4.5 Stability at higher temperatures

Major draw back associated with biomacromolecule based artificial antenna complex is the denaturation of proteins and nucleic acid at elevated temperatures. DNA/cBSA/Dye film on the glass surface was heated at 80 ^{0}C and emission spectra were collected as a function of time , after the film was cooled back to room temperature. Emission spectra shows that even after 21 days emission intensity decrease is minimum (**Figure 4.8**). The robust nature of the self-assembled antenna complex improved further the usefulness of the system in ultimate device fabrication.

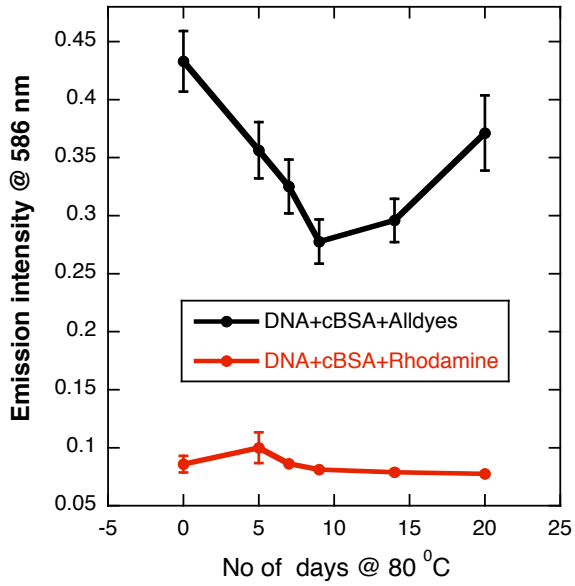

Figure 4.8 Emission intensity at 586 nm (emission of Rhodamine) vs time of incubation of DNA/cBSA/dye film and DNA/cBSA/Rhodamine film at 80 ^{0}C. Films were cooled down to room temperature for 2-3 hours before taking the collecting spectra.

4.5 Conclusion

Biomaterial based artificial antenna complex is not a strange thing compared to naturally occurring photosynthesis complex. In fact the design is entirely inspired by plant photosystems. Very high concentrations of organic dyes in solutions cause drastic decrease in their quantum yields. If dyes arrange too close to each other, non-fluorescence dimmers can form that act as excitation sinks and deplete excitation. Nevertheless in photosystem I and II chlorophyll concentration range from 0.5 to 0.25 M[161]. Plant photosystems overcome this problem by organizing their chromophores in protein scaffolds, which enable to increase the local dye concentration at the same time optimize energy transfer efficiency[162]. Protein and DNA based scaffold reported here serve exactly the same purpose. Since all the components in the system self assembled according to their binding affinities, complex synthetic efforts are omitted although finely tuned order and distances couldn't be obtained. In fact recent structural data and theoretical models explain that precise distances and symmetrical order of chromophores are not necessary for efficient energy transfer process. In a randomly arranged network of chromophores a highly optimal configuration can be found by statistical sampling[163]. The protein DNA based antenna complex can be further expand to harvest light over near IR range and will be useful for fabricate solar light harvesting complex that efficiently capture and convert solar energy to chemical energy.

References

1. Wagner, E., Zenke, M.; Cotten, M.; Beug, H. and Birnstiel, M. L. *Proc. Natl. Acad. Sci. USA*. **1990**, *87*, 3410 -3414.
2. Kumagai, A. K.; Eisenberg, J. B. and Pardridge, W. M. *J. Biol. Chem*. **1987**, *262*, 15214-15219.
3. DeSantis, G. and Jones, J. B. *Curr. Opin. Biotechnol*. **1999**, *10*, 324-330.
4. Polizzi, K. M.; Bommarius, A. S.; Broering, J. M. and Chaparro-Riggers, F. *Curr. Opin. Biotechnol*. **2007**, *11*, 220-225.
5. Murphy, A. and óFágáin, C. *J. Biotechnol*. **1996**, *49*, 163-171.
6. Krikstopaitis, K.; Kulys, J. and Tetianec, L. *Electrochem. Commun*. **2004**, *6*, 331-336.
7. Roberts, M. J.; Bentley, M. D. and Harris, J. M. *Adv. Drug Deliv. Rev*. **2002**, *54*, 459-476.
8. Futami, J.; Kitazoe, M.; Murata, H. and Yamada, H. *Expert Opin. Drug Discov*. **2007**, *2*, 261-269.
9. Chu, F. S.; Lau, H. P.; Fan, T. S. and Zhang, G. S. *J. Immunol. Methods*.**1982**, *55*, 73-78.
10. Rhaese, S.; Briesen, H.; RÜbsamen-Wagmann, H.; Kreuter, J. and Langer, K. *J. Controlled Release*. **2003**, *92*, 199-208.
11. Kitazoe, M.; Murata, H.; Futami, J., Maeda, T.; Sakaguchi, M.; Miyazaki, M.; Kosaka, M.; Tada, H.; Seno, M. and Huh, N. *J. Biochem*. **2005**, *137*, 693-701.

12. Fischer, D.; Bieber, T.; Brüsselbach, S.; Elsässer, H. P. and Kissel, T. *Int. J. Pharm*. **2001**, *225*, 97-111.

13. Futami, J.; Kitazoe, M.; Maeda, T.; Nukui, E.; Sakaguchi, M.; Kosaka, J.; Miyazaki, M.; Kosaka, M.; Tada, H. and Seno, M. *J. Biosci. Bioeng*. **2005**, *99*, 95-103.

14. Davis, B. G. *Curr. Opin. Biotechnol*. **2003**, *14*, 379-386.

15. Kang, Y. and Pardridge, W. M. *Pharm. Res*. **1994**, *11*, 1257-1264.

16. Kohen, R.; Kakunda, A. and Rubinstein, A. *J. Biol. Chem*. **1992**, *267*, 21349-21354.

17. Ma, C.Y. and Nakai, S. *J. Dairy. Sci*. **1980**, *63*, 705-714.

18. Basu S. and Sen, S. *J. Chem. Inf. and Model.,* **2009** *49*, 1741-1750; Strickler, S. S., Gribenko, A. B., Keiffer, T. R., Tomlinson, J., Reihle, T., Lolandze, V. V., Makhatadze, G. I., *Biochem.,* **2006**, *45*, 2761-2767.

19. Hoare, D. G. and Koshland Jr, D. E. *J. Am. Chem. Soc*. **1966**, *88,* 2057-2058.

21. Dennis M. Krizek, Margaret E. Rick, Current Protocols in Cell Biology, Unit 6.7, Wiley Online Library; Johansson, B. G., Scand. J. Clin. & Lab Invest., **1972**, *29*, 7-19.

22. Buranaprapuk, A.; Leach, S. P. and Kumar, C. V. *Biochim. Biophys. Acta*. **1998**, *1387*, 309-316.

23. Jonassen, H.B.; Bertrand, J.A.; Groves, Jr. F.R.; Stearns, R.I. *J. Am. Chem. Soc*. **1957**, *79*, 4279- 4282.

24. Kumar, C. V. and Chaudhari, A. *J. Am. Chem. Soc*. **2000**, *122*, 830-837.

25. Wrolstad, R.E.; Decker, E. A.; Schwartz, S. J.; Sporns, P. *Hand book of food analytical chemistry, water, enzyme, enzymes, lipids and carbohydrates*. *Volume* 1. John Wiley & sons, Inc., **2004**.

26. Nelson, D. R. and Huggins, A. K. *Anal. Biochem*., **1974**, *59*, 46-53.

28. Maehly, A.C.; Chance, B . *Methods Biochem. Anal*. **1954**, *1*, 357

28. Y. Pocker, J. T. Stone, *Biochem*., **1967**, *6*, 668–678.

29. Bhambhani, A. and Kumar, C. V. *Micropor. Mesopor. Mater*. **2008**, *109*, 223-232.

30. Tsuge, H.; Natsuaki, O and Ohashi, K . *J. Biochem*. **1975**,*78*, 835-843; J. G. Voet, J. Coe, J. Epstein, V. Matossian, T. Shipley, *Biochem*., **1981**, *20*, 7182–7185; Nilsson, A. and Lindskog, S. *Eur. J. Biochem*. **1967**, *2*, 309-317; Fanelli, A. R.; Antonini, E. and Caputo, A. *Biochim. Biophys. Acta*. **1958**, *30*, 606-615.

31. Pecsok, R. L.; Garber, R. L. and Shield, D. *Inorg. Chem*., **1965**, *4*, 447-451.

32 J. G. Voet, J. Coe, J. Epstein, V. Matossian, T. Shipley, *Biochem*., **1981**, *20*, 7182–7185.

33 Nilsson, A. and Lindskog, S. *Eur. J. Biochem*. **1967**, *2*, 309-317.

34 Fanelli, A. R.; Antonini, E. and Caputo, A. *Biochim. Biophys. Acta*. **1958**, *30*, 606-615.

35. Hodak, J.; Etchenique, R.; Calvo, E. J.; Singhal, K.; Bartlett, P. N. *Langmuir* **1997**, *13*, 2708-2716.

36. Gratzer, W. B. and Cowburn, D. A. *Nature.* **1969**, *222*, 426-431.

38. Sugihara, A.; Iwai, M. and Tsujisaka, Y. *J.Biochem*. **1982**, *91*, 507-513; Hosseinkhani, S.; Ranjbar, B.; Naderi-Manesh, H. and Nemat-Gorgani, M. *FEBS Lett*. **2004**, *561*, 213-216; Habeeb, A. *Biochim. Biophys. Acta* . **1996**, *115*, 440-454.

39. Duff, M. R. and Kumar, C. V *J. Phys. Chem. B*. **2009**, *113*, 15083–15089; Duff, M. R. and Kumar, C. V. *Langmuir*. **2009**, *25*, 12635-12643.

40. Pillai, C.K.S.; Sharma, C.P. *J. Biomater.Appl.* **2010** , *25*, 291.

41. Arshady, R. *Introduction to Polymeric Biomaterials*; Citus Books: London, 2003; p 46.

42. Klok, H.-A . *J. Polym. Sci., Part A: Polym. Chem*. **2005** , *43*, 1

43. Gauthier, M.A.; Klok, H.-A . *Chem.Commun*. **2008** , 2591.

44. Lele, B.S.; Murata, H.; Matyjaszewski, K.; Russell, A.J . *Biomacromolecules*. **2005**, *6*, 3380.

45. Hoffman, A.S.; Stayton, P.S.; Bulmus, V.; Chen, G., Chen, J.; Cheung, C.; Chilkoti, A.; Ding, Z.; Dong, L.; Fong, R.; Lackey, C.A.; Long, C.J.; Miura, M.; Morris, J.E.; Murthy, N.; Nabeshima, Y.; Park, T.G.; Press, O.W.; Shimoboji, T.; Yang, H.J.; Monji, N.; Nowinski, R.C.; Cole, C.A.; Priest, J.H.; Harris, M.J.; Nakamae, K.; Nishino, T,; Miyata, T. *J. Biomed. Mater. Res*. **2000** ,*52*, 577.

46. Vandermeulen, G.W.M.; Klok, H.A. *Macromol. Biosci*. **2004**, *4*, 383.

47. Klok, H.-A . *Macromolecules.* **2009** ,*42*, 7990.

48. Heredia, K.L.; Maynard, H.D . *Org. Biomol. Chem*. **2007**, *5*, 45.

49. Thordarson, P.; Le Drougmaguet, B.; Velonia, K. *Appl. Microbiol. Biotechnol*. **2006**, *73*, 243.

50.. Matyjaszewski, K.; Tsarevsky, N. V . *Nat. Chem.* **2009** , *1* , 276.

51. Hillmyer, M. A . C*urrent Opinion in Solid State & Materials Science*. **1999** , *4* , 559.

52. Hadjichristidis, N.; Pitsikalis, M.; Iatrou, H. *Adv Polym Sci*. **2005** , *189*, 1.

53. Nicolas, J.; Mantovani, G.; Haddleton, D. M. *Macromol. Rapid Commun*. **2007**, *28*, 1083.

54. Greenburg, A.G.; Kim, H.W. *Critical Care*. **2004**, *8*, S61.

55. Piras, A.M.; Dessy, A.; Chiellini, F.; Chiellini, E.; Farina, C.; Ramelli, M.; Valle, E.D. *Biochimica et Biophysica Acta* . **2008**, *1784*, 1454.

56. Voet, D.; Voet, J.G. *Biochemistry*, 3rd ed.; Wiley : Hoboken, 2004; Chapter 7, p. 186.

57. Gao, W.; Liu, W.; Mackay, J.A.; Zalutsky, M.R.; Toone, E.J.; Chilkoti, A. *Proc. Natl. Acad. Sci. U. S. A*. **2009**, *106*, 15231.

58. Phillips, W.T.; Klipper, R.W.; Awashthi, V.D.; Rudolph, A.S.; Cliff, R.; Kwasiborski, V.; Goins, B.A. *J. Pharmacol. Exp. Ther*.**1999**, *288*, 665.

59. Shi, Q.; Huang, Y.; Chen, X.; Wu, M.; Sun, J.; Jing, X . *Biomaterials.* **2009**, *30*, 5077.

60. Topoglidis, E.; Campbell, C.J.; Cass, A. E. G.; Durrant, J.R. *Electroanalysis.***2006** , *9*, 882.

61. Gu, H-Y.; Yu, A-M.; Chen, H-Y . *J. Electroanal. Chem*. **2001**, *516*, 119

62. Tess, M.E.; Cox, J.A. *J. Pharm. Biomed. Anal*. **1999**, *19*, 55.

63. MacLean-McDavitt, D.S.; Robertson, J.D.; Jay, M. , *Pharm. Res*. **2002**, *20*, 435.

64. Muramatsu, M.; Kanada, K.; Nishida, A.; Ouchi, K.; Saito, N.; Yoshida, M.; Shimoaka, A.; Ozeki, T.; Yuasa, H.; Kanaya, Y . *Int. J. Pharm*. **2000**, *119*, 77.

65. Adhikari, B., Majumdar, S . *Prog. Polym. Sci*. **2004**, *29*, 699.

66. Ding, B.; Yamazaki, M.; Shiratori, S . *Sens. Actuators, B*. **2005**, *106*, 477.

67. Jia, S.; Fei, J.; Deng, J.; Cai, Y.; Li, J . *Sens. Actuators, B*. **2009**, *138*, 244.

68. Yang, J.; Hu, N.; Rusling, J.F. *J. Electroanal. Chem.* **1999**, *463*, 53.

69. Lu, Z.; Huang, Q.; Rusling, J.F . *J. Electroanal. Chem*. **1997**, *423*, 59.

70. Maehly, A.C.; Chance, B . *Methods Biochem. Anal*. **1954**, *1*, 357.

71. Bhambhani, A.; Kumar, C.V . *Microporous Mesoporous Mater*. **2008**, *109*, 223.

72. Woody, R.W. In *Circular Dichroism and Conformational Analysis of Biomolecules*; Fasman, G.D., Ed.; Plenum Press: New York, 1996; p 25

73. Gratzer, W.B.; Cowburn, D.A . *Nature*. **1969**, *222*, 426.

74. Przywarska-Boniecka, H.; Panejko, E.; Tyrnda, L.; Biernat, J . *Materials Science.* **1978***, 4*, 139.

75. Antoniotti, S.; Santhanam, L.; Ahuja, D.; Hogg, M.G.; Dordick, J.S. *Organic Letters*. **2004***, 6*, 1975.

76. Ratner, B.D.; Hoffman, A.S.; Schoen, F.J.; Lemons, J.E. *Biomaterials Science: An introduction to materials in medicine*; Academic Press: San Diego, 1996; p 417.

77. Wiegand, C.; Abel, M.; Ruth, P.; Wilhelms, T.; Schulze, D.; Norgauer, J.; Hipler, U.-C . *J. Biomed. Mater. Res., Part B*. **2008**, *90*, 710.

78. Xu, Y.; Liang, J.; Hu, C.; Wang, F.; Hu, S., He, Z . *J. Biol. Inorg. Chem*. **2007**, *12*, 412.

79. Polizzi, K.M.; Bommarius, A.S.; Broering, J. M.; Chaparro-Riggers, J.F. *Curr. Opin. Chem. Biol*. **2007**, *11*, 220.

80. Drury, J.L.; Mooney, D.J . *Biomaterials*. **2003***, 24*, 4337.

81. Ying, Q; Chu, B. *Macromolecules* **1987**, *20*, 362-366.

82. Boyer, C.; Huang, X.; Whittaker, M.R.; Bulmus, V.; Davis, T.P. *Soft Matter* **2011**, *7*, 1999.

83. Zhang, Y.-Y.; Hu, X.; Tang, K.; Zou, G.-L . *Process Biochemistry*. **2006**, *41*, 2410.

84. Sakai, H.; Yuasa, M.; Onuma, H.; Takeoka, S.; Tsuchida, E. *Bioconjugate Chem*. **2000**, *11*, 56.

85. Cooper, C.; Dubin, P.; Kayitmazer, A.; Turksen, S. *Curr. Opin. Colloid. In.* **2005**, *10*, 52-78

86. Gibson, T. D.; Pierce, B. L. J.; Hulbert, J. N.; Gillespie, S. *Sens. Actuators. B.Chem* . **1996**, *33*, 13-18.

87. Yu, A.; Caruso, F. *Anal.Chem.* **2003**, *75*, 3031-3037.

88. Ku, M.; Bertoncello, P.; Ding, H.; Paddeu, S.; Nicolini, C. *Biosens.Bioelectron.* **2001**, *16*, 849- 856

89. Braia, M.; Porfiri, M. C.; Farruggia, B.; Picó, G.; Romanini, D. *J. Chromatogra. B.* **2008**, *873*, 139-43.

90. Holler, C.; Zhang, C. *Biotechnol. Bioeng.* **2008**, *99*, 902-909.

91. Kaibara, K.; Okazaki, T.; Bohidar, H. B.; Dubin, P. L. *Biomacromolecules.* **2000**, *1*, 100-107.

92. Mattison, K. W.; Brittain, I. J.; Dubin, P. L. *Biotechnol. Prog.* **1995**, *11*, 632-637.

93. Sinha, V. R.; Trehan, A. *J. Control. Release.* **2003**, *90*, 261-80

94. Blanco, D.; Alonso, M. J. *Eur. J. Pharm. Biopharm.* **1998**, *45*, 285-94

95. Weinbreck, F.; Minor, M.; Kruif, C. G. *J. Microencapsul.* **2004**, *21*, 667-79

96. Koker, S. De; Cock, L. J. De; Rivera-Gil, P.; Parak, W. J.; Auzély Velty, R.; Vervaet, C.; Remon, J. P.; Grooten, J.; Geest, B. G. De *Adv. Drug. Deliver. Rev*. **2011**, *63*, 748–61

97. LaVan, D. A; McGuire, T.; Langer, R. *Nat. Biotechnol*. **2003**, *21*, 1184–91

98. Johnston, A. P. R.; Cortez, C.; Angelatos, A. S.; Caruso, F. *Curr. Opin. Colloid. In*. **2006**, *11*, 203–209.

99. Ariga, K.; Lvov, Y. M.; Kawakami, K.; Ji, Q.; Hill, J. P. *Adv. Drug. Deliver. Re*. **2011**, *63*, 762–71

100. Villiers, M. M. de; Lvov, Y. M. *Adv. Drug. Deliver. Re*. **2011**, *63*, 699–700.

101. Peyratout, C. S.; Dähne, L. *Angew. Chem. Intl. Edit*. **2004**, *43*, 3762–83

102. Oh, J. K.; Drumright, R.; Siegwart, D. J.; Matyjaszewski, K. *Prog. Polym. Sci*. **2008**, *33*, 448–477.

103. Vinogradov, S. . *Curr. Pharm. Des*. **2006**, *12*, 4703–4712

104. Gauthier, M. A.; Klok, H.-A. *Chem. Comm.* **2008**, *23*, 2591-2611; Klok, H.-A. *Macromol.* **2009**, *42*, 7990; Gauthier, M. A.; Klok, H.-A. *Biomacromol.* **2011**, *12,* 482-493; Daniel, M.; Root, M. J.; Klok, H.-A. *Biomacromol.* **2012**, *13*, 1438-1447

105. Romanini, D.; Braia, M.; Angarten, R. G.; Loh, W.; Picó, G. *J. Chromatogr. B.* **2007**, *857*, 25-31.

106. Xu, Y.; Mazzawi, M.; Chen, K.; Sun, L.; Dubin, P. L. *Biomacromolecules.* **2011**, *5*.

107. Azegami, S.; Tsuboi, A.; Izumi, T.; Hirata, M.; Dubin, P. L.; Wang, B.; Kokufuta, E. *Langmuir.* **1999**, *15*, 940-947.

108. Picó, G.; Bassani, G.; Farruggia, B.; Nerli, B. *Int. J. Biol. Macromol.* 2007, *40*, 268-75.

109. Almeida, N. L.; Oliveira, C. L. P.; Torriani, I. L.; Loh, W. *Colloids and surfaces. B.* **2004**, *38*, 67-76.

110. Tribet.C. *Physical chemistry of polymers* . Radeva. T., Ed.; Marcel Dekker Inc: New York, **2001**; p 687.

111. Moreira, I. S.; Fernandes, P. A.; Ramos, M. J. *Proteins.* **2007**, *68*, 803-812.

112. Díaz-Rodríguez, A.; Davis, B. G. *Curr. Opin. Chem. Biol.* **2011**, *15*, 211-9

113. Duff, M. R.; Kumar, C.V. *Langmuir.* **2009**, *25*, 12635-12643

114. Duff, M. R.; Kumar, C. V. *J. Phys. Chem.* B. **2009**, *113*, 15083–15089.

115. Thilakarathne, V.; Briand, V.A.; Zhou, Y.; Kasi, R.M. ; Kumar., C.V. *Langmuir*. **2011**, *27*, 7663-7671.

116. Mattison, K. W.; Dubin, P. L.; Brittain, I. J . *J. Phys. Chem.* B. **1998**, *102*, 3830-3836

117. Park, J. M.; Muhoberac, B. B.; Dubin, P. L.; Xia, J.. *Macromolecules.* **1992**, *25*, 290-295.

118. Sturtevant, J. M. *Annu. Rev. Biochem.* **1987**, *38*, 463-88.

119. Breslauer, K. J.; Freire, E.; Straume, M. *Methods Enzymol.* **1992**, *211*, 533-567.

120. Hoare, D.G .; Koshland Jr, D.E . *J.Am.Chem.So*c.**1966**, *88*, 2057-2058

121. Kumar, C. V.; Chaudhari, A. *J. Am. Chem. Soc.,* **2000**, *122*, 830-837.

122. Maurstad, G.; Kitamura, S.; Stokke, B. T. *Biopolymers*. **2012**, *97*, 1–10

123. Bharadwaj, S.; Montazeri, R.; Haynie, D. T. *Langmuir.***2006**, *22*, 6093–101.

124. Guardado-Calvo, P.; Muñoz, E. M.; Llamas-Saiz, A. L.; Fox, G. C.; Kahn, R.; Curiel, D. T.; Glasgow, J. N.; Raaij, M. J. van *J.Virol*., **2010**, *84*, 10558–68.

125. Wu, T.; Gong, P.; Szleifer, I.; Vlcek, P.; Subr, V.; Genzer, J. *Macromolecules*. **2007**, *40*, 8756–8764

126. Gary-Bobo, C. M.; Solomon, A. K. *J. Gen. Physiol.* **1968**, *52*, 825-53

127. Sparks, D. L.; Phillips, M. C. *J. Lipid. Res.* **1992**, *33*, 123-30.

128. Woody, R.W. In *Circular Dichroism and Conformational Analysis of Biomolecules*; Fasman, G.D., Ed.; Plenum Press: New York, 1996; p 25.

129. Gratzer, W.B.; Cowburn, D. A. *Nature*, **1969**, *222*, 426

130. Smith, J. ; Beck, W. ; *Biochem. Biophys. Acta* **1967**, *147*, 324-333.

131. Azegami, S.; Tsuboi, A.; Izumi, T.; Hirata, M.; Dubin, P. L.; Wang, B.; Kokufuta, E. *Langmuir.* **1999**, *15*, 940-947.

132. Carlsson, F.; Linse, P.; Malmsten, M. *J.Phys. Chem. B.* **2001**, *105*, 9040-9049.

133. Seyrek, E.; Dubin, P. L.; Tribet, C.; Gamble, E. A. *Biomacromolecules.* **2003**, *4*, 273-82.

134. Petit, F.; Audebert, R.; Iliopoulos, I. *Colloid. Polym. Sci.* **1995**, *273*, 777-781

135. Borrega, R.; Tribet, C.; Audebert, R. *Macromolecules.* **1999**, *32*, 7798-7806.

136. Tan, W. B., Cheng, W., Webber, A., Bhambhani, A., Durff, M. R., and McLendon, G., and Kumar, C. V., *J. Biol. Inorg. Chem*., (**2005**) *10*, 790-799.

137. Kumar, C. V. and Chaudhari, A., *J. Am. Chem. Soc*., **2000**, *122*, 830-837.

138. Bysell, H.; Hansson, P.; Malmsten, M. *J. Colloid. Interf. Sci*. **2008**, *323*, 60–9.

139. Månsson, R.; Bysell, H.; Hansson, P.; Schmidtchen, A.; Malmsten, M. *Biomacromolecules*. **2011**, *12*, 419–24.

140. Bysell, H.; Hansson, P.; Malmsten, M. *J. Phys. Chem. B*. **2010**, *114*, 7207–15.

141. Shen, Z.; Chen, Y.; Barriau, E.; Frey, H. *Macromol. Chem. Phys*. **2006**, *207*, 57–642.

142. Droege, P. *Bulletin.Sci.Technol.Soc*. **2002**, *22*, 87-99.

143. Lewis, N.S. Science. **2007**. *315*. 798-801.

144. Lewis, N.S., and Nocera, D.G. *Proc.Natl.Acad.Sci.USA*. **2006**.*103*.15729-15735.

145. McDermott, G.; Prince, S. .; Freer, A. .; Hawathornthwaite-Lawless, A. M.; Papiz, R. J.; Isaacs, N. W. *Nature*. **1995**, *374*, 517–521.

146. Miller, R. a; Presley, A. D.; Francis, M. B. *J. Am. Chem. Soc*. **2007**, *129*, 3104–9

147. Cotlet, M.; Vosch, T.; Habuchi, S.; Weil, T.; Müllen, K.; Hofkens, J.; Schryver, F. De. *J. Am. Chem. Soc*. **2005**, *127*, 9760–8.

148. Dutta, P. K.; Varghese, R.; Nangreave, J.; Lin, S.; Yan, H.; Liu, Y. *J. Am. Chem. Soc.* **2011**, *133*, 11985–93.

149. Stein, I. H.; Steinhauer, C.; Tinnefeld, P. *J. Am. Chem. Soc*. **2011**, *133*, 4193–5.

150. Duff, M.R. and Kumar, C. V. *J. Photochem. Photobio. Sci*., **2008**, *7,* 1522-30.

151. Hazra, P., Chacraboarty, D. and Sarkar, N. *Biochem. Biophys.Res.Commun.* **2004**,*314,*543-549.

152. Duff, M.R., Tan, W.B., Bhambhani, A., Perrin Jr, B.S., Thota, J., Rodger, A. and Kumar, C.V. *J.Phys.Chem.B* , **2006**,*110*, 20693-20701.

153. Yen, S., Gabbay, E., and Wilson, W. *Biochemistry*, **1982**, *21*, 2070-2076.

154. Kumar, C. V.; Duff, M. R. *J. Am. Chem. Soc* .**2009**, *131*, 15966–15967

155. Turro, N.J. *Modern molecular photochemistry*. The Benjamin/Cummings publishing Co. Menlo park. CA. 1978. Pp 296-310.

156. Pjura, P.E., Grzekowiak, K., and Dickerson, R.E. Binding of Hoechst 33258 to the minor groove of B-DNA. *J.Mol.Biol*, **1987**,*197*,257-271.

157. Barbero, N., Barni, E., Barolo, C., Qualiotto, P., Viscardi, G., Napione, L., Pavan, S., and Bussolino, F. *Dyes.Pigments*. **2009**, *80*, 307-313.

158. Zhu, J., Li, J. J. and Zhao, J. W. Sensors. *Actuators.B*. **2009**, *128*, 9- 13.

159. Posokhov, Y. O.; Merzlyakov, M.; Hristova, K.; Ladokhin, A. S. *Anal. Biochem*. **2008**, *380*, 134–6.

160. Johansson, E.; Choi, E.; Angelos, S.; Liong, M.; Zink, J. I. *J. Sol-Gel. Sci. Techn*. **2007**, *46*, 313–322.

161. Beddard, G. S.; Porter, G. *Nature*. **1976**, *260*, 366–367

162. Scholes, G. D.; Fleming, G. R.; Olaya-Castro, A.; Grondelle, R. van *Nat. Chem*. **2011**, *3*, 763–74.

163. Scholak, T.; Melo, F. de; Wellens, T.; Mintert, F.; Buchleitner, A. *Phys. Rev. E*. **2011**, *83*, 2–5.